
Electronic Theses and Dissertations, 2004-2019

2010

A Wearable Head-mounted Projection Display

Ricardo F. Martins
University of Central Florida



Part of the [Optics Commons](#)

Find similar works at: <https://stars.library.ucf.edu/etd>

University of Central Florida Libraries <http://library.ucf.edu>

This Doctoral Dissertation (Open Access) is brought to you for free and open access by STARS. It has been accepted for inclusion in Electronic Theses and Dissertations, 2004-2019 by an authorized administrator of STARS. For more information, please contact STARS@ucf.edu.

STARS Citation

Martins, Ricardo F., "A Wearable Head-mounted Projection Display" (2010). *Electronic Theses and Dissertations, 2004-2019*. 1643.

<https://stars.library.ucf.edu/etd/1643>

A WEARABLE HEAD-MOUNTED PROJECTION DISPLAY

by

RICARDO F. MARTINS
B.S. Fairleigh Dickinson University, 2001
M.S. University of Central Florida, 2003

A dissertation submitted in partial fulfillment of the requirements
for the degree of Doctor of Philosophy
in the Department of Modeling and Simulation
in the College of Sciences
at the University of Central Florida
Orlando, Florida

Fall Term
2010

Major Professor: Thomas Clarke

© 2010 (Ricardo F. Martins)

ABSTRACT

Conventional head-mounted projection displays (HMPDs) contain of a pair of miniature projection lenses, beamsplitters, and miniature displays mounted on the helmet, as well as a retro-reflective screen placed strategically in the environment. We have extended the HMPD technology integrating the screen into a fully mobile embodiment. Some initial efforts of demonstrating this technology has been captured followed by an investigation of the diffraction effects versus image degradation caused by integrating the retro-reflective screen within the HMPD. The key contribution of this research is the conception and development of a mobile-HMPD (M-HMPD). We have included an extensive analysis of macro- and microscopic properties that encompass the retro-reflective screen. Furthermore, an evaluation of the overall performance of the optics will be assessed in both object space for the optical designer and visual space for the possible users of this technology.

This research effort will also be focused on conceiving a mobile M-HMPD aimed for dual indoor/outdoor applications. The M-HMPD shares the known advantage such as ultra-lightweight optics (i.e. 8g per eye), unperceptible distortion (i.e. $\leq 2.5\%$), and lightweight headset (i.e. ≤ 2.5 lbs) compared with eyepiece type head-mounted displays (HMDs) of equal eye relief and field of view. In addition, the M-HMPD also presents an advantage over the preexisting HMPD in that it does not require a retro-reflective screen placed strategically in the environment. This newly developed M-HMPD has the ability to project clear images at three different locations within near- or far-field observation depths without loss of image quality. This particular M-HMPD embodiment was targeted to mixed reality, augmented reality, and wearable display applications.

To my wife, whom I owe the bountiful delight of our shared experiences I will always love you. To our two great children, who have brought me great wisdom I thank you.

To my parents, who have supported me and taught me never to surrender to life's trials and tribulations. For all of the lifelong support, I will always be grateful.

To my lifelong friends, whom I shared many joyful nights, thank you for your presences.

To the memory of all my grandparents, who have showed me reverence you will always be missed.

ACKNOWLEDGMENTS

First and foremost, I want to thank my advisor, Thomas Clarke, for providing me the opportunity to work collaboratively on this research effort.

I want to express my utmost gratitude to my committee members, Peter Kincaid, Randall Shumaker, and Vesselin Shaoulov for your comments, suggestions and great input in developing this work.

I would like to thank Glenn Boreman from the College of Optics/CREOL for his support and honesty during the years of my graduate program.

I want to express my fullest admiration to my wife, Sandra Martins who has showed me a new meaning of love you are ingrained in my soul. To my children, Samantha (5 yrs old) and Nathan (1.75 yrs old) Martins I understand the truest form of love through your eyes, may God bless you always.

I cannot express the amount of gratitude towards my family, and to my friends who have surpassed simple friendship and will be lifelong family members especially; Aldwin Polanco, Hong Liu, Mike Cordoba, and Vesselin Shaoulov you guys are an integral part of my live, thank you.

Finally, I would like to thank the support of the Office of Naval Research through contract N00014-03-10677, the Florida Photonics Center of Excellence (FPCE), and the National Science Foundation (NSF) grant IIS/HCI 03-07189. Special thanks goes to Fresnel Technology, Inc. for donating Fresnel lenses, to 3M Corporation and Reflexite, Inc. for their contributions of retro-reflective screens, Optical Research Associates for the student license of CODE V[®], and Breault Research for the student license of Advanced Systems Analysis Program (ASAP[®]).

TABLE OF CONTENTS

LIST OF FIGURES	ix
LIST OF TABLES	xii
LIST OF ACRONYMS/ABBREVIATIONS	xiii
CHAPTER ONE: INTRODUCTION.....	1
1.1 Defining the Mobile Head-Mounted Display (MHMD).....	4
1.2 Related Research.....	5
1.3 HMPD Overall Optical Layout.....	6
1.4 HMPD Optomechanical Design	8
1.4.1 Polarized HMPD Design.....	11
1.4.2 Eye-tracking HMPD Design.....	12
1.5 Motivation.....	14
1.6 Research Summary	15
1.7 Dissertation Outline	15
CHAPTER TWO: EXPERIMENT ONE: DIFFRACTION OF PHASE CONJUGATE MATERIAL IN A NEW HMD ARCHITECTURE.....	17
2.1 Introduction.....	17
2.2 Concept of a new see-through head-mounted displays (HMD).....	19
2.2.1 Optical lens design.....	21
2.3 Experimental Results of Phase Conjugate Material.....	24
CHAPTER THREE: EXPERIMENT TWO: PRJECTION BASED HEAD-MOUNTED DISPLAYS FOR WEARABLE COMPUTERS	28

3.1 Introduction.....	28
3.2 Review of the Optical Layout for the Wearable HMPD.....	30
3.3 Optical Lens Design.....	32
3.4 Experimental Results of PCM	33
CHAPTER FOUR: EXPERIMENT THREE: A MOBILE HEAD-WORN PROJECTION	
DISPLAY	38
4.1 Introduction.....	38
4.2 M-HMPD System	41
4.2.1 Microdisplay Device.....	43
4.2.2 Projection Optics.....	44
4.2.3 Retro-reflective screen.....	48
4.3 Display Results	51
CHAPTER FIVE: EXPERIMENT FOUR: THE MACROSCOPIC AND MICROSCOPIC	
PROPERTIES OF HIGH GAIN SCREENS	53
5.1 Introduction.....	54
5.2 Macroscopic Properties.....	56
5.3 Microscopic Properties	58
5.3.1 Simulation Results of a Gaussian Image	60
5.3.2 Simulation Results of an MTF Resolution Target and Bitmap Portrait Image.....	63
CHAPTER SIX: CONCLUSION AND FUTURE WORK.....	
APPENDIX: A COMPACT MICROLENSLET-ARRAY-BASED MAGNIFIER.....	69

APPENDIX: B MAGNIFYING MINIATURE DISPLAYS WITH MICROLENSLET ARRAYS	77
APPENDIX: C HEAD-MOUNTED DISPLAY BY INTEGRATION OF PHASE-CONJUGATE MATERIAL	87
APPENDIX: D COMPACT MICROLENSLET ARRAYS IMAGER	103
LIST OF REFERENCES	113

LIST OF FIGURES

Figure 1: A monocular HMD configuration consisting of a miniature display, illumination system, and collimating optics worn on the head.	4
Figure 2: (a) First order layout of the HMPD, (b) miniature projection optics, (c) HMPD system	7
Figure 3: HMPD Optical Layout.	7
Figure 4: Monocular lens-mount assembly.....	9
Figure 5: Overall Display Exploded OptoMechanical Design	10
Figure 6: (a) OLED HMPD 3D view ; (b) OLED HMPD Side view.....	10
Figure 7: Design of the p-HMPD.....	12
Figure 8: Design of the ET-HMPD.....	13
Figure 9: Current HMPD	19
Figure 10: Conceptual design	20
Figure 11: Design Layout	21
Figure 12: Lens assembly	23
Figure 13: Head-mounted projection display	23
Figure 14: Astigmatism in arcmin	23
Figure 15: Projection optics.....	24
Figure 16: MTF curves	24
Figure 17: Experimental setup to investigate diffraction of the microstructure	25
Figure 18: Coordinate system for computing diffraction	26
Figure 19: Intensity plot of both microstructures	27

Figure 20: First Order Layout of HMPD Conceptual Design	31
Figure 21: Wearable HMPD Concept. While a grayscale picture can only be shown here for publication, the display allows full color.....	32
Figure 22: Monocular Lens-Mount Assembly.....	33
Figure 23: Different Types of Microstructures.....	35
Figure 24: HMPD Bench Setup.....	36
Figure 25: Computer-Generated Test Image	36
Figure 26: Capture Test Image with Lights Off (Scenario 1).....	36
Figure 27: Capture Test Image with Lights On 15 lux (Scenario 2)	36
Figure 28: (a) First order layout for one eye of the see-through M-HMPD with retro-reflective screen placed along Path 2. (b) Assembly of a binocular see-through M-HMPD with a robust titanium mounting structures and the integrated retro-reflective screen. (c) User wearing the binocular M-HMPD.	41
Figure 29: Monocular Lens-Mount Assembly.....	46
Figure 30: The MTF plots for a projected scene located at (a) 1.5 m, (b) 3.5 m, and (c) infinity across the full 12 mm of the projection optics.....	47
Figure 31: Distortion plots for a projected scene located at (a) 1.5 m, (b) 3.5 m, and (c) infinity across the full 12 mm of the projection optics.....	48
Figure 32: Monocular Lens-Mount Assembly.....	50
Figure 33: Image (a) represents the test image to be superimposed in the outdoor scene (b) is the augmented reality image captured outdoors by a digital camera at the optics exit pupil location. While currently at reduced resolution given the need for new microstructure films,	

the parrots were successfully superimposed on outdoor trees seen as a detailed texture in the background.....	52
Figure 34: First order layout of the M-HMPD implementing ideal optical components to solely retrieve the corner-cube screen image degradation information.....	59
Figure 35: (a) Bitmap image of the object source.	61
Figure 36: Imaging and irradiance distribution of an MTF grey-scale bitmap object source: (a) original object source, (b) image with 256 μm corner cube microstructures, (c) image with 128 μm corner cube microstructures, (d) image with 64 μm corner cube microstructures, (e) image with 32 μm corner cube microstructures, (f) image with 16 μm corner cube microstructures, (g) image with 8 μm corner cube microstructures.	65
Figure 37: Grey-scale bitmap object source: (a) original grey-scale object source, (a) image with 16 μm corner cube microstructures, (b) image with 8 μm corner cube microstructures.....	65

LIST OF TABLES

Table 1 Specification of projection optics..... 22

LIST OF ACRONYMS/ABBREVIATIONS

3D	Three-Dimensional
AOI	Area Of Interest
AR	Augmented Reality
ARC	Augmented/Artificial Reality Center
CRT	Cathode Ray Tube
CSCE	Computer Supported Cooperative Environment
DARE	Distributed Augmented Reality Environment
DIVE	Distributed Interactive Virtual Environment
DVS	Distributed Virtual System
FOV	Field of View
HCI	Human-Computer Interaction
HPS	Human Patient Simulator
HMD	Head Mounted Display
HWD	Head Worn Display
HWPD	Head Worn Projection Display
IPD	Inter-Pupillary Distance
IREDD	Infrared Emitting Diode
ISO	International Standard Organization

LAN	Large Area Network
LCD	Liquid Crystal Display
LOD	Level Of Detail
M-HWPD	Mobile-Head Worn Projection Display
MIMD	Multiple Instruction Multiple Data
MR	Mixed Reality
NTP	Network Time Protocol
OLED	Organic Light Emitting Display
ODALab	Optics Diagnostics and Applications Lab
P2P	Peer-To-Peer
RT	Real Time
RTOS	Real-Time Operating System
THMD	Teleportal Head-Mounted Display
VA	Visual Acuity
VE	Virtual Environment
VGA	Video Graphic Array
VR	Virtual Reality
WAN	Wide Area Networks
XGA	Extended Graphics Array

CHAPTER ONE: INTRODUCTION

Head-mounted displays (HMDs) are devices that allow a person to alter their perspective of the real world into a predefined computer generated augmented world, where he or she can experience possibilities that would be impossible otherwise. This augmented world can be defined as a simulated environment. The individual components comprising an HMD are a miniature display, an optical system to magnify our miniature display, and illumination systems to enhance the brightness of our display. These components assemble cohesively to provide the means for our software media to create the simulated environment. The user wearing the HMD experiences a ubiquitous sense of an enhanced environment that is controlled by a pre-existing computer-generated scene displaying a three-dimensional (3D) realm. Gaining the connection between the physical and the simulated worlds depends on the successful design and integration of the HMD. Successful designs of an HMD can only be achieved if full consideration is given to the user's needs to complete the required simulated tasks.

There are two major configurations to an HMD, specifically video see-through, and an optical see-through design. [[Sutherland, I., 1965](#)], [[Rolland, J., et al., 1995](#)] With optical see-through HMDs, the real world is seen through a beamsplitter (i.e. partially transparent mirror) which is placed in front of the user's eyes. The beamsplitters' primary operation is to reflect the computer generated images into the user's eyes, thus superimposing the computer-generated imagery on top of the real world. In contrast, in a video see-through HMD, the real-world view is captured with two video cameras mounted on the headset, and the computer-generated images captured by the cameras are electronically combined and perceived as a video representation of the real world. In this configuration, users do not have a direct view to the real world. Two major

obstacles that we must overcome in a video see-through configuration are, electronic latency and view point offsets. [[Holloway, R., 1994](#)], [[Yamazaki, T., et. al., 1990](#)]

Electronic latency (i.e. lag) is the time it takes between when the head moves and when the visual scene is updated to reflect this movement. This update is referred to as an *update rate* and is the frequency with which each visual scene is displayed to the user. Both the lag and update rate have been found to be contributors to simulator sickness and cybersickness. [[Biocca, F., 1992](#)] [[Kalawsky, R. S., 1993](#)] [[Pausch, R., and Conway, M., 1992](#)] Therefore, the need to develop an HMD with low latency and increasing the update rate is desirable for video see-through HMD technology.

Moreover, view point offset is also a critical issue in video see-through HMD systems. [[Cakmakci, O., and Rolland, J., 2006](#)] The magnitude of the viewpoint offset has been found to impact the sensorimotor adaptation. [[Biocca, F., and Rolland, J., 1998](#)] Orthoscopic displays which do not introduce a view-point offset have been built for a modest FOV. [[State, A., et. al., 2005](#)] In this orthoscopic display, [[State, A., et. al., 2005](#)] the FOV was 26 x 19.6 degrees. It was suggested that it is difficult, if not impossible, for video-based see-through HMDs to perfectly match the natural viewpoint of the user for wide FOV displays. [[Biocca, F., and Rolland, J., 1998](#)]

One solution to the problem that can cause cybersickness resulting from view point offset, latency, and update rate issues, is to decrease the FOV. This option runs counterproductive to the goal of most HMD designers. Typically, a given application generates the requirement for the FOV. Moreover, requirements of applications such as movies or computer gaming may be satisfied with a moderate FOV of 15 - 20 degrees. In applications such

as flight simulators, extended FOVs (i.e. 40 – 120 degrees) are required, which in turn are responsible for the cybersickness in such applications. The finite resolution of miniature displays also plays a role on the visual acuity which directly correlates to the maximum FOV.

Another more practical solution to the problem of cybersickness is to decrease the HMD's overall weight. Evidence has shown that the added weight rearranges the relationships between motor commands for head movement and feedback from the head and neck. [[DiZio, P., and Lackner, J. R., 1992](#)] With an increase of the effective weight placed on the head, an increased inertia is created and can shift the center of gravity of the head position. It has been observed that wearing an HMD weighing more than two pounds can elicit symptoms of motion sickness. [[DiZio, P., and Lackner, J. R., 1992](#)] Therefore, it is desirable for an HMD designer to pay special attention to the center of gravity and total overall weight of the device.

The optimal solution to combat cybersickness and motion sickness is to develop an optical see-through HMD that does not impede on the user's natural vision. [[Rolland, J., et al., 1995](#)] One such HMD was developed by Vio in the United Kingdom, Virtual I/O glasses, with a generous amount of look-around and look-under vision, and reports zero incidents of sickness. [[Buckert-Donelson, A., 1995](#)] The ability to view the outside world and one's own body provide the needed visual reference to prevent onset sickness. The desired HMD configuration is a lightweight optical see-through system that develops an augmented reality perspective, where synthetic imagery is combined with the real world to mitigate motion or cybersickness. [[Barfield, W., et al., 1995](#)] [[Metzger, P. J., 1993](#)]

1.1 Defining the Mobile Head-Mounted Display (MHMD)

HMDs are complex optical systems that present either dynamic data or imagery primarily to the user wearing the device. A monocular HMD in its simplistic form, as shown in Fig. 1, consisting of a single miniature display, illumination system, and collimating optics worn on the head. Furthermore, the HMD can increase in complexity through several possible configurations. The system can include two miniature displays allowing for a binocular view that permits a stereoscopic scene. The HMD can be designed to occlude the environment for an immersive virtual environment with an integrated beam splitter, a see-through configuration can allow for an augmented environment. In the occluded virtual environment, the user has an ambiguous sense of the real world where he/she is completely controlled by the images rendered on the miniature display. In contrast, in an augmented environment, the user merges the real world and a computer-generated environment into a single enhanced environment greatly improving the required objectives.

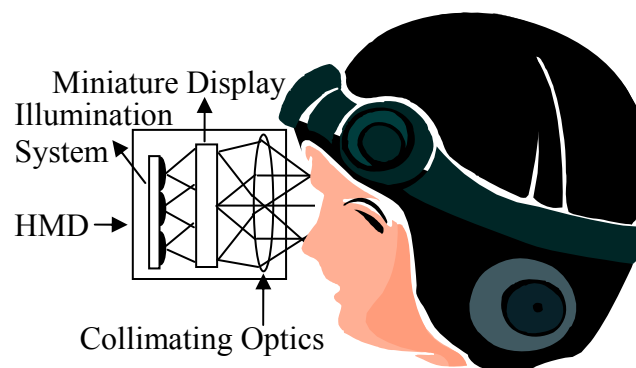


Figure 1: A monocular HMD configuration consisting of a miniature display, illumination system, and collimating optics worn on the head.

All of the individual HMD components, such as the miniature display, illumination system, and collimating optics, may adapt several different technologies. For example, the HMD miniature display can take the form of cathode ray tube (CRT), liquid crystal display (LCD), liquid crystal on silicon (LCOS), digital light processor (DLP), or organic light emitting display (OLED). An external illumination system in conjunction with the LCD, LCOS, or DLP may be an array of white light emitting diodes (LEDs) or three separate red, green, and blue LEDs to form white light, a light pipe, and a fiber optics light guide, CRTs are a self-sufficient displays that do not require an external illumination system; they incorporate a fluorescent screen that emits light when electrons emitted by an electron gun strike the screen. OLEDs also do not require an external illumination system since one of their many layers is an emissive electroluminescent light source. The emissive electroluminescent layer material emits light when an electric current is passed through it. Once the light is emitted by the miniature display the collimating optics can take on either of two main configurations, eyepiece or a projection based design. The design goal of both configurations is to magnify the miniature display at a designed FOV.

1.2 Related Research

Several research groups have been developing and improving HMDs for the past two decades. The majority of the research groups have been focusing on eye-point misalignment and registration concerns, but only a few institutions have actually developed HMD and more specifically head-mounted projection displays (HMPDs). The HMPD is comparable to an HMD as they both have an optical system, miniature displays, display electronics, and headset. The

major difference between them is in the optical configuration. In an HMPD the optical system conjugates an image rendered by the miniature display (i.e. located on the headset) onto a retro-reflective screen, because of the characteristics of the screen all of the light is reflected back to the user and concentrated at the exit pupil plane, as shown in Fig. 2 (i.e. where the user places their eye). [[Hua, H., et. al., 2000](#)] [[Hua, H., and Rolland, J. P., 2002](#)] [[Hua, H. and Gao, C., 2007](#)] Since the light exits the headset the user has the unique ability to occlude the computer generated image. [[Inami, M., et. al., 2000](#)] This is a major advantage over existing video see-through HMDs as they cannot provide real-time occlusion as all of the light is confined within the headset. An HMPD provides a means of augmenting the natural environment which is comparable to the human visual system without significant electronic latency. Although, the latency did not perceive to be a problem multiple research teams have designed and developed see-through HMPD to reduce the amount of latency that could be contributed to cybersickness.

1.3 HMPD Overall Optical Layout

The first HMPD system was assembled from commercial off-the-shelf components (COTS) and was demonstrated for medical visual applications by Parsons and Rolland, and Kijima and Ojika. [[Parsons, J., and Rolland, J. P., 1998](#)], [[Kijima, R., and Ojika, T., 1997](#)] Kawakami and Tachi demonstrate a non-head-mounted configuration that utilized two video projectors combined with a retro-reflective screen. [[Kawakami, N., et. al., 1999](#)] Some years later, Inami and Tachi's research team further extended their research to include a stereoscopic display configuration with an HMPD. [[Inami, M., et. al., 2000](#)]

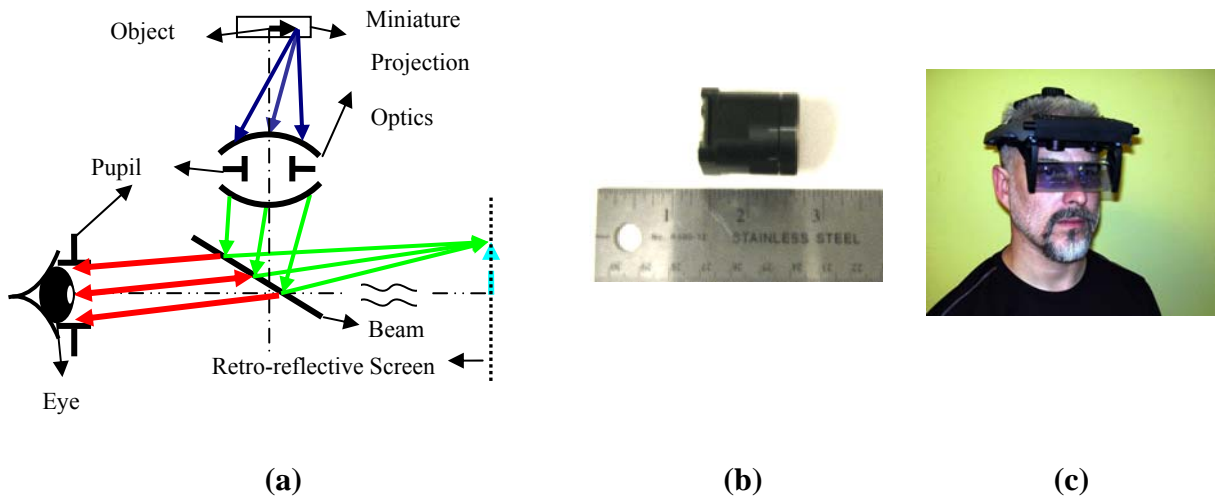


Figure 2: (a) First order layout of the HMPD, (b) miniature projection optics, (c) HMPD system

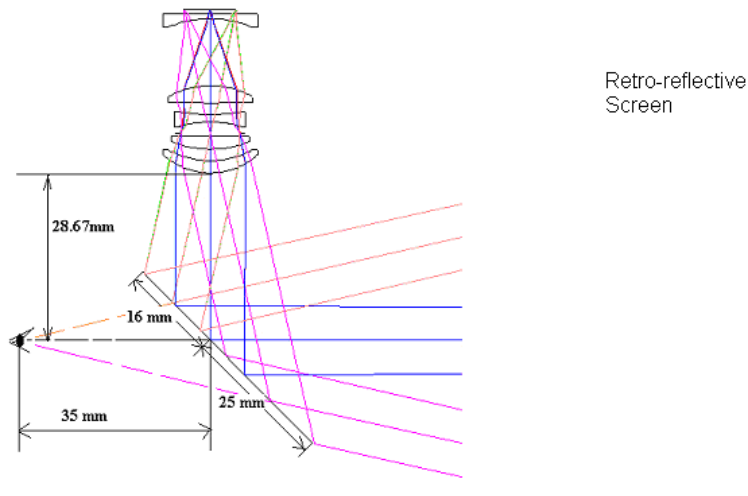


Figure 3: HMPD Optical Layout.

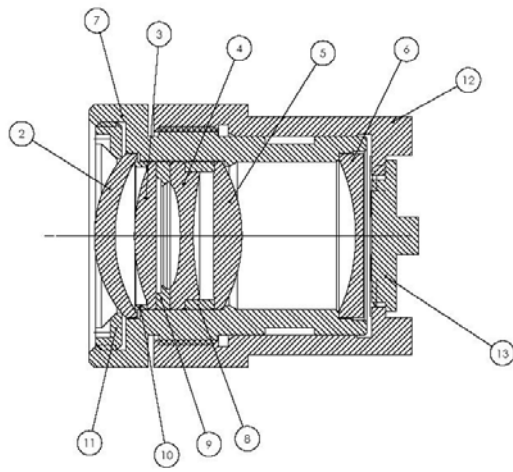
In order to provide images to the eyes of the user, as well as maximize light efficiency throughput, a retro-reflective screens is utilized instead of conventional diffusing projection screens. The use of such optical screens (a.k.a. high gain screens) is critical to enabling the operation of the HMPD with sufficient light throughput. As shown in Fig. 3, the HMPD optical

layout is presented; a miniature display is located at or beyond the focal plane of the projection optics and used to magnify computer-generated image. A beamsplitter is placed after the projection lens at 45 degrees with respect to the optical axis, bending the light at 90 degrees away from the eyes and towards the retro-reflective screen. This configuration creates the opportunity to overlay the retro-reflective screen seamlessly onto the environment to enable a virtual environment.

Moreover, the screens can be placed in the environment without the prerequisite of calibration. Because of the optical characteristics of the retro-reflective screen, the light rays are reflected back onto themselves in the opposite direction upon interfacing with the surface, allowing the light to reach the users eyes. A user can thus perceive the stereoscopic images from the exit pupils of the overall optics assembly (i.e. projection optics together with the beamsplitter), which is optically co-located with the users eyes.

1.4 HMPD Optomechanical Design

Figure 4 shows a detailed cross-section of the monocular optomechanical sub-assembly, complete with the lens elements and miniature display. This module was made as compact as possible and the optics was assembled in the optical shop for optimal alignment of the various components, including the miniature display.



ITEM NO.	QTY.	PART NO.	DESCRIPTION
1	1	rays-hmdrmd2	
2	1	30718-01	LENS 1
3	1	30718-02	LENS 2, DIFFRACTIVE
4	1	30718-03	LENS 3, ASPHERE
5	1	30718-04	LENS 4
6	1	30718-05	LENS 5
7	1	30718-06	LENS MOUNT
8	1	30718-07	SPACER, LENS 3 & 4
9	1	30718-08	SPACER, LENS 2 & 3
10	1	30718-09	SPACER, LENS 1 & 2
11	1	30718-10	RETAINER
12	1	30718-12	MOUNT, MICRO DISPLAY
13	1	30718-13	OLED MICRO DISPLAY

Figure 4: Monocular lens-mount assembly.

A preliminary study of the overall mechanical design approach was completed to ergonomically mount in the HMPD optical sub-assembly to the next higher assembly. One approach was to mount the display module (i.e. miniature display & associated optics and optical mechanical housings) onto ITT Industries' off-the-shelf AN/AVS-9 type night vision goggles helmet-mounting plate, which can be easily be clipped onto a standard flight helmet. This approach required developing a custom up-down mechanism for proper viewing. A second approach, which was adopted as a prototype, was to mount the HMPD components by re-Engineering NVIS's off-the-shelf HMD, nVisor SX.

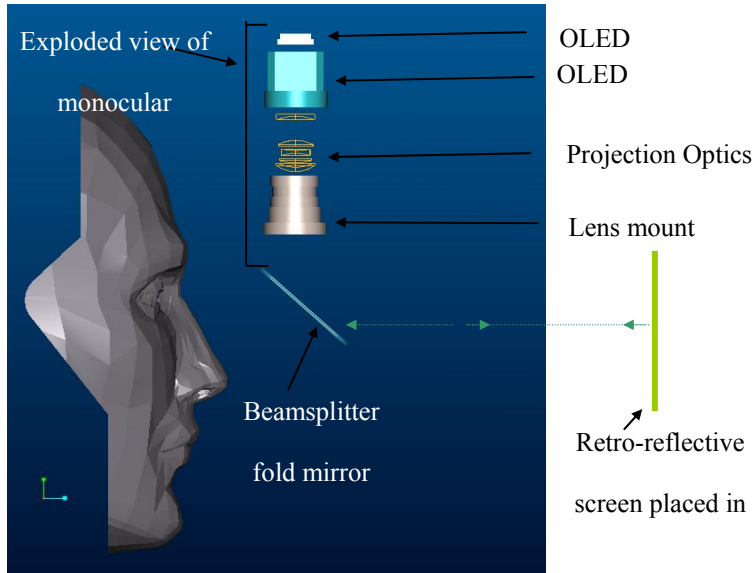


Figure 5: Overall Display Exploded OptoMechanical Design

Figure 5 shows the exploded view of the HMPD, revealing the major components of the monocular sub-assemblies. For simplicity, other elements such as retaining rings and spacers are not shown. The prototype HMPD is shown in Fig. 6. (a-b), which consists of a lightweight shell with a comfortable head fitting system and a full range IPD (Interpupillary Distance) mechanism that is currently being used on NVIS nvisor SX HMD products.

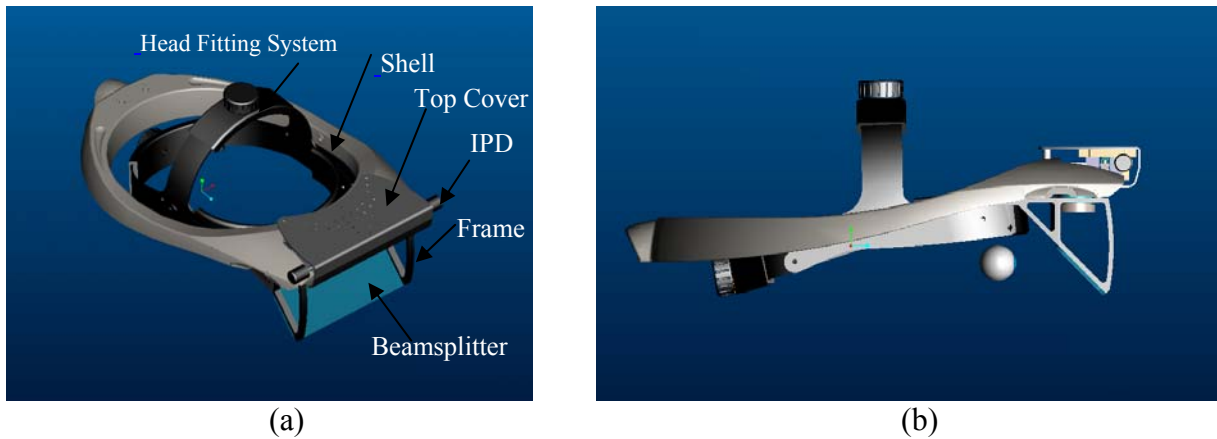


Figure 6: (a) OLED HMPD 3D view ; (b) OLED HMPD Side view

This was an innovative solution for a low-cost embedded display for use in training and simulation in deployed ground and air vehicles. As previously mentioned HMDs based on conventional eyepiece designs, even with see-through optics, suffer from poor registration between the out-the-window (OTW) scenes. One of two main advantages of projection based HMDs is the natural cut out of the virtual environment by the real environment where the optical screen ends. This provides the user with the correct dimensions between the real environment and the OTW scene. All other areas of the physical environment are visible through the display optics.

1.4.1 Polarized HMPD Design

Another approach to designing an HMPD is to take advantage of some polarizing displays. In a typical HMPD, the light flux passes through the beamsplitter twice, thus reducing the overall illumination by 50% in each pass. Therefore, to minimize losses, a polarizing display source can be utilized in combination with a polarized beamsplitter and a quarter-wave retarder plate, as shown in Fig. 7. [[Zhang, R. and Hua, H., 2008](#)] Another benefit of the polarized HMPD (p-HMPD) design lies in the compactness which is a critical factor in HMD systems to reduce size and weight. Another benefit to this design and presented by Hua's research team was in developing a p-HMPD. The illumination was significantly increased and her design achieved the theoretical value of 19.3% efficiency, compared with approximately 4-10% efficiency with convention HMPDs. With the use of a p-HMPD this configuration is limited to microdisplay that operates on polarized light. For example, LCD, DLPs, and LCOS displays all operate on polarized light although a recent technology such as OLEDs are randomly polarized. If we

consider using a p-HMPD with an OLED we must polarize the emitted light before the beamsplitter which may lead to similar illumination efficiencies as an HMPD. Therefore, the p-HMPD is specific to the particular display that will be integrated into the design of the HMD.

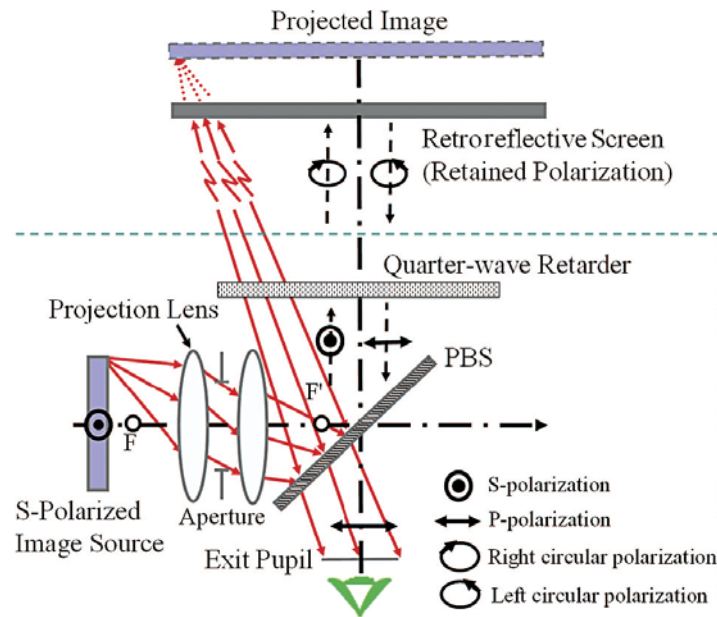


Figure 7: Design of the p-HMPD.

1.4.2 Eye-tracking HMPD Design

We can further enhance an HMPD by tracking the user’s pupil as discussed by Curatu, Hua, and Rolland, as shown in Fig. 8. [Curatu, C., et. al., 2005], [Curatu, C., et. al., 2006] Curatu designed and integrated a near infrared camera within an HMPD to track the gaze angle of the user. The optical system was designed in such a manner that the infrared sensor and HMPD optical system was shared on the same optical axis further reducing cost, weight, and complexity, as shown in Fig 8. The eye-tracking HMPD (ET-HMPD) could aid in reducing or

possibly eliminating registration issues by tracking the user's eye gaze angle and displaying the appropriated computer rendered images through the ET-HMPD. [Azuma, R., 1993], [Azuma, R., 1995], [Azuma, R., and Gary B., 1994], [Azuma, R., and Gary B., 1995], [Genc, Y., et. al., 2000]

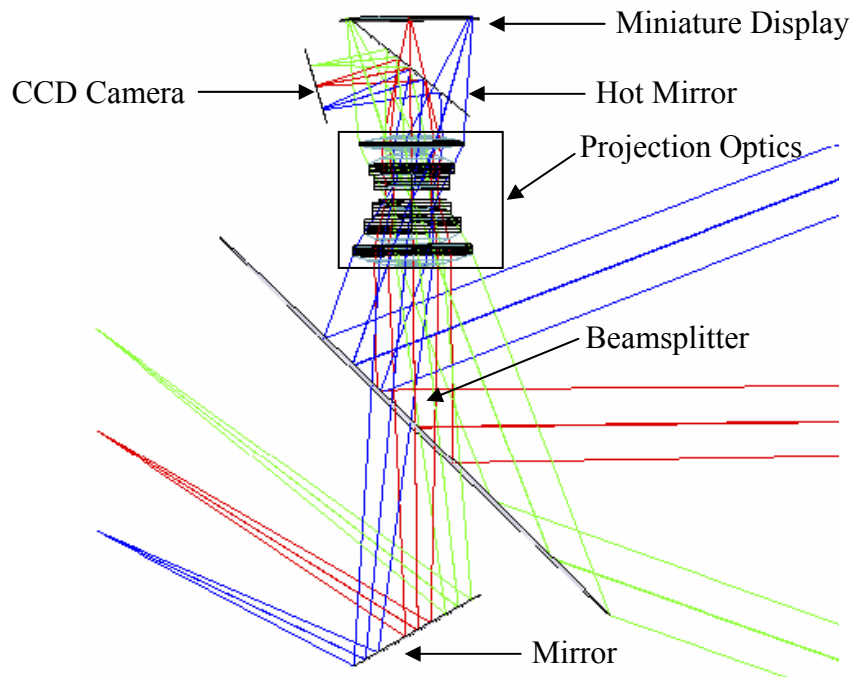


Figure 8: Design of the ET-HMPD.

With the various HMPDs developed that target specific limitations over other HMDs one such problem that the HMPD faces is mobility. In all designs of the HMPD a retro-reflective screen is placed in the environment, therefore mobility is confined within the screen. Thus, a need to venture with unlimited boundaries is required to provide more flexibility and allow for mobile applications to benefit from the HMPD technology. Since the HMPD is considerably lighter (i.e. ≤ 1.5 lbs) at unperceivable distortion levels (i.e. $\leq 2.5\%$) this technology can benefit mobile applications.

1.5 Motivation

A challenge in developing an modular augmented reality HMD is achieving a high visual acuity system with sufficient resolution and brightness. There are many HMD systems that are currently used in an augmented reality environment, but are limited to a confined space. Current HMD systems utilize either an eyepiece optical design or free-form prism, which is one special case of an eyepiece optical system. These particular designs currently accommodate the vast amount of augmented reality applications.

An issue found with eyepiece or free-form prism HMD designs is the undesirable amount of image distortion and overall optical weight versus FOV present in the visual scene. The image distortion is inherent in all eyepiece systems because of the location of its exit pupil, which is outside the optical system. This also results in an increased optical aperture as the FOV is increased. Thus with an increased aperture more optical components are inevitably required, thus increasing the overall weight of the system. The current optical designers must balance the distortion and weight while controlling the maximum amount of FOV required by the desired application. Moreover, the increased weight may fatigue the user's neck thus drastically limiting the amount of training that can be comfortably achieved. Therefore, we must improve on HMD technology by improving optical performance and possibly extending its virtual environment to satisfy both indoor and outdoor applications. This would remove any limitations on augmented reality training.

1.6 Research Summary

The purpose of this research effort is to present a mobile HMD in the form of an HMPD that can achieve a large FOV without increasing image distortion or optical weight. In addition, we will investigate the imaging properties of the retro-reflective screen as one of the main components of the HMPD system.

A solution to the undesirable distortion and weight issues are to develop an optical see-through mobile-HMPD (M-HMPD) that elevates the undesirable features of an eyepiece system. The undesirable features are large amounts of distortion $\geq 8\%$, and total weight ≥ 2.5 lbs. By implementing an M-HMPD we can integrate a retro-reflective screen within the headset construct. The M-HMPD form can achieve a diagonal FOV ≤ 90 degrees without increasing the distortion or optical weight. The benefit of an M-HMPD is the optical system is based on projection optics where the exit pupil is located within the optics thus creating symmetry around the pupil. To the author's knowledge, such device parameters have not been achieved by an eyepiece or free-form prism optical system.

The research presented in this body of work provides a revolutionary M-HMD design that can benefit deployable applications in settings such as urban combat training facilities, for example.

1.7 Dissertation Outline

This dissertation is organized in the following manner: Chapter 2 demonstrates the embodiment of the see-through M-HMPD. This section describes the configuration of the M-HMPD and the first order optical characteristics of the lens design. The conclusion of this chapter describes the

current M-HMPD and extends to the future work on developing a retro-reflective screen for imaging applications.

Chapter 3 describes experimentally the M-HMPD and its ability to render computer-generated images in an indoor environment as a viable wearable system. While in Chapter 4 we will extend the capabilities of the M-HMPD to render images in an outdoor setting. Moreover, in this chapter we will include a discussion of the retro-reflective screen and extend our discussion to include different types of commercially viable solutions for fabricated retro-reflective screens.

Chapter 5 details a rigorous model of an imaging retro-reflective screen and will be the second part of this research effort on improving the M-HMPD system. A mathematical model will be developed to describe the optical characteristics of the retro-reflective screen and a means of improving the screen for our mobile applications. The characteristics of the model will be composed of two parts which are the macroscopic and microscopic optical properties. At the end of this section a summary of the results and future work will be included.

Finally, in Chapter 6 we summarize the results and contributions of the work developed as well as a discussion the potential for future work to improve the M-HMPD.

CHAPTER TWO: EXPERIMENT ONE: DIFFRACTION OF PHASE CONJUGATE MATERIAL IN A NEW HMD ARCHITECTURE¹

Conventional head-mounted displays (HMDs) consisting of a pair of miniature projection lenses, beam splitters, and miniature displays mounted on the helmet, as well as phase conjugate material placed strategically in the environment have been redesigned to integrate the phase-conjugate material into a complete see-through embodiment. Some initial efforts of demonstrating the concept was followed by an investigation of the diffraction effects versus image degradation caused by integrating the phase-conjugate material internally in the HMD. The key contribution of this chapter lies in the conception, and assessment of a novel see-through HMD. Finally, the diffraction efficiency of the phase-conjugate material is evaluated, and the overall performance of the optics is assessed in both object space for the optical designer and visual space for possible users for this technology.

2.1 Introduction

3D visualization devices, which have succeeded in penetrating real world markets, have evolved into three formats: standard monitors/shutter glasses, head-mounted displays (HMDs), and projection-based displays such as CAVEs. [[Buxton, D., Fitzmaurice, G. W., 1998](#)] Each of the three common approaches currently imposes a significant increase in cost. In addition, monitors with shutter glasses are limited in capability, and CAVEs are prohibitive in cost and limited to

¹ Martins, R.F. and Rolland, J.P. "Diffraction of Phase Conjugate Material in a New HMD Architecture,"*SPIE AeroSense: Helmet and Head-Mounted Displays VIII: Technologies and Applications*, SPIE Proceedings Vol. **5186**, p. 277-283, , Editors: C. E. Rash and C. E. Reese, September 2003.

fully support only one user at a time without perceptual distortions. HMDs currently provide a fine balance of affordability and unique capabilities such as creating mobile and secure displays, [[Davis, L., et. al., 2003](#)] spanning the virtual environments continuum first proposed by Milgram, [[Milgram, P., and Kishino, F., 1994](#)] and enabling teleportal capability with face-to-face interaction. [[Biocca, F., and Rolland, J., 2000](#)]

Most future display technologies will be linked to the telecommunication networks. Mobile and distributed systems are driven by concrete real world applications testable in real environments. The overall thrust of the research is to develop HMD technologies that support outdoor helmet mounted displays specifically aimed at mobile augmented reality navigation and information systems. This effort led to the conceptual novel design of a see-through HMD that will provide a solution for an improved outdoor virtual environment.

A recent novel type of HMD is the head-mounted projection display (HMPD), which may be thought as a miniature projector mounted on the head with a phase conjugate material placed strategically in the environment. In Fig. 9. the display presented in this chapter builds on the HMPD concept, however the novelty lies in the integration of the phase conjugate material within the HMD. Such display is also light weight but can be used outdoors. [[Martins, R. F., and Rolland, J. P., 2003](#)] The weight of the optics is less than 8g per eye in the current conception. This technology developed lies beyond the boundaries of any conventional HMDs and projection-based displays because it opens the door from an indoor environment tethered to the phase conjugate material placed in the environment to a mobile system with the capability to be outdoors. Such configuration allows 3D visualization capability with a large FOV (i.e. $30^\circ < \text{FOV} < 90^\circ$ diagonal), lightweight optics (i.e. 8g per eye) and low distortion (i.e. $< 1.5\%$ at the

edge of the FOV). Distortion may easily be constrained at the expense of other field aberrations to be less than one percent depending on the targeted application because of the pupil location within the optics by design. A potential drawback of the new HMD compared to the original HMPD is the loss of some of the natural occlusion cues that might be desired in targeted applications. The conceptual design of the HMD is presented in Section 2. In Section 3, the optical design is detailed. Finally, Section 4 presents an analysis of diffraction blur and experimental validation.



Figure 9: Current HMPD

2.2 Concept of a new see-through head-mounted displays (HMD)

The conceptual design for the see-through HMD was achieved and patented in the Optical Diagnostics and Application Laboratory (ODA Lab) and the actual design was finalized under the Synthetic Natural Environment program of the US Army. This design shown in Fig. 10 has incorporated projection optics and phase conjugate material within the HMD, thus eliminating the requisite use of an external phase conjugate material. [Rolland, J. P., et. al., 2001] A key component of this design is not only the integration of the phase conjugate material and projection optics but also the use of a lens located near the material that facilitates the operability of this technology. Because of its stand alone capability, this display extends the use of

projection head mounted displays to clinical guided surgery, medical simulation training, and outdoor augmented see-through virtual environment for military training and wearable computers.

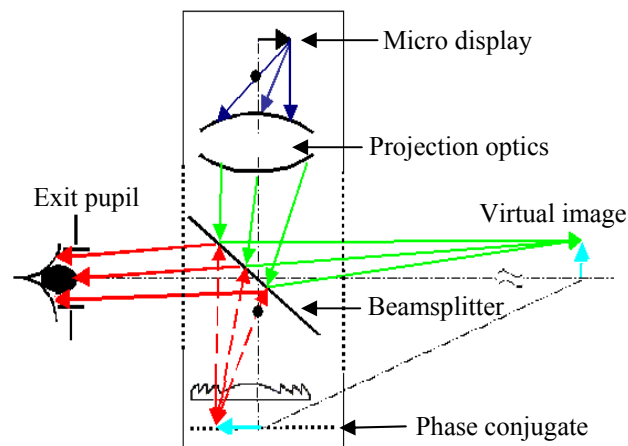


Figure 10: Conceptual design

In a first design layout, Fig. 11 provides an illustration of how the see-through HMD can be worn on a user's head. From this design it is not sufficient to solely place the phase conjugate material in close proximity to the user's head because of the vast amount of diffraction blur (i.e. approximately 9.7 arcmin) caused if we discard the use of an additional optical element. Therefore, the use of an optical element was implemented in order to image the phase conjugate material at or approximately near the virtual image plane.

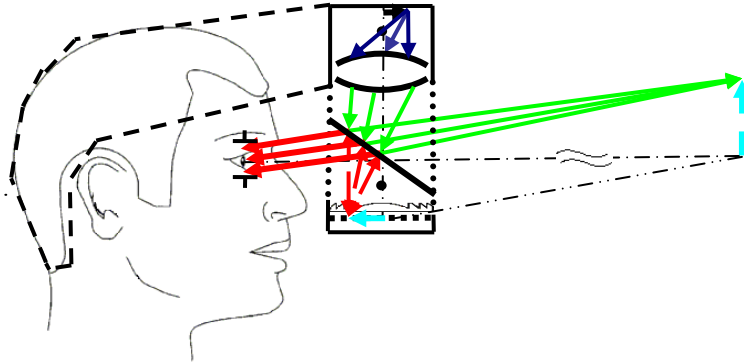


Figure 11: Design Layout

2.2.1 Optical lens design

The projection optics of the HMPD is composed of a binocular system, which consists of two identical optical lenses. The difference in the design of a projection lens for the HMD from other common projection optics is the requirement for lightweight and compactness. In the optical design of the HMD, we employed a combination of plastic, glass, and diffractive optics in order to reach lightweight and compactness. The miniature display selected was based on illumination requirements and was a 0.6" Organic Light Emitting Diode (OLED), manufactured by eMagin Corp., with 800x600 pixels and a 50- μm pixel size. Given the miniature display, wide field-of-view (FOV) and high resolution is always two contradictory but desirable requirements. [Fischer, R. E., 1994] Besides the consideration of resolution, there are two aspects of limitation on the targeted FOV. One aspect is that a flat beam splitter imposes a maximum FOV of 90°; the other aspect is the significant retro-reflectivity drop-off of commercially available phase conjugate materials beyond $\pm 35^\circ$ of incidence, which imposes an upper limit of 70° on FOV for a flat retro-

reflective screen. [Hua, H., et. al., 2000] Table 1 summarizes the overall design specifications of the 42° optics for the see-through head-mounted display.

Table 1 Specification of projection optics

Parameter	Specification
Object: Color OLED	
a. Size	0.6" inch in diagonal
b. Active display area	Rectangle, 9 mm x 12 mm
c. Resolution	800 x 600 pixels 1.3 arcmin
Lens:	
a. Type	Projection lens
b. Effective focal length	19.5 mm
c. Exit pupil diameter	12 mm
d. Overall length	25.7 mm
e. No. of diffractive surface	1
Other Parameters:	
a. Wavelength range	486-656nm
b. FOV	42.0° in diagonal
c. Distortion	<1.5% over entire FOV

The starting point of this design is a patented 4-element lens shown in Fig. 12. [Hua, H., et. al., 2002] The HMPD built with this optics is also shown in Fig. 13. In this design, in order to achieve lightweight, both the aspheric and the DOE lenses are made of plastic. The overall weight of the lens system is about 8 grams per eye. Fig. 15 shows the layout of the optical system that will be integrated in the new HMD. The purpose of employing a DOE is to correct the secondary spectrum and residual spherical aberrations for apochromatic imaging, in place of using high-index lanthanum crown glasses. [Hua, H., et. al., 2002] [Ogawa, H., 1999] [Caldwell, J. B., 1999] [Ha., Y., and Rolland, J. P., 2002]

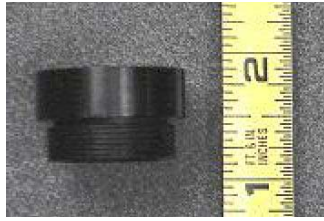


Figure 12: Lens assembly



Figure 13: Head-mounted projection display

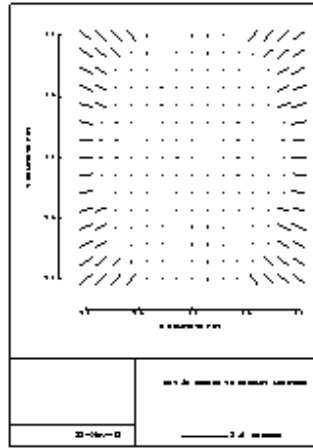


Figure 14: Astigmatism in arcmin

Fig. 16 shows the polychromatic diffraction modulation transfer function (MTF) for the full 12-mm pupil, which is presented across the five respective field angles. The target OLED display (see Table 1) has a spatial frequency of 24 lp/mm given a 50- μ m pixel size. We note that the modulation ratio of the design at 24 lp/mm is approximately 60% across the FOV. Therefore, we can scale the FOV without reducing the MTF below a design criterion of 20% at 24 lp/m, but we must consider that the performance is currently limited by the miniature display size. In the HMD optics, the main aberrations to control were astigmatism and field curvature, which means

a perfect point on the miniature display can either be displayed in visual space as a blurred spot or as an elongated line due to these aberrations. [Ha., Y., and Rolland, J. P., 2002] Therefore, to minimize any residual aberrations in visual space a field lens near the miniature display was placed to compensate and correct these effects. An analysis of the optical design shown in Fig. 17 illustrates the amount of astigmatism in visual space across the FOV in term of the visual measurement in arc minutes, and the direction of the lines show the direction along which a perfect point would be elongated in visual space. The result shows that across the FOV, the accommodation shift and astigmatism are less than 1.2 arc minutes. After designing the projection optical system, a future endeavor will be to fabricate and assemble the complete see-through HMD as shown in Fig. 11.

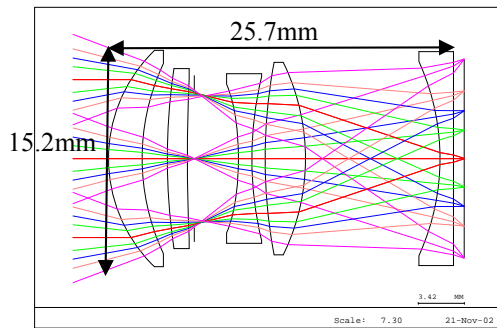


Figure 15: Projection optics

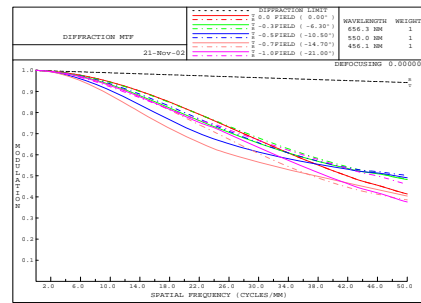


Figure 16: MTF curves

2.3 Experimental Results of Phase Conjugate Material

Placing the phase conjugate material internally in the HMD we investigated two commercially available types of retro-reflective material: micro-beads and micro-corner-cube arrays. The micro-bead arrays operate on specular reflection, whereas the micro-corner-cube arrays utilize total internal reflection (TIR). At the current status of commercially available retro-reflective

materials, manufacturers have yet to optimize the material for imaging conditions. Instead the material is currently specific for traffic control and other safety applications. For an ideal case of a perfect phase conjugation the incoming rays emitted by the micro display should be retro-reflected with respect to the incident light without any deviation. Furthermore, the retro-reflected rays are not returned individually, instead a cone of diffracted light is returned producing an amount of image degradation. The amount of light in the observation plane depends on the microstructure and the retro-reflective properties of the materials employed. [Hua, H., et. al., 2000] We can define the amount of light retro-reflected from the phase conjugate material to the user's eye by basing the analysis on the diffraction efficiency of the microstructure geometry. This approach yields accurate results, providing that first the microstructure is large compared to the wavelength, and the diffracted field is observed far from the phase conjugate material; based on these conditions we can treat the diffraction of light as a scalar phenomenon.

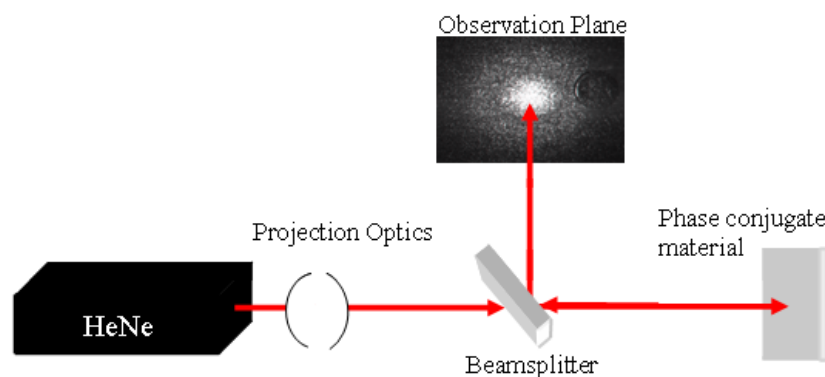


Figure 17: Experimental setup to investigate diffraction of the microstructure

A theoretical formulation is provided to verify some experimental data from the setup shown in Fig. 17. To characterize the imaging with retro-reflective materials, we consider the point-spread function (PSF) given by the modulus square of the complex amplitude in the image plane $|U(x_2, y_2, z)|^2$. We consider for simplicity an imaging scheme in the far field condition where $z \gg k/2(x_1^2 + y_1^2)$, and where we express the intensity $I(x_2, y_2, z)$ at the image plane, located away from the microstructure in the general case, caused by diffraction of the microstructure geometry $A(x_1, y_1, 0)$. [Goodman, J. W., 1968]

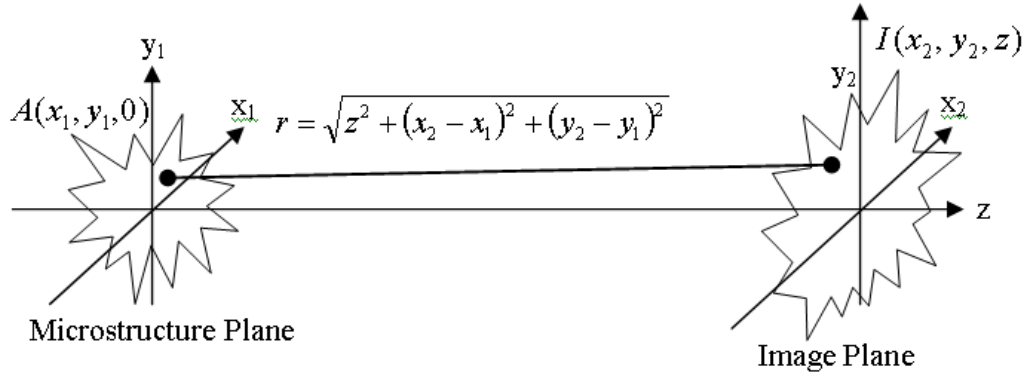


Figure 18: Coordinate system for computing diffraction

In the far field approach laid out in Fig. 18, $I(x_2, y_2, z)$ is given by

$$I(x_2, y_2, z) \propto |\mathfrak{F}\{A(x_1, y_1, 0)\}|^2, \quad (2.1)$$

where \mathfrak{F} denotes the Fourier transform. The normalized intensity distribution of a micro-bead structure, which has circular apertures, yields a Bessel function of the first kind in the observation plan or airy diffraction pattern. The corner-cube material on the other hand has the diffraction pattern of a pentagon, which we can assume for the analysis to be a deformed square aperture function resulting in an intensity distribution $\sin^2(\pi x_2)/(\pi x_2)^2$ in the one dimensional case. The theoretical intensity plot shown in Fig. 19 shows the micro-bead material producing

larger side lobes, which generates less intensity in the main lobe, compared to a localized and more confined intensity from the corner-cube material. The amount of intensity in the main lobe is related to the level of brightness acquired in the image plane. Therefore, for an improved image quality, the phase conjugate material with a corner cube microstructure integrated in the HMD will provide better results in an imaging condition.

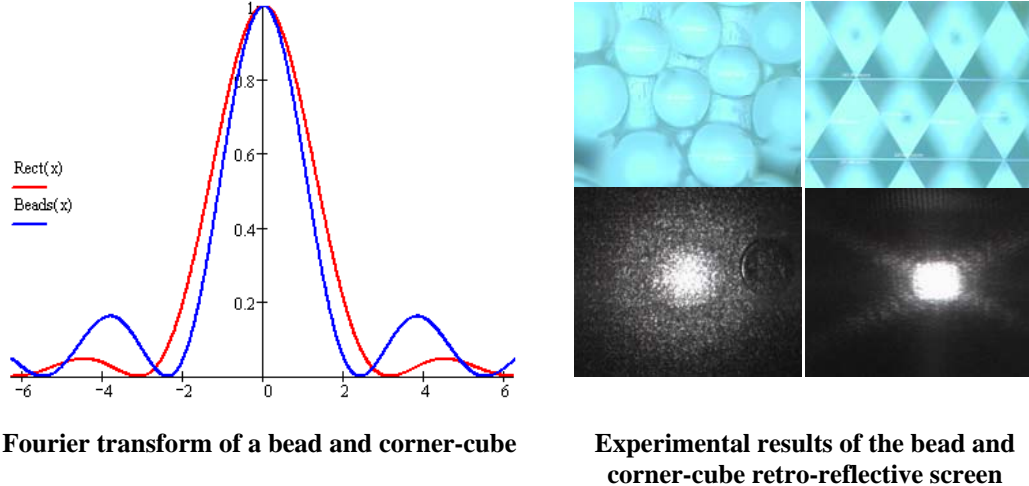


Figure 19: Intensity plot of both microstructures

CHAPTER THREE: EXPERIMENT TWO: PROJECTION BASED HEAD-MOUNTED DISPLAYS FOR WEARABLE COMPUTERS¹

The projection based head-mounted display (HMD) constitutes a new paradigm in the field of wearable computers. Expanding on our previous projection based HMD, we developed a wearable computer consisting of a pair of miniature projection lenses combined with a beam splitter and miniature displays. Such wearable computer utilizes a novel conceptual design encompassing the integration of phase conjugate material (PCM) packaged inside the HMD. Some of the applications benefiting from this innovative wearable HMD are for government agencies and consumers requiring mobility with a large field-of-view (FOV), and an ultra-light weight headset. The key contribution of this chapter is the compact design and mechanical assembly of the mobile HMD.

3.1 Introduction

Projection optics as opposed to eyepiece design has emerged as a new optical design for 3D visualization in HMDs. [[Fischer R. W., 1996](#)] [[Arrington, K. F., and Geri, G. A., 2000](#)] [[Hua, H., et. al., 2000](#)] [[Rolland, J. P., et. al., 2004](#)] The HMD is a key component for 3D visualization tasks such as surgical planning, medical training, and engineering design. [[Davis, L., et. al., 2002](#)] A recent innovation to the HMD field is the head-mounted projection display (HMPD), which may be thought of as a miniature projector mounted on the head with PCM strategically

¹ Martins, R., Shaoulov, V., Ha, Y., and Rolland, J. P., “Projection based head-mounted displays for wearable computers,” Proc. SPIE **5442**, 104–110, 2004.

placed in the environment. The HMPD is an emerging technology that lies on the boundary of conventional HMDs and projection displays such as the Cave Automatic Virtual Environment (CAVE) technology. [[Kijima, R., and Ojika, T., 1997](#)] [[Cruz-Neira, C., et. al., 1993](#)] [[Inami, M., et. al., 2000](#)] [[Ha, Y., and Rolland, J. P., 2004](#)] It yields 3D visualization capability with a large FOV (i.e. up to 70 degrees with a flat retroreflective screen based on current off-the-shelf PCM), lightweight optics with low distortion, and correct occlusion of virtual objects by real objects. [[Hau, H., et. al., 2001](#)]

The early HMPDs conceived in the Optical Diagnostics and Application Laboratory (ODALab) consisted of a pair of miniature projection lenses combined with a beam splitter and miniature displays, all mounted in a headset, as well as PCM placed strategically in the environment, as shown in Fig. 9. The PCM is placed in the environment allowing users to view computer-generated images embedded in the real environment. The stereoscopic images seen by the viewer are projected from the HMPD retro-reflected from the PCM to the respective viewers' eyes, allowing stereoscopic perception. The PCM is flexible and can be used to partially or completely surround the users or to inexpensively cover any surface or object of various shapes within the environment. Fig. 9 is an example of a dynamic volumetric augmented reality (AR) object of a human's femur perceived by the user wearing the HMPD. [[Hau, H., et. al., 2002](#)] The virtual femur retains the physical properties of the real object, but it can also dynamically take on any visual property including animation. The only hindrance of such HMPD system is the mobility outside of the PCM area because of the attachment of the external PCM placed in the real environment.

The outdoors HMPD that we proposed builds on the previous HMPD concept, however the novelty is the integration of the PCM within the HMPD. [[Martins, R., et. al., 2003](#)] This technology expands the boundaries of the conventional HMDs and projection-based displays because it opens the door from an indoor environment tethered to the PCM, to a mobile system with potential outdoors application such as Military Operations on Urbanized Terrain (MOUT). [[Julier, S., et. al., 2000](#)] The proposed wearable HMPD configuration allows for 3D visualization capability with a large field of view (FOV), lightweight optics and low distortion. The outdoor HMPD design comprises of lightweight projection optics and integrated PCM in the headset that eliminates the requisite use of an external PCM. A key component of the design is not only the integration of the PCM but also the use of a lens in combination with this novel projection enclosed system clearly facilitating the operability of the technology. [[Martins, R., and Rolland, J. P., 2003](#)]

In this chapter, a review of the conceptual design for the outdoor HMPD is presented in Section 2. In Section 3, we demonstrate a 42-degree projection optics module. Finally, in Section 4 we present an analysis of imaging by utilizing commercially available phase conjugate material with an experimental validation and conclusion for improving the image quality.

3.2 Review of the Optical Layout for the Wearable HMPD

Fig. 20 provides the conceptual design of an outdoor HMPD, which was achieved in the ODALab and was finalized in collaboration with the United States Army STRICOM, Synthetic Natural Environment (SNE) project. [[Martins, R., and Rolland, J. P., 2003](#)]

The fundamental principle of the outdoor HMPD is enabled by projection optics that projects a real image on the PCM where the rays are then retroreflected from the PCM back to the user's eye. Due to the nature of the PCM, rays hitting the surface are reflected back on themselves in the opposite direction. Therefore, a user can perceive the virtual projected image at the exit pupil of the optics. [Rolland, J. P., et. al., 2001] If the projected image and PCM are conjugate to each other, the user can clearly view the virtual image. Previously we demonstrated that not placing the PCM at the same location as the projected real image would lead to a degraded and blurred image, rendering the virtual images useless. A solution to rendering of clear virtual images was to place a lens between the projection optics and the PCM, in order to conjugate the PCM and the projected real images. By conjugating the PCM and the projected real images in a compact solution, we enabled a wearable outdoor HMPD. However, other issues arose, which led to a degraded virtual image quality. We will further address these issues in Section 4.

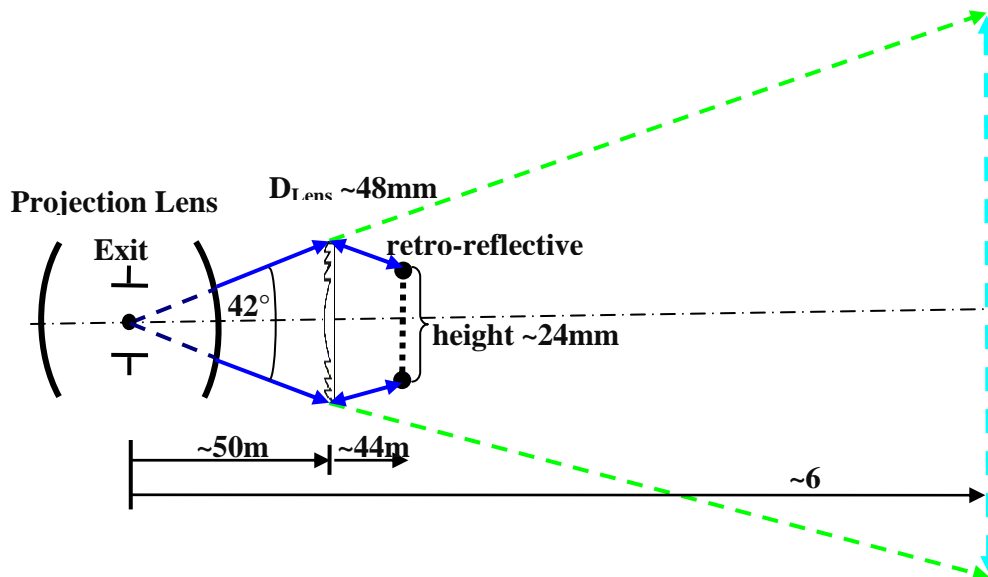


Figure 20: First Order Layout of HMPD Conceptual Design

3.3 Optical Lens Design

The HMPD conceptual design shown in Fig. 21 is an example of how the integration of the miniature and lightweight projection optics and the PCM can be placed on the head as a wearable headset.

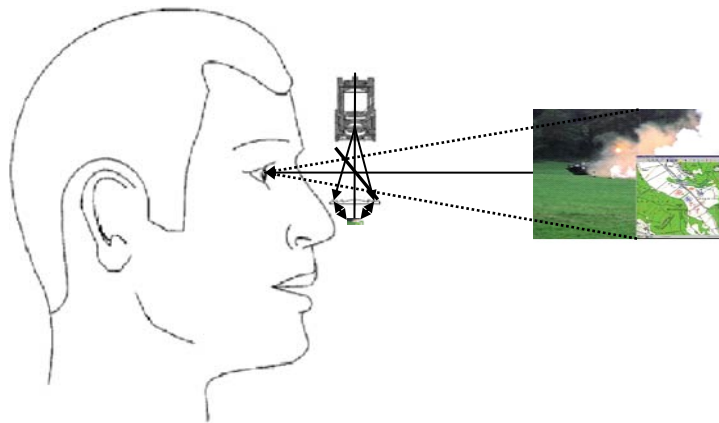


Figure 21: Wearable HMPD Concept. While a grayscale picture can only be shown here for publication, the display allows full color.

The lens module of the projection optics intergraded together with the miniature display is demonstrated in Fig. 21. The miniature display selected was based on illumination requirements. An off-the-shelf 0.6in diagonal Organic Light Emitting Display (OLED) with resolution of 800x600 pixels and 15 μ m pixel size manufactured by eMagin Corp. was integrated into the lens module. Other off-the-shelf miniature displays use external light sources adding to overall length and weight. The self-emitting property of the OLED allows for an ultra lightweight and compact solution for a wearable HMPD. The optical design is composed of a main module consisting of four lenses and a field lens close to the miniature display. The projection lens for the wearable HMPD was designed with a combination of a diffractive optical

element (DOE), plastic components, and aspheric surfaces ensuring both compactness and high image quality, while achieving a 42-degree FOV. The wearable HMPD was designed for a 15mm eye relief and might be further modified before the final prototype is built. The eye relief, accounting for the tilt of the beam splitter and the lens module, is less than 26mm, therefore the prototype will not accommodate eyeglasses. The state-of-the-art compact lens was manufactured within 1 in length and lightweight optics of 8 grams per eye.



Figure 22: Monocular Lens-Mount Assembly.

3.4 Experimental Results of PCM

We investigated two different types of commercially available PCMs, micro-optical beads and microcorner-cube arrays geometries, approximately $100\ \mu\text{m}$ in size, as shown in Fig. 23 (a) and (b). The characteristics of the non-uniform micro-bead array are described by combination of Snells law and specular reflection, while the micro-corner-cube array utilize total internal reflection, both providing the required retroreflective property.

Currently the commercially available PCMs are not optimized for imaging, rather for applications such as traffic control and other safety purposes. For the ideal case of a perfect retroreflector, the incoming rays emitted by the miniature display should be reflected back parallel and in the opposite direction to the incident light without any deviation. The

commercially available PCMs partially reflect rays that are not parallel to the incident light, instead they deviate within ± 15 -degree cone. This deviation produces a cone of light reflected from the PCM, which provides more illumination for devices such as “stop signs” and “firefighter’s vests”, for example. Therefore, image degradation in the virtual image is produced since the rays are reflected back in a cone instead of parallel to the incident light.

Due to the imperfections of the micro-optical beads, shown in Fig. 23(a), such as the randomness of the radiuses and the separation between two consecutive beads, the retroreflected rays deviate from being reflected parallel to the incident light. The micro-optical beads over the micro-corner-cube yielded a greater loss of light efficiency, which is needed when overcoming indoor ambient light or outdoor illumination.

The next PCM tested was the micro-corner-cube array geometry based on an array of pyramids, shown in Fig. 23 (b), which benefits from a uniform spacing, but the faces of the pyramid are not planar and 90- degrees with each two planes of the pyramid. In addition, if the surface of the pyramid is slightly curved, the incident rays will encounter a curved mirror altering the desired optical path for an ideal retroreflection. Therefore, not all of the rays will reflect parallel to the incoming rays, rather they will deviate thus producing image degradation. Finally, to yield an ideal imaging conditions for any PCM we need to satisfy the strenuous uniformity and surface criteria to control the incoming rays to achieve perfect retro-reflection.

To produce the desired retro-reflection we need either an optimized corner cube array shown in Fig. 23 (c) or a custom-built microlenslet array, as shown in Fig. 23 (d), which will have uniform radii of curvature and separation of the lenses as well as a consistent performance of the microlenses across the array. The manufacturing of such PCM provides some fabrication

challenges that will need to be further investigated. Thus, in our further implementation the micro-corner-cube PCM was selected based on the increased light efficiency over the micro-optical beads.

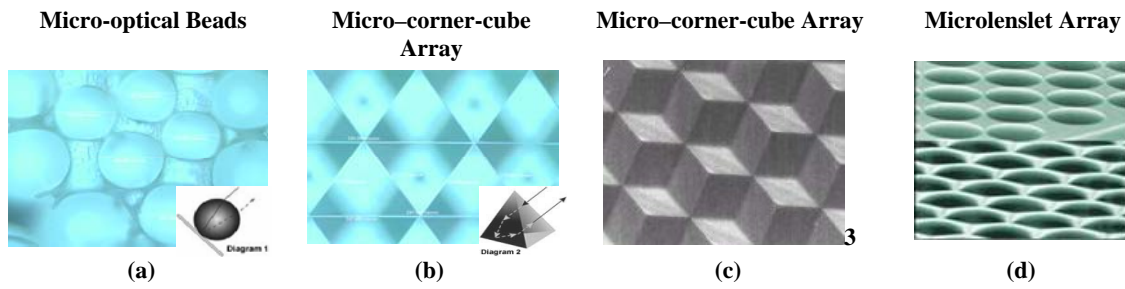


Figure 23: Different Types of Microstructures

With the micro-corner-cube array a bench test was assembled to validate the conceptual design of the wearable HMPD and to qualitatively investigate the image degradation produced by the PCM. Fig. 24 demonstrates the bench setup for the wearable HMPD with the manufactured projection optics on the left. The projection optics will re-image the computer-generated test image shown in Fig. 25, on the PCM. Although we use a grayscale test image, the OLED has the capability of projecting color images. The test image was projected on the micro-corner-cube array and then captured on a CCD camera at the exit pupil location, which simulates a user's eye. Two scenarios were under consideration to qualitatively investigate the image quality: Scenario 1 was with the room lights off and Scenario 2 was with the room lights on (i.e. 15 lux).

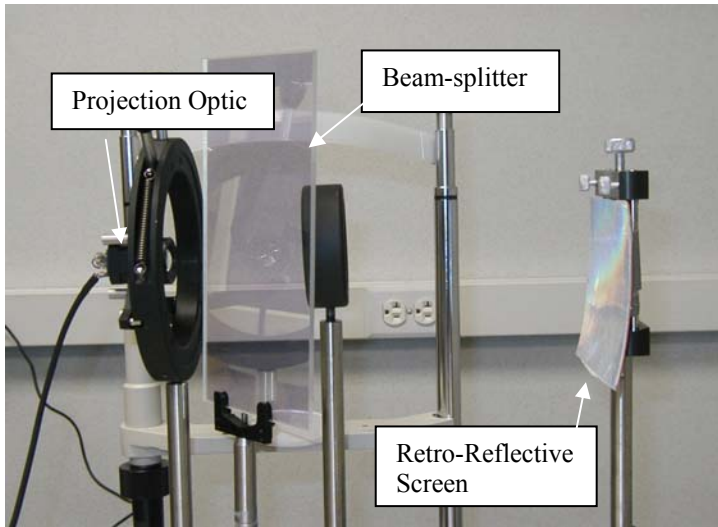


Figure 24: HMPD Bench Setup



Figure 25: Computer-Generated Test Image

We started our investigation with scenario 1 for the wearable HMPD and captured the 42-degree FOV image at 1500mm as shown in Fig. 26. Next, we investigated scenario 2 and captured the projected virtual image and the environment to provide a full see-through wearable HMPD, as shown in Fig. 26. The difference between the scenarios are in Fig. 26 the camera was focused on the same image plane, while in scenario 2 the camera was focused on the background of the laboratory.



Figure 26: Capture Test Image with Lights Off (Scenario 1)



Figure 27: Capture Test Image with Lights On 15 lux (Scenario 2)

Fig. 26 and 27 qualitatively demonstrate the difference in the image quality between scenario 1 and scenario 2. Comparing both the computer-generated test image shown in Fig. 21 and the results of scenario 1 and 2 shown in Fig. 26 and 27 demonstrate that scenario 1 yields a better representation of the test image than scenario 2. In scenario 2 the ambient light from the room was less than the microdisplay illumination, therefore, the image was visible but the contrast of the virtual images was decreased. In addition, the PCM was not optimized to perfectly retro-reflect all of the light back to the user's eye or in our case the CCD camera, leading to a further decrease in the contrast ratio.

CHAPTER FOUR: EXPERIMENT THREE: A MOBILE HEAD-WORN PROJECTION DISPLAY¹

A recent advancement was achieved in the integration and miniaturization of a binocular head-mounted projection display (HMPD) conceived for fully mobile users. The devised display, referred to as Mobile HMPD (M-HMPD), offers see-through capability through custom-designed, light-weight projection optics and an integrated commercial-off-the-shelf (COTS) retro-reflective screen to display full color stereoscopic rendered images augmenting the real world. Moreover, the light-weight optical device (i.e., approximately 8g per eye) has the ability to project clear images at three different locations within near- or far-field observation depths without loss of image quality. In this chapter, we first demonstrate the miniaturization of the optics, the optical performance, and the integration of these components with the retro-reflective screen to produce an M-HMPD prototype. We then show results that demonstrate the feasibility of superimposing computer-generated images on a real outdoor scene with the M-HMPD.

4.1 Introduction

The preferred features of the existing head-mounted display systems (HMD) are cost effectiveness, portable and light-weight packaging with an ergonomic form factor, and providing at least a 20 degree field-of-view (FOV). A recent review of HMDs was reported in [[Cakmakci O., & Rolland J., 2006](#)]. Among HMDs, the head-mounted projection display (HMPD) design has attracted much interest because of its wide FOV (i.e., greater than 40 degrees) distortion-free

¹ Martins, R., Shaoulov, V., Ha, Y., and Rolland, J. P, "A mobile head-worn projection display," Opt. Express **15**, 14530-14538, 2007.

images. Additionally, customized HMPD designs can be achieved providing ergonomic form factor integrated with high quality, miniature-projection optics. Fischer, the initial developer of the HMPD systems, employed a combination of projection optics and a retro-reflective screen placed in the environment, to develop a projection-based HMD assisted by a crane. [[Fischer, R. E., 1994](#)] The first prototype was developed with commercial, off-the-shelf (COTS) large aperture projection optics and furthermore, a COTS retro-reflective screen was used. The major benefit of using a retro-reflective screen instead of various other projection screens is that the small scattering angle of the screen maximizes the brightness of the projected image. Since 1998, Rolland and her team have designed a few generations of HMPDs utilizing custom designed projection optics integrating a combination of glass and plastic components, thus reducing the overall weight of the system (i.e., to approximately 6 grams per eye). Furthermore, Rolland and her team employed aspheric surfaces and diffractive optical elements (DOEs) to improve the overall image quality. [[Rolland, J. P. et. al., 2005](#)]

Until recently, the limiting factor of the HMPD technology was the requirement of placing a retro-reflective screen in the environment, thus restricting its use only to indoor areas. Although such approach is sufficient for certain tasks, the exclusion of all applications that cannot be performed in limited indoor areas is not practical. Thus, the need to use the HMPD systems outdoors was the driving force behind the research reported in this chapter. Our work was focused on conceiving and developing an assembled HMPD with a retro-reflective screen integrated within the system itself, as opposed to tethering the retro-reflective screen to the environment, thus providing full mobility. Furthermore, such HMPD system will be referred to as a mobile HMPD (M-HMPD.) Although such integration presents several challenges, which

will be addressed later in this chapter, the positive results obtained with the conceived system provide the impetus for the continuation of our research to move the M-HMPD technology described here to a full-scale commercial solution.

In this chapter, we will first review the principle of a binocular M-HMPD integrating projection optics, an imaging lens, and a retro-reflective screen, and shows the newly developed assembly of the first M-HMPD prototype. Next, we will attempt to demonstrate the feasibility of replacing the eyepiece-based HMDs with large FOVs (>20 degrees), extensively used since the 1960s for various indoor and outdoor applications, with projection based M-HMPD. Furthermore, we shall establish the requirements for a custom-designed, retro-reflective screen for imaging applications and we shall demonstrate a typical augmented reality (AR) image captured outdoors using the M-HMPD described in this chapter. Finally, we conclude with an overall assessment of the M-HMPD technology and a discussion of follow-up research that is planned by our group to further advance this emerging technology.

Previously, in a feasibility analysis, we demonstrated a monocular bench setup consisting of a retro-reflective screen and an imaging lens (L_1) along an alternate optical path (Path 2) provided by a beam splitter, as shown in Fig. 9 (a). [[Martins, R. et. al., 2004](#)] The bench setup was assembled with a 100 mm diameter lens L_1 along with an approximate 100-mm by 100-mm section of a COTS retro-reflective screen. The reported results were promising for the integration of a retro-reflective screen within an HMPD. Therefore, the research progressed into the miniaturization of the bench prototype and furthermore into an actual head-mounted design, which is first demonstrated in this chapter, and is shown in Fig. 9 (b-c). The driving criterion for the M-HMPD prototype design was compactness while using a COTS lens and retro-reflective

screen. In addition to the demonstration of the M-HMPD concept in an actual HMPD system, a new design to mount the display is presented that incorporates a flexible hat for mounting optical components and distributing the weight uniformly on the user's head. This ensures sufficient comfort, thus the headset can be worn for extended periods of time. [Oranchak, A., and Rolland, J., 2006]

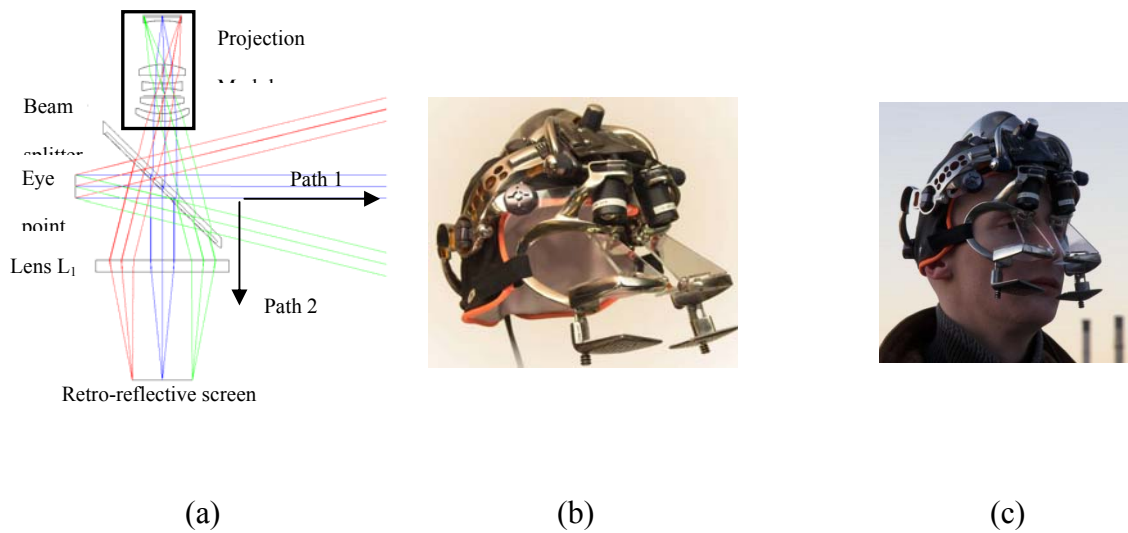


Figure 28: (a) First order layout for one eye of the see-through M-HMPD with retro-reflective screen placed along Path 2. (b) Assembly of a binocular see-through M-HMPD with a robust titanium mounting structures and the integrated retro-reflective screen. (c) User wearing the binocular M-HMPD.

4.2 M-HMPD System

The M-HMPD, similar to the HMPD, utilizes a micro-display, which is custom designed for system specifications such as FOV and visual performance, located at, or beyond, the focal point of the projection optics, as shown in Fig. 28 (a). The essence of the M-HMPD innovation is in relaying the physical retro-reflective screen from the environment to the headset, thus integrating it within the headset at the conjugate image plane location of the projection optics. This is

achieved by imaging the retro-reflective screen in the M-HMPD using an imaging lens L_1 . Without such imaging lens, the integration would lead to a non-resolvable virtual image, since the retro-reflective screen would not lie in the image plane. Quantitatively, in the configuration without L_1 , the amount of blurring produced would result in an unfocused image with a resolution of ≥ 400 arcmin, rendering the image undistinguishable. An imaging lens L_1 is thus placed between the projection optics and the retro-reflective screen, allowing the physical screen to be optically imaged in front of the user. The imaging distance can be varied by adjusting the imaging conjugates of the projection optics and the location of the retro-reflective screen with respect to the focal point of L_1 . For example, if it is desirable to work with a collimated image, the projection optics is optimized to form an image at optical infinity, and the image of the retro-reflective screen will be set to infinity by placing it at the focal point of L_1 . However, in many instances, the optical image will reside at a finite distance from the user, and thus the physical screen will be placed within the focal point of L_1 .

In its current design that uses a COTS lens L_1 , the entire optical system has an overall length of approximately 120 mm measured from the micro-display to the retro-reflective screen. In practice, one could design the lens L_1 to be telecentric, although we would sacrifice our design criterion for the most compact solution provided our COTS Fresnel lens. In this configuration, a 15-mm eye relief was selected in order to maximize the compactness of the system. An eye relief of 25 mm has been recommended with a 95th percentile human head circumference, with a minimum of 15 mm needed for eyeglasses to be comfortably worn with the HMPD without the beam splitter intruding on the face (MIL-STD-1472D). Although the 15-mm eye relief does not

provide adequate distance for all users with eyeglasses, we can custom fit for near- and far-sightedness by refocusing the projection optics.

Theoretically, the most compact overall length is achieved with the shortest focal length possible for L_1 , but the latter is limited by the diameter or equivalent F-number of L_1 . Because of the retro-reflective screen properties (i.e. the light falling on the retro-reflective screen is reflected back on itself), in principle, the imaging lens L_1 only needs to satisfy first-order imaging properties, given that the optical aberrations induced by L_1 will cancel upon double pass (i.e. the optical path difference, or the OPD, will be zero if all the light is perfectly retro-reflected back on itself.) Thus, a compact Fresnel lens can serve as the imaging optics in place of L_1 . However, as the F-number decreases, the grooves of the Fresnel lens get deeper, affecting the light transmission properties of the Fresnel lens. Therefore, in practice, an F-number of 0.7 may be considered to minimize transmission losses, which is close to the limits of state-of-the-art fabrication techniques.

4.2.1 Microdisplay Device

The development of the M-HMPD prototype reported in this chapter is based on a COTS organic, light-emitting micro-display (OLED), with a 0.6-inch diagonal, composed of 800 by 600 pixels, as the imaging source for the projection optics. The major benefit of selecting the OLED micro-display compared to other COTS micro-displays is that its composition (as a series of thin-film, organic substrates sandwiched between two conductors producing a self-emitting display source on a chip) reduces the bulkiness of the electronic components as well as removing the requirement for an external light source. [[Oranchak, A., and Rolland, J., 2006](#)] Such a micro-

display highly facilitates the design of a compact and light-weight optical assembly, and minimizes the complexity of the opto-mechanical assembly as well. Our requirement for the most compact display narrowed our choice to an OLED SVGA micro-display for the design. The tradeoff in OLEDs is reduced brightness compared to custom designed LED-based illumination schemes that are commonly used in LCOS, LCD, and DLP micro-displays. [[Bogaert, L. et. al., 2007](#)] Because one of the HMD main research goals is establishing the most compact solutions, the geometry of the M-HMPD presented in this chapter will provide a path to viable compact commercial solutions as OLED micro-displays, or equivalent self-emitting technologies emerge. As a result, approaches using external illumination that are highly relevant for today's product development may become less relevant for the long-term advancement of HMD technology. [[Rapaport, A. et. al., 2006](#)]

4.2.2 Projection Optics

The FOV specified for the projection optics was driven by the visual requirement for angular resolution of the display, estimated as the ratio of the FOV to the total number of pixels. Therefore, the projection optics was designed with a 42 degree diagonal FOV, yielding a 2.4 arcmin resolution, set by the angle subtended by one pixel of the micro- display. With a given display height and FOV, the effective focal length of the projection optics was 19.85 mm. The chosen FOV combined with the binocular requirements imposed by the user's face limited the diameter of L_1 to 30.5 mm. In addition, the projection module was tilted by approximately 10 degrees as shown in Fig. 28 (b) to eliminate the possibility of contact between L_1 and the user's face. This tilt angle further imposed a required compensating tilt of the beam splitter, also shown

in Fig. 28 (b), for the user to perceive correctly aligned images. Finally, the compactness of the system was limited by the distance from L_1 to the 29-by-22 mm retro-reflective screen. This distance was determined by the focal length of L_1 with respect to the F-number. In order to reduce the cost of implementing the prototype of the current system design, a COTS F/1 imaging lens was selected, yielding a focal length of 30.5 mm and a profile consisting of 5 grooves/mm.

Various applications may require different operating distances, but state-of-the-art HMDs offer only one optical image plane located at some fixed distance from the user. Our projection optics was optimized across multiple image locations, i.e., three in the case of the current system (1.5 m, 3.5 m and infinity), so various operating distances set manually for different applications might be used at equivalent resolutions measured in human perception studies. [Fidopiastis, C., 2006] For example, if the tasks to be performed are solely in the far field, it is optimal to set the distance of the optical image for each eye to be located beyond 6 m (i.e., at optical infinity), and the optics is optimized under such imaging conditions. On the other hand, if the desired application only involves the manipulation of objects in the near field, the optics should be designed to form a sharp optical image at about 1m to 1.5 m. Therefore, the same optics can be used for various applications by refocusing, which we accomplish by using the system with a slight rotation of the optics barrel, as shown in Fig. 29.



Figure 29: Monocular Lens-Mount Assembly

In addition, the M-HMPD was designed for a 12 mm exit pupil, which comfortably allows for natural eye movements within the 42 degrees FOV without vignetting. It is important to note that the pupil of the optical system is located within the optics in HMPD, which together with the integration of the beam splitter oriented at 90 degrees, yields the projection optics pupil to be the optical conjugate of the eye's pupil. Also, because the pupil is internal to the projection optics, the M-HMPD can be more easily corrected for optical distortion. In contrast, conventional eyepiece-based HMDs provide an external pupil making it not only challenging to control distortion but also to minimize the weight of the eyepiece optics, given that the size and the weight of the optics increases respectively linearly and cubically with FOV. This allows for more compact optics with large FOVs, while minimizing some optical aberrations as discussed below. In the current projection system, we characterized the optical performance by evaluating the polychromatic modulation transfer function (MTF) curves (i.e., vertical axis of each plot) for the full 12 mm pupil. The MTF shows the degradation of the contrast across increased spatial frequency (i.e., horizontal axis of each plot) of the image for three optical images distances (1.5 m, 3.5 m, and infinity). The maximum spatial frequency at which we evaluated the MTFs was set by the 15 μm pixel size of the miniature display. The spatial frequency of the MTF was based on the Nyquist frequency set by the pixel diagonal size, which is approximately 24 cycles/mm. The lens was designed to support a minimum criterion of 20% modulation across all FOVs for a 3 mm effective pupil at 24 cycles/mm. If this performance metric is satisfied across the full pupil, it will be satisfied for the 3 mm effective pupil as well as for all of its decentered values. The MTF curves across the full 12 mm pupil are shown in Fig. 30. Results show that the design

exceeds the design specifications required to produce a well-balanced image quality across the entire FOV. The fact that the MTFs across the three different image depths are quite similar in value indicates that our projection optics have been corrected effectively for all three image distances.

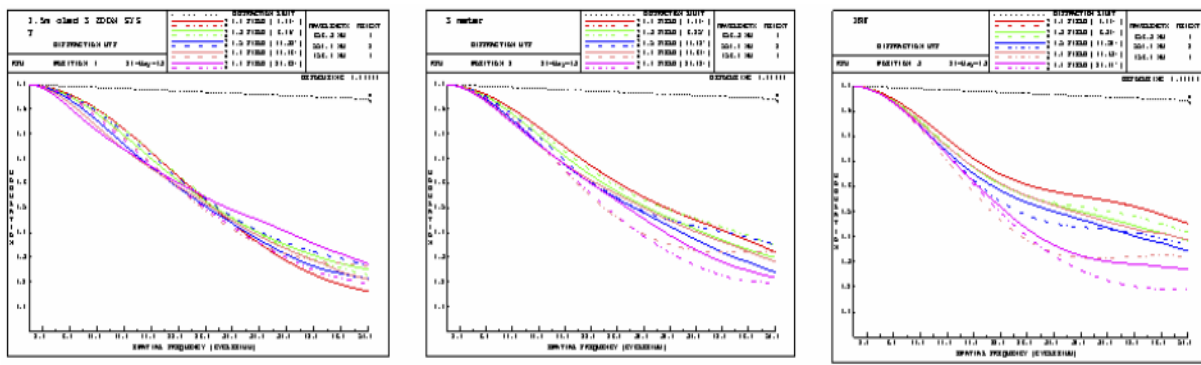


Figure 30: The MTF plots for a projected scene located at (a) 1.5 m, (b) 3.5 m, and (c) infinity across the full 12 mm of the projection optics.

Another key benefit to a projection-based HMD versus an eyepiece HMD is the low percent distortion across the image. In the current projection system, we were able to limit distortion to a maximum of 1% across all of the three image distances, as shown in Fig. 31. By utilizing a projection system, the inherent properties of a symmetrical lens system around the aperture stop substantially reduces distortion, coma, and lateral chromatic aberrations. In contrast, if an eyepiece system has an external stop, symmetry is not possible. An eyepiece system is commonly accepted as well corrected for distortion if distortion is limited to 3-5%, although distortions in the range of 8-12% are common with a FOV of 60 degrees.

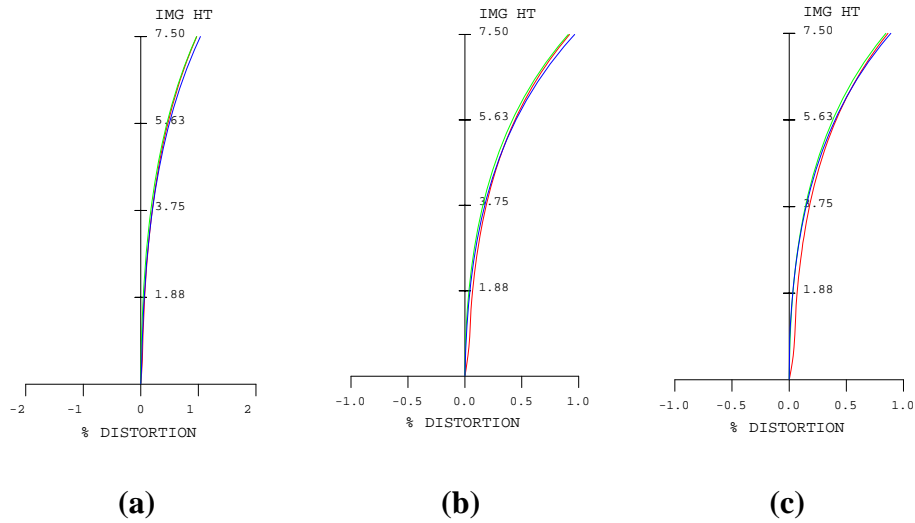


Figure 31: Distortion plots for a projected scene located at (a) 1.5 m, (b) 3.5 m, and (c) infinity across the full 12 mm of the projection optics.

4.2.3 Retro-reflective screen

The M-HMPD system is currently hindered by the COTS retro-reflective screen. Various COTS retro-reflective screens were investigated and found to be fabricated with corner-cube microstructures of approximately 150 micrometers. By integrating such retro-reflective screens with imaging optics, the microstructures are magnified by L_1 and become visible on the image plane, which reduces the perceived computer-generated image resolution. In addition, the large corner-cube microstructures yield an additional degradation in image sharpness caused by the retro-reflected rays departing a maximum of 150 μm from their incident location on the Fresnel lens, causing non-canceling optical aberrations for the Fresnel lens. To eliminate the loss of resolution caused by the retro-reflective screen, we have established design requirements for a custom-designed, retro-reflective screen that would result in a miniaturization of the

microstructures to less than the human visual acuity to optimize visual performance. Throughout our further discussion, we will consider only corner-cube-based retro-reflective screens.

There are two key aspects of imaging with an integrated retro-reflective screen for imaging purposes. The first is the construction of the corner-cube microstructure in terms of retro-reflected angle, and the second is the magnification produced by L_1 . Provided that the retro-reflective screen is manufactured with the three perfectly orthogonal surfaces, the rectilinear propagation from a point entering the surface lens L_1 will also exit at approximately the same position after retro-reflection. By satisfying this condition, the incident and retro-reflected angles will be equal for a corner-cube design with orthogonal surfaces. We can also conclude that the properties of the retro-reflective screen are of greater importance than those of L_1 , since the light entering the lens exits the lens at approximately the same location after being retro-reflected. Thus L_1 , regardless of its physical properties except those affecting its transmission, will yield a zero optical path difference between the incident and transmitted light, canceling the optical aberrations. The second requirement of the retro-reflective screen is the required aperture size and depth of the trihedral corner-cube after the magnification produced by the lens L_1 . It should be noted that if we implement a shorter focal length, the magnification of the microstructures will increase and the pixel width of the image at the screen will decrease, making it even more difficult to fabricate a miniaturized microstructure. If we consider the first order layout, as shown in Fig. 32, the height of the virtual image $h_{projection}$, given by the projection optics module, is perceived at a distance $z_{projection}$ and will subtend a FOV with a half angle $\theta_{half-FOV}$, as given by

$$h_{projection} = z_{projection} \tan(\theta_{half-FOV}). \quad (4.1)$$

Therefore, the image seen through L_1 located at a distance z_{image} will yield a slightly magnified image with respect to the OLED size h_{OLED} and distance z_{OLED} given by:

$$Magnification = \left(\frac{h_{image}}{h_{OLED}} \right) = \left(\frac{z_{image}}{z_{OLED}} \right). \quad (4.2)$$

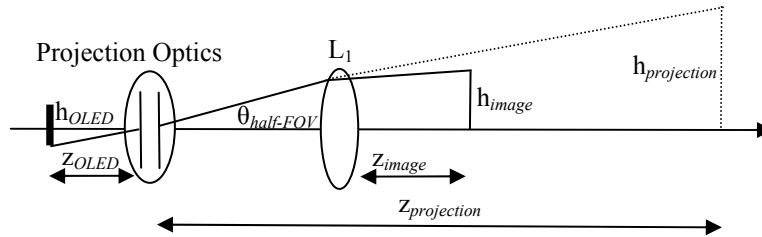


Figure 32: Monocular Lens-Mount Assembly.

When an image is formed on the retro-reflective screen with the appropriate magnification defined by Eq. (2), we can separate the image into individual pixels and compare the pixel area versus the trihedral aperture area. In the condition where a single pixel area is smaller than the area of a single trihedral aperture, multiple pixels, each with their own corresponding color, will be inverted with respect to their neighboring pixels. This occurrence is caused by the corner-cube construction, which will invert the incoming pixel information. Consequently, a local inversion will occur within a finite area reducing the resolution. In our case, the COTS screen has a ratio of pixel area to trihedral aperture area of approximately 25/1. Therefore, we expect that the image will clearly show artifacts, such as an array of magnified corner-cube structures, as well as an AR image with a loss in resolution compared with the initial 800 x 600 OLED resolution. In contrast, with the area of a single pixel being greater than the aperture area of the trihedral corner-cube, the local inversion will only occur on each emitted pixel color. Inverting the color of any individual pixels will not directly affect the overall AR

image. Therefore, it is desirable that the custom-designed, retro-reflective screen have a smaller trihedral aperture area than pixel area.

4.3 Display Results

To show the feasibility of the integration process into an HMPD form, we assembled the M-HMPD and qualitatively assessed its visual performance outdoors late in the afternoon on a cloudy day. One additional step was taken to enable the M-HMPD to function outdoors; a laptop computer was used to render the visual scene along with two polarizers located in front of the beamsplitter, which attenuated the ambient light to adjust the relative illumination of the AR image with respect to the outdoor illumination. An alternative to the polarizers will be to employ emerging electrochromatic technology to adaptively control the outdoor light that goes through the beam splitter. Our experience indicates that a challenge associated with this emerging technology will be the deposition of electrochromatic material on a curve substrate. The test image shown in Fig. 33 (a) was captured by placing a digital camera at the exit pupil location of the M-HMPD, and the result is shown in Fig. 33 (b). As expected, the image clearly resolves the magnified corner-cube microstructures from the COTS retro-reflective screen, while reducing the overall SVGA resolution. Moreover, a loss in resolution occurred because the large microstructures ultimately reduced the test image from 530 by 404 pixels to 106 by 80 pixels. This loss in resolution is precisely consistent with the 25/1 ratio of the corner cube size to OLED pixel size discussed in Section 2.3. Current research is in progress to fabricate an array of miniature trihedral microstructures with orthogonal surfaces of depths of 8-10 μm . [[Hockel, H., et al., 2005](#)] Thus, it is our hypothesis that the loss of resolution can be overcome by developing a custom retro-reflective screen with trihedral microstructures having a depth d and a length of

the aperture a to be less than or equal to half a pixel width (i.e., $d = 6^{-0.5} \cdot a$). [[Hockel, H., et al., 2005](#)] For our application, we require a trihedral length of approximately 11 μm with a corner-cube depth of 4.5 μm . This will ensure that the custom-designed screen maintains the fidelity of the AR image.



(a)



(b)

Figure 33: Image (a) represents the test image to be superimposed in the outdoor scene (b) is the augmented reality image captured outdoors by a digital camera at the optics exit pupil location. While currently at reduced resolution given the need for new microstructure films, the parrots were successfully superimposed on outdoor trees seen as a detailed texture in the background.

CHAPTER FIVE: EXPERIMENT FOUR: THE MACROSCOPIC AND MICROSCOPIC PROPERTIES OF HIGH GAIN SCREENS¹

Abstract

Retro-reflective screens (i.e. high gain screens) have been implemented in numerous applications ranging from illumination enhancements on traffic signs to imaging devices such as mobile head-worn projection displays (M-HWPD), for example. In these applications, the light hitting the surface of a high gain screen is retro-reflected towards an observer to increase the brightness in a light deprived environment. The amount of light retro-reflected towards an observer can be decomposed into its perspective macroscopic and microscopic properties and is the key contribution of this chapter. The macroscopic property represents the illumination characteristics due to the microstructures solid angle, whereas the microscopic properties describe the obtainable resolution performance provided by the miniature microstructures physical dimensions. In an imaging application utilizing the M-HWPD a balance of both properties must be achieved to maintain optimal imaging capabilities. We begin the chapter with an introduction into high gain screens and their benefits in illumination and imaging applications. More specifically, we will discuss the screen's role and importance on the M-HWPD. Then we will use radiometric equations to define the macroscopic properties of the screen. We will conclude with an in-depth analysis using Breault Research's (BRO) illumination software ASAP to qualitatively describe the microscopic properties. The intent of this analysis will be to establish

¹ Martins, R., Shaoulov, V., and Clarke, T., "The Macroscopic and Microscopic Properties of High Gain Screens," Opt. Express, in progress.

fabrication requirements for a high gain screen to render video realistic images through the M-HWPD.

5.1 Introduction

High gain screen are utilized in applications such as, movie cinema, traffic signs, and safety apparel and some fundamental work has been completed to understand their properties although a complete framework of its respective macroscopic and microscopic properties are yet to be expressed in a comprehensive manner. The goal of this chapter will be to represent the macroscopic properties in terms of its illumination characteristics then we will further explain the high gain screens microscopic properties which relates to the diffraction effects due to the physical microstructures of the screen. These microstructures take the form as an array of either spherical beads (i.e. also referred to as cat's eye reflectors), or corner-cubes (i.e. also referred to as prismatic reflectors) and their main purpose is to enhance the visibility in a dark environment. [[Liepmann, T. W., 1994](#)] [[Zurasky, J. L., 1976](#)] [[O'Brien, D. C., and Edwards, D., J., 1999](#)] [[Sewards, G. H., and Cort, P. S., 1999](#)] Both the spherical beads and corner-cubes can be modeled as optical components in which the incident rays are approximately equal to the reflected ray angles. The main differences between reflectors are the spherical bead brings the incident light to a focus which then is reflected by a metallic mirror surface, whereas a corner-cube arrangement has three orthogonal highly reflective metallic mirror surfaces to reflect the incident light. [[Yuan, J., et. al., 2002](#)] The mutually orthogonal surfaces ensure that the incoming light entering the corner-cube will be reflected back parallel to the incident angle. Both of these two common microstructures have been extensively researched for its retroreflectance in

illumination applications, [[Yuan, J., et. al., 2002](#)] [[Zhu, X., et. al., 2000](#)] [[Hua, H., et. al., 2000](#)] but has yet to be fully investigated for its imaging capability as a high gain screen in applications that incorporate optical systems with limited space to illuminate the image source. Such applications that will benefit from this research are the head-mounted projection displays (HMPD), mobile head-worn projection displays (M-HWPD), and commercial home theater systems, for example. In both the HMPD and M-HWPD a high gain screen is incorporated with a projection optical system to reduce the reflected cone angle, therefore improving the illumination of an already deprived illumination source. [[Martins, R., et. al., 2007](#)] Moreover, commercial home theater systems integrate a high power lamp as their light source to produce a uniform image on a nearly Lambertian screen. The drawbacks to the projection lamps are they are expensive to replace, they produce several hundred watts of heat, and are cumbersome. It would be more beneficial to replace these lamps with light emitting diodes (LEDs) which are extremely efficient and can be integrated in a smaller foot-print. The limitation in replacing the lamps are the amount of light reaching the user's eye will be significantly less, although if we implement a high gain screen we can drastically alter the amount of light and reach an equivalent uniformity using an LED instead of a high powered and expensive lamp. In both applications much can be benefited in understanding the properties that make up high gain screens thus providing the ability to improve and alter these screens to greatly impact in a beneficial manner their end user.

The need to fully understand the imaging capabilities arose with the invention of the M-HWPD. [[Martins, R., et. al., 2006](#)] Currently, commercial off-the-shelf (COTS) high gain screens fabricated with corner-cube microstructures are primarily manufactured for their enhanced illumination, although yielding low precision requirements (i.e. applications, which are

able to tolerate higher deviation angles). Therefore, when the COTS high gain screens was applied in our imaging application, it inherently induced image blur due to the angular spread of light, and loss of resolution from the microstructures apertures. [[Hua, H., et. al., 2002](#)] In our imaging application we aspired towards an optimal brightness of the retroreflected light and minimal image degradation. Therefore, we intend to decompose the high gain screen into its respective properties such as, the macroscopic and microscopic properties. The macroscopic properties express the high gain screens' brightness, whereas the microscopic properties describe the microstructure and its contribution to the resolution of the image. In both cases the image is affected by both properties, therefore a full investigation was established to understand how to best design an ideal imaging high gain screen. Our research primarily focused on the corner-cube microstructures as they provided higher brightness due to their triangular aperture, and decreased image degradation compared with a spherical bead retroreflector.

5.2 Macroscopic Properties

In the existing M-HWPD, we integrated a high gain screen to retroreflect light from a miniature display in a bright environment. [[Martins, R., et. al., 2006](#)] The inherently narrow solid angle of a high gain screen makes this technology more attractive compared with a Lambertian diffusing screen. We will describe the macroscopic properties by comparing the ratio of the luminance between a high gain screen to a diffusive screen. The resulting brightness will be expressed as a function of the ratio of their solid angles. The luminance ratio is given by the following equations,

$$L_{HGS} = \frac{\Phi_{display}}{A_{screen} \cdot \Omega_{HGS}} \cdot HGS_{efficiency} \quad (5.1)$$

$$L_{Diffuser} = \frac{\Phi_{display}}{A_{screen} \cdot \Omega_{Diffuser}} \cdot Diffuser_{efficiency} \quad (5.2)$$

$$\frac{L_{HGS}}{L_{Diffuser}} = \frac{HGS_{efficiency}}{Diffuser_{efficiency}} \cdot \frac{\Omega_{Diffuser}}{\Omega_{HGS}} \quad (5.3)$$

where L_{HGS} denotes the luminance of the high gain screen, $L_{Diffuser}$ is the luminance of a diffusive screen, $\Phi_{display}$ is the flux emitted within the solid angle enclosed by the half-angle α . If we assume no losses in the optics then the solid angle is given as $\Omega = 2\pi(1 - \cos(\alpha))$, and A_{screen} is give as the area of the screen. [Dereniak, E. L., and Boreman, G. D., 1996] Given the efficiency of the material $HGS_{efficiency}$ we can compute the amount of brightness observed at the screen. In the case of a COTS high gain screen a typical subtended angle is given as $\alpha = 7.5$ degrees, thus the solid angle was computed as $\Omega_{HGS} = 0.054$ steradians, whereas a diffusing screen has a solid angle $\Omega_{Diffuser} = 2\pi$. If we assume the efficiency of the high gain screen and the diffusive screen to be approximately equal, for simplicity, than the ratio of the luminance is the ratio of the screen's solid angle. Therefore, a high gain screen will always be superior in brightness as long as the solid angle is less than 2π . This can be realized by comparing the amount of brightness observed by a lower power laser having a negligible solid angle with the brightness of the sun in both cases the laser has significantly more brightness than the sun. Therefore, as previously discussed a low power LED can appear greatly brighter then a high powered lamp subtending a hemisphere of 2π steradians.

5.3 Microscopic Properties

To express the microscopic properties we implemented the optical configuration of the M-HMPD, [[Martins, R., et. al., 2006](#)] which is the basis of our research investigation. The microstructures that encompass our high gain screen were custom developed with the commercially available software ASAP by BRO Research. We began our model by developing a gray-scale bitmap object source with a Gaussian profile to better understand the image resolution as well as the noise associated with various aperture sized corner-cubes microstructures. Next, we replaced the Gaussian source with a bitmap image of a modulation transfer function (MTF) resolution target to simulate how high and low frequency are effected by our custom designed high gain screen. In addition, a second gray-scale bitmap image of two small children was used as a qualitative investigation to assess a typical image rendered by the M-HMPD. Furthermore, in our model of the optical layout we removed all optical aberrations of our projection optics by incorporating an ideal projection optical system, ideal 50/50 beamsplitter, and an ideal Fresnel lens. This allowed us to decouple the optical aberrations from the affects of the corner-cube microstructures.

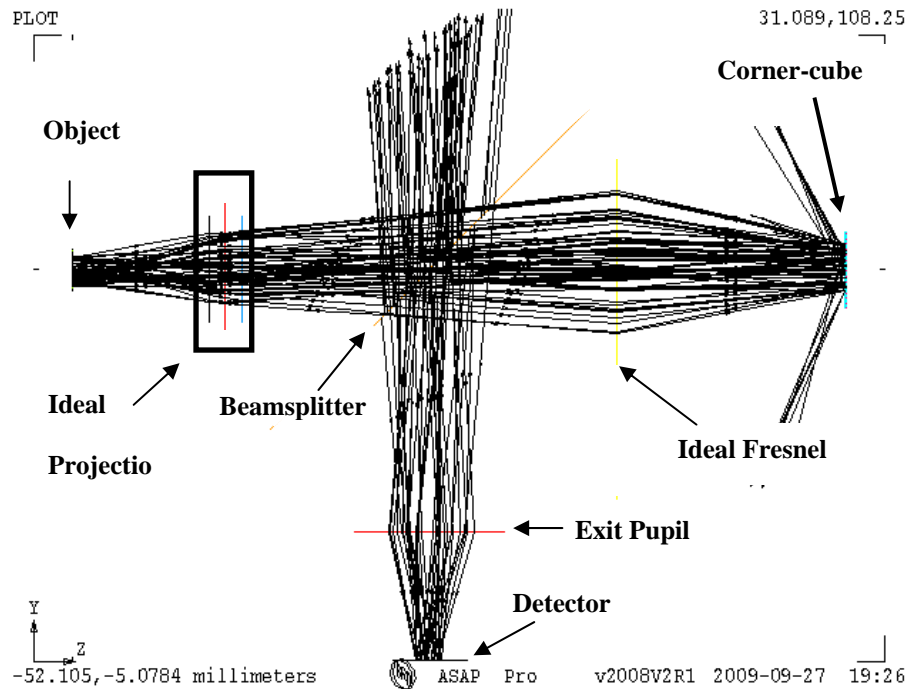


Figure 34: First order layout of the M-HMPD implementing ideal optical components to solely retrieve the corner-cube screen image degradation information.

The optical layout of Fig. 34 comprises of an ideal projection optics system with an effective focal length (EFL) of 19.5 mm and a field-of-view (FOV) of 20°, an ideal 50/50 beamsplitter, an ideal Fresnel lens with an EFL of 30.48 mm and F-number of 1.0, and finally an array of corner-cubes varying in aperture sizes of 256 μm , 128 μm , 64 μm , 32 μm , 16 μm , and 8 μm . Moreover, we designed our model of the high-gain screen with an array of corner-cube spaced 1 μm apart from one another to simulate the current fabrication limitations of diamond turning or photo-etching. [Hockel, H., et. al., 2005] In addition, we represented the exit pupil as an ideal lens having a focal length relative to the human eye's focal length of 17 mm. The detector size was chosen to be 2.5 mm by 2.5 mm with 626 x 626 pixels yielding a 4 μm pixel.

The intent of selecting such detector with those characteristics was to simulate the visual acuity of 1 arc-min as a boundary condition for our simulation. We could have designed our detector with a greater visual acuity by increasing the amount of pixels, although this would have increase our computational time and would have created meaningless results as we are bounded by the human visual acuity. With the boundary conditions implemented and the configuration for the simulated M-HMPD developed we ray traced our gray-scale image sources with 550 million rays at a single wavelength of 656 nm. Such configuration parameters were used in ray tracing our object sources of the Gaussian object, MTF resolution target, and bitmap portrait image and finally all simulation results are further presented in this chapter.

5.3.1 Simulation Results of a Gaussian Image

We quantify the microscopic properties of the high gain screen by taking a cross section of both the normalized autocorrelation of the final image with the normalized autocorrelation of the object source. The difference between the normalized autocorrelation of the image and object source was taken to extract the noise generated by the array of corner-cubes microstructures, as shown in Fig. 35(a) – (v). We preformed some post-processing of our object source to compensate for the lateral demagnification of 0.9144 as seen on the image plane. After completing the scaling of our object source the pixel of our object to image were not perfectly aligned as a result a slight shift in the noise can be seen in our results. Although the noise is slightly shifted it does not degrade or diminish the outcome of our results. The desired goal of imaging our bitmap gray-scale images was to achieve a corner-cube size with no residual artifacts such as discontinuities in the irradiance profile. Therefore, a range of corner-cube sizes

was selected to qualitatively examine the irradiance across our simulated images. The results clearly depict a uniform irradiance profile when the noise is well below 1% at which the corner-cube aperture size reaches $16\ \mu\text{m}$ and below. Through this preliminary investigate of imaging our Gaussian object source can we begin to make the prediction that manufacturing a high gain screen with $16\ \mu\text{m}$ or less with produce a uniform irradiance distribution although we will need to extend our predictions to assess the resolution quality of our image.

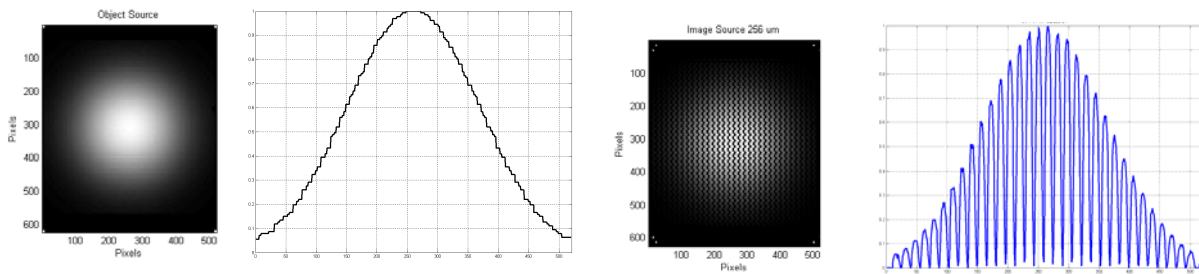
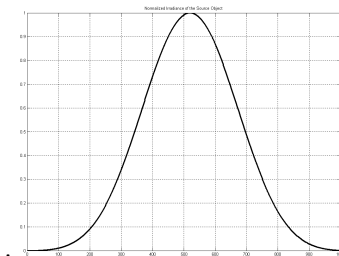


Figure 35: (a) Bitmap image of the object source.

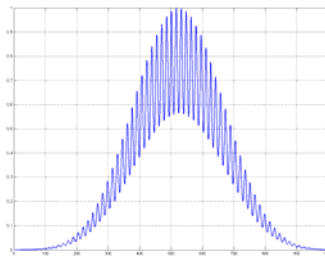
(b) Normalized cross-section of the object source.

(c) Simulated image source with an array of $256\ \mu\text{m}$ corner cube microstructures.

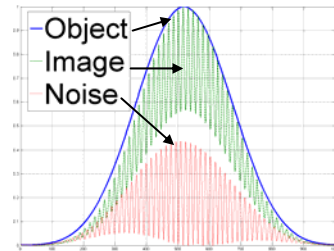
(d) Cross-section of the normalized irradiance profile from the image source.



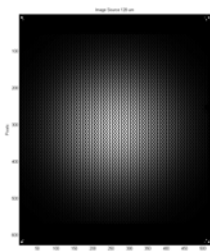
(e) Normalized cross-section autocorrelation of the object source.



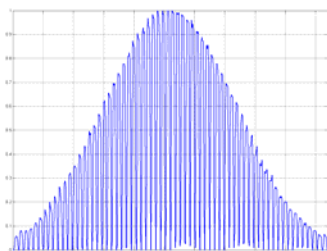
(f) Normalized cross-section autocorrelation of the image source.



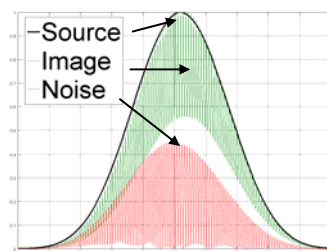
(g) The difference between both normalized autocorrelation of the object and image source cross-sections.



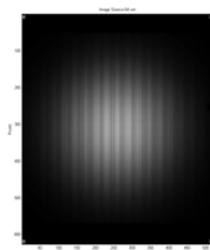
(h) Simulated image source with an array of 128 μm corner cube microstructures.



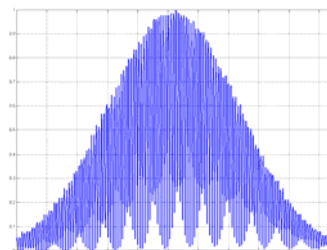
(i) Normalized cross-section of the image source.



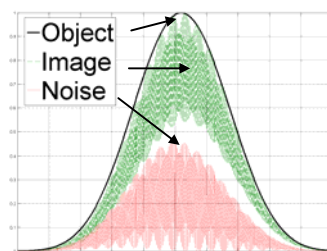
(j) The difference between both normalized autocorrelation of the object and image source cross-sections.



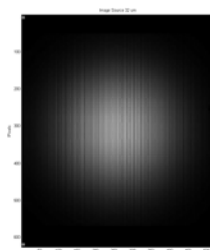
(k) Simulated image source with an array of 64 μm corner cube microstructures.



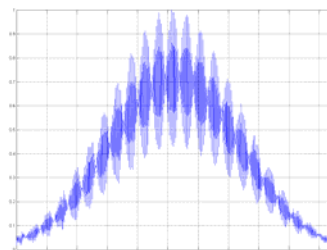
(l) Normalized cross-section of the image source.



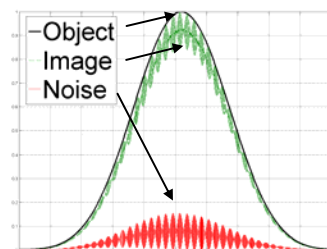
(m) The difference between both normalized autocorrelation of the object and image source cross-sections.



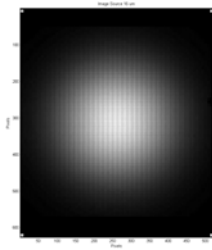
(n) Simulated image source with an array of 32 μm corner cube microstructures.



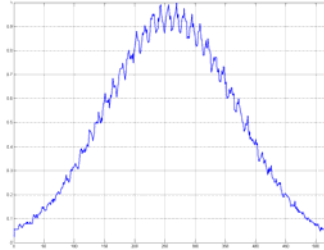
(o) Normalized cross-section of the image source.



(p) The difference between both normalized autocorrelation of the object and image source cross-sections.



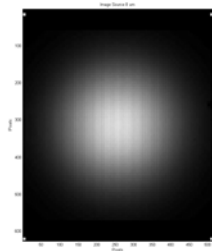
(q) Simulated image source with an array of 16 μm corner cube microstructures.



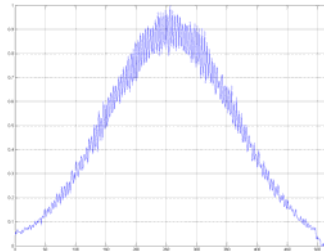
(r) Normalized cross-section of the image source.



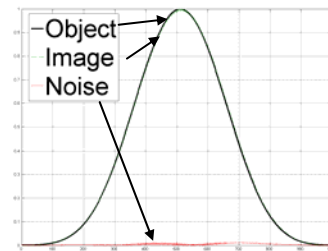
(s) The difference between both normalized autocorrelation of the object and image source cross-sections.



(t) Simulated image source with an array of 8 μm corner cube microstructures.



(u) Normalized cross-section of the image source.



(v) The difference between both normalized autocorrelation of the object and image source cross-sections.

5.3.2 Simulation Results of an MTF Resolution Target and Bitmap Portrait Image

In qualitatively assessing the resolution capabilities of our custom designed high gain screen we replaced the Gaussian source with an MTF resolution target to observe the effects of our varying corner cubes. From our previous results with the Gaussian source we expect that the MTF resolution target to perform well at and below 16 μm . As expected the MTF resolution target at 256 μm was illegible as shown in Fig. 36 (b), although the image resolution progressively improved through miniaturizing the corner-cubes aperture, as shown in Fig. 36 (c) – (g) . It was

not until the corner cube size was miniaturized to an aperture of 16 μm did the object and image source appear visually similar.

Previously, the Gaussian gray-scale image demonstrated low noise levels at and below 16 μm , although in our MTF resolution test we can clearly observe residual artifacts at 16 μm . As we mentioned earlier, the detector was designed to simulate the human visual acuity therefore the detector will sample approximately 3 pixels per corner cube at 16 μm whereas with a corner-cube aperture of 8 μm the detector will sample approximately 1 pixel per corner cube. In the case of an 8 μm corner-cube the resolution of the detector is the limiting factor ultimately reaching the human visual acuity. To fully understand the impact of the residual effect between the 16 μm and 8 μm corner-cube apertures a final simulation was conducted using a bitmap image of the author's children.

The majority of people are not accustomed in determining the visual performance of an MTF resolution targets, as a result an extension to this research was completed with a more familiar image, such as a portrait of two children, as shown in Fig. 37 (a). It is clearly evident by comparing both the object source to the image of either the 16 μm or 8 μm corner-cube apertures the artifacts produced by the 16 μm corner-cube, as shown in Fig. 37 (b), is perceptively discernible in our simulated image, whereas our 8 μm corner-cubes produced a replica of our object source, as shown in Fig. 37 (c). In summary, based on our results of the macroscopic and microscopic properties we request a fabricated high gain screen composed of an array of corner-cubes to accommodate the combination of both properties in order to obtain an optimal retro-reflective screen for the M-HWPD.

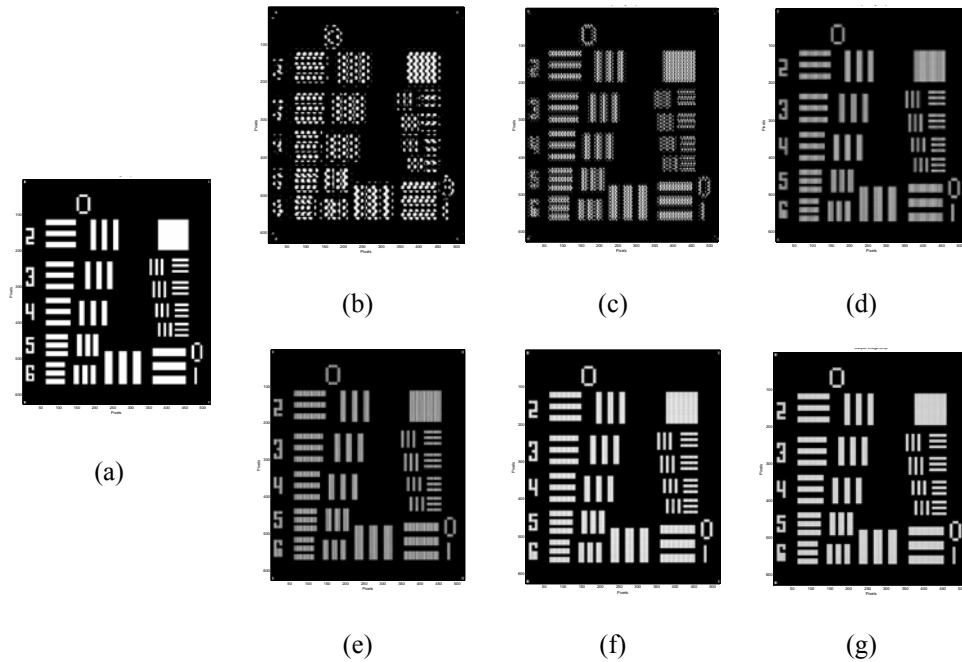


Figure 36: Imaging and irradiance distribution of an MTF grey-scale bitmap object source: (a) original object source, (b) image with 256 μm corner cube microstructures, (c) image with 128 μm corner cube microstructures, (d) image with 64 μm corner cube microstructures, (e) image with 32 μm corner cube microstructures, (f) image with 16 μm corner cube microstructures, (g) image with 8 μm corner cube microstructures.

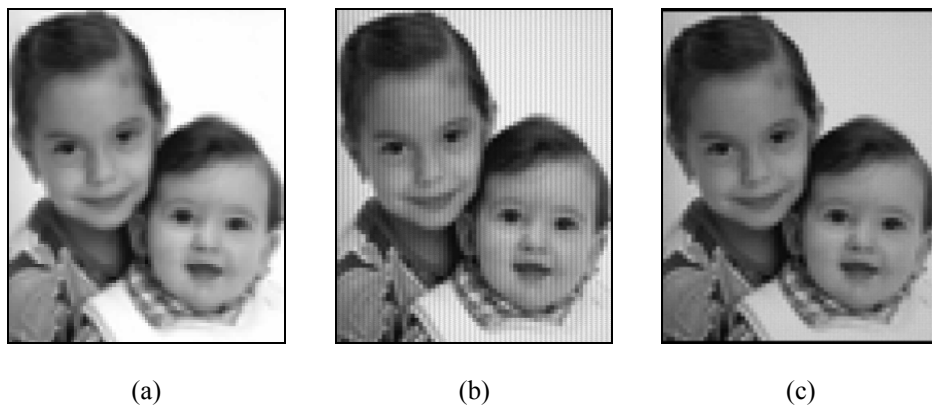


Figure 37: Grey-scale bitmap object source: (a) original grey-scale object source, (a) image with 16 μm corner cube microstructures, (b) image with 8 μm corner cube microstructures.

CHAPTER SIX: CONCLUSION AND FUTURE WORK

The research presented in Chapter 2 led to the design and the development of a novel HMD optical system consisting of a single unit assembly composed of a micro display, projection optics, and phase conjugate material all internally mounted inside the HMD. This unique design provides the capabilities of several applications such as, augmented reality for urban combat, guided surgery, and wearable computers allowing the user to view computer generated images in a see-through environment setting. This novel design also led to the assessment of two types of phase conjugate material that may be implemented in the ultra light weight head-mounted display assembly.

The research presented in Chapter 3 led to the conceptual design of a novel single unit optical system consisting of an assembly of OLED microdisplay, projection optics, and PCM integrated into the HMPD. This unique design enables applications such as augmented reality for urban combat, MOUT, guided surgery, and wearable computers, for example, allowing the user to view computer-generated images in an indoors or outdoors environments. This novel design also led to specific design requirements for manufacturing custom PCM that will be integrated in our ultra lightweight, wide field of view HMPD assembly to improve the image quality.

The research presented in Chapter 3, demonstrated a fully integrated, see-through, wearable M-HMPD as a novel method of utilizing HMPD technology for mobile outdoors applications. Currently, the integration yields optical elements in close proximity to the user's mouth that could present condensation and fogging with cool outdoor temperatures. An immediate solution is to embed a dense fabric cover to shield the retro-reflective screen and the Fresnel lens from unwanted condensation and potential other environment effects. With the

addition of light control devices, for example photo or electrochromatic windows to attenuate the environmental light, and a custom designed retro-reflective screen, the M-HMPD design can ultimately provide SVGA quality computer generated images superimposed on top of the natural environment at various levels of illumination. Future research will focus on the development of custom designed, nano-fabricated, retro-reflective microstructures, as well as novel micro-optics designs to replace the Fresnel lens and retro-reflective screens for more compact solutions. Finally, the development of an electrochromatic window for the M-HMPD can provide a feasible solution for adjustment of the ambient light, thus achieving optimized imaging in outdoor environments.

The research presented in Chapter 4, described how high gain screens can be described by decomposing the screen into two respective properties that both must be considered in the fabrication process. In this chapter, we have defined the macroscopic properties in terms of its radiometric quantities and have shown the importance of controlling the deviation angle to be approximately zero to enhance the brightness of our rendered image. In addition, we qualitatively described the microscopic properties in terms of its illumination uniformity and respective resolution characteristics. We further linked the illumination and resolution performance to the corner-cubes physical dimensions. It is important to note the desired dimensions of the corner-cubes were based on the current configuration of the M-HWPD, thus under this configuration the dimensions were selected to be below our visual acuity of 1 arc-min resulting in an 8 μm corner-cube aperture. For example, in a movie theater configuration the corner-cubes can be several orders of magnitude larger and will still satisfy both the macro- and microscopic properties.

As part of our future work we will investigate in greater detail the contrast difference between the object source and resulting image. Although, it is believed that the loss in contrast is a multiple of several contribution of which can be linked to the 1 μm separation between individual corner-cubes, the 25% light received on our detector from our double pass system, and the amount of light retro-reflected at the edge of the field. In addition, with the configuration of the M-HWPD the system is not configured to be telecentric on the high gain screen that is the chief rays are not parallel to the optical axis, thus we produce a varying F-number across our detector reducing the entrance cone on our corner-cubes. As a result, as the field angle increases the acceptance angle of light entering our corner-cubes will decrease limiting the amount of retro-reflected light returned onto our detector.

**APPENDIX: A COMPACT MICROLENSLET-ARRAY-BASED
MAGNIFIER**

Vesselin Shaoulov, Ricardo Martins, and Jannick P. Rolland

*Center for Research and Education in Optics and Lasers,
School of Optics, University of Central Florida, Orlando, Florida 32816*

Received November 21, 2003

An ultracompact optical imaging system allowing various magnifications or demagnifications and based on microlenslet arrays is presented for the first time to our knowledge. This research generalizes recent findings regarding microlenslet-array-based 1:1 relay systems [Appl. Opt. **42**, 6838 (2003)]. Through optical ray tracing, the feasibility of magnifying gray-scale images through a stack of two dissimilar microlenslet arrays is demonstrated for the first time to our knowledge. Results presented specifically demonstrate that a compact imaging system operating at a magnification of 2 is feasible with an overall length of —9 mm. Optical aberrations of the most basic configuration are evaluated, and optimization is discussed. © 2004 Optical Society of America

OCIS codes: 350.3950, 110.2960, 220.4830, 350.5730.

The imaging properties of microlenslet arrays and associated baffle for binary (i.e., black and white) imaging, such as the imaging needed in copiers and scanners, were first investigated by Anderson.¹ Later microlenslet arrays were found to be a useful tool in designing ultracompact imaging relay systems, as well as in realizing three-dimensional integral photography.²⁻⁶ Current state-of-the-art micro-optics fabrication facilities make possible the manufacturing of microlenslet arrays of extremely short focal length with apertures of various shapes and size comparable with wavelength. Microlenslet arrays with refractive, diffractive, anamorphic, spherical and aspherical, and positive and negative optical surfaces are currently available.

The design of many optical imaging systems requires extremely compact and lightweight magnifying systems, for example, the magnification of miniature organic light-emitting diode displays in head-mounted projection displays (HMPDs), one of the applications driving our research, which does not have stringent resolution requirements in the magnification process.⁷ An ultracompact solution would be extremely beneficial for such an

application because it would allow for improved design, increased field of view, and overall higher performance. With conventional design techniques, even some of the most compact custom-designed conventional magnification 1:2 systems present an overall length of ~ 120 mm and weight of 700 g. To overcome such restrictions in size, an alternative approach had to be investigated. Optical magnification systems based on microlenslet arrays could provide a useful solution for such applications.

In this Letter we propose the use of microlenslet arrays to create compact, lightweight, and potentially cost-effective optical magnification systems for imaging at various magnifications. Previous work demonstrated the feasibility of imaging with microlenslet arrays in the special case of 1:1 relay systems. A key contribution of this Letter is the replacement of bulk macro-optic systems by multi-aperture micro-optics. Another key contribution of this Letter is the generalization of imaging with microlenslet arrays for various magnifications or demagnifications. Specifically, we establish the detailed relationships necessary to describe the most general case of imaging with two stacks of microlenslet arrays and the appropriate baffles. Also, the simulation of such an imaging system is presented, which validates its feasibility.

There are numerous possible configurations that can be used to create an optical 1: M magnifying system with a stack of two dissimilar microlenslet arrays.⁸ The general case for a stack of two microlenslet arrays is illustrated in Fig. 1. Provided that the microlenses in the first and the second arrays are of focal lengths f_1 and f_2 , respectively, the overall length (OAL) of such a system, defined as the distance from the object to the final image plane, is given by

$$OAL = \frac{(m_1 + 1)^2}{m_1} f_1 + \frac{(m_2 + 1)^2}{m_2} f_2, \quad (1)$$

where the first and the second microlenslet arrays operate at magnifications of magnitudes m_1 and m_2 , respectively. The magnitude of the overall magnification M of the system is defined as

$$M = m_1 m_2, \quad (2)$$

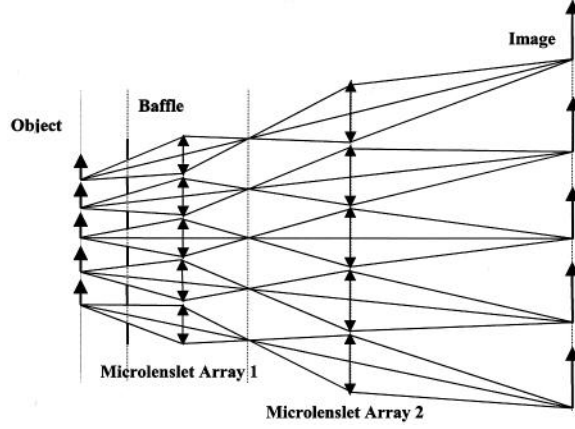


Fig. 1. Optical layout of 1: M imaging with a stack of two arrays of microlenses.

Two key aspects of imaging with a stack of two microlenslet arrays are lensletization and ghost images.² The key to overcoming ghost-image formation in a system consisting of arrays of microlenslets is placing an array of baffles of the correct size at the appropriate location in the system.² The minimum of the function given by Eq. (1), after substituting for m_2 with Eq. (2), yields the most compact configuration of the two microlenslet arrays and is given by

$$\frac{\partial \text{OAL}}{\partial m_1} = 0, \quad (3)$$

which yields

$$m_1 f_2 (m_2 - 1)(m_2 + 1) = m_2 f_1 (m_1 - 1)(m_2 + 1), \quad (4)$$

One of the solutions to Eq. (4) yields $m_1 = m_2 = M = 1$, which simplifies the system to a microlenslet-arraybased 1:1 relay $2f$ system.² Furthermore, if M is given, Eq. (4) may be solved for m_1 to minimize OAL. In this case it can be shown that

$$m_1 = \left(\frac{M f_1 + M^2 f_2}{M f_1 + f_2} \right)^{1/2}. \quad (5)$$

Furthermore, in all cases (i.e., $\forall M$), to best eliminate ghost images in the final image plane, the intermediary subimages after the first microlenslet array must not overlap to allow placement of a baffle at the entrance pupil of the system. Such a condition naturally requires $m_1 < 1$. Without loss of generality let $f_2 = \gamma f_1$. Then Eq. (5), which sets the minimum OAL, combined with

the requirement that $m_1 < 1$, leads to a system with an overall demagnification (i.e., $M < 1$). Thus for $M > 1$ a configuration can be established, but it will not correspond to the minimum OAL. It should be noted, however, that the most compact arrangement might not correspond to optimal first-order image quality, as previously found in 1:1 relay systems.² Specifically, first-order image quality is also highly dependent on image lensletization. Overcoming this effect is less straightforward than suppressing ghost images. It requires overlapping of the individual subfields of view of each individual pair of lenses at the expense of an increase in OAL and a natural decrease in resolution.²

To validate the feasibility of the conceived 1:2 imaging system, an $F/5$, 500-mm focal-length microlenslet array was selected in the front location without loss of generality, and an $F/8.3$, 1000-mm array was selected in the back location. Furthermore, the microlenses in each array were square plano-convex lenses with a thickness of 150 μm . The microlenslet arrays operate at $m_1 = 0.5$ and $m_2 = 4$, respectively. In such a configuration it can be shown from basic principles that the second lenslet in each pair is the aperture stop of the system; therefore the baffle has to be placed in the location of the entrance pupil, which is a conjugate of the aperture stop. Furthermore, the baffle must be established for the correct magnification of the pupils. In the case investigated, a set of microbaffles with a computed diameter of 40 mm was placed at the appropriate location in the system.

A software model for imaging assessment was developed with custom-developed software based on the Advanced Systems Analysis Program (ASAP). The optical layout of the system, made of 11 x 11 micro-lenses in each array, is shown in Fig. 2. An analysis of the minimum number of rays satisfying 99% accuracy of the ray-traced image was performed, and it was found that the minimum number of rays needed was 2.5×10^9 . With the current state of hardware and software such accuracy would require more than 3 weeks of computational time. Based on the accuracy of the ray-trace analysis shown in Fig. 3, an accuracy of 97% was selected for image quality feasibility because it satisfies both the criterion of ~ 48 h computational time on a 2.8-GHz PC and the criterion of more than 95% accuracy commonly accepted as a threshold for assessing feasibility.⁹

Results of the simulation shown in Fig. 4 demonstrate that a 1:2 relay lens based on a stack of two dissimilar microlenslet arrays can be achieved with no ghost images, yet a small residual lensletization.

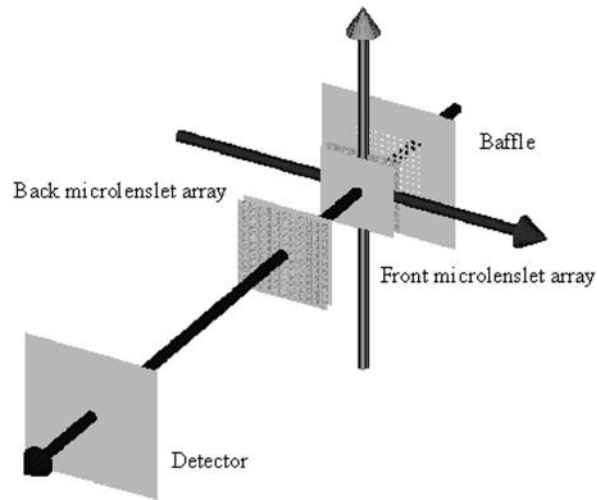


Fig. 2. ASAP layout of 1:2 microlenslet-array-based magnification system with two 11 x 11 arrays of microlenses and the appropriate baffle. From right to left, the baffle, the two dissimilar microlenslet arrays made of square plano-convex lenses, and the detector upon which an image will be formed given an object in front of the baffle are shown.

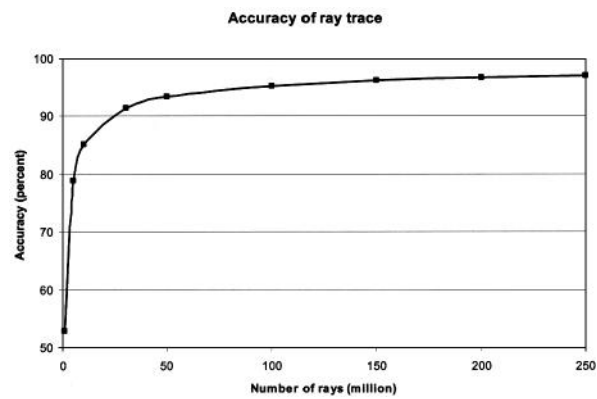


Fig. 3. Accuracy of the ray trace in percents as a function of the number of rays emitted from the object.

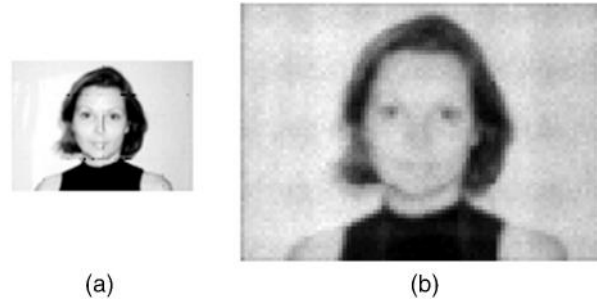


Fig. 4. Imaging of a gray-scale object through a 1:2 microlenslet-array-based magnifying system: (a) object and (b) magnified image.

of the image may be observed. Such lensletization would be overcome in a final optimized configuration by further overlapping the subfields of view. With commercially available microlenslet arrays, such a system would have an overall length of 8.7 mm and a weight of ~ 1 g. An analysis of the image quality of the system shows that the diffraction-limited point-spread function is $41.67 \mu\text{m}$. Such a spot size is large compared with the $10 \mu\text{m}$ pixel size found in most commonly available CCD cameras. A smaller pixel size of $10 \mu\text{m}$ may be achieved by increasing the apertures of the microlenslets in both arrays to $410 \mu\text{m}$ in the front and $500 \mu\text{m}$ in the back. However, increasing the apertures of microlenslets while keeping their focal length invariant naturally occurs at the expense of decreasing the working F number. Such a decrease leads to a more complex performance-optimization task, yet it does not compromise the feasibility of the design. In this case the OAL is still compact and ~ 9.5 mm. Such resolution requires simulations with more pixels to cover an equivalent field of view and thus fewer rays per pixel, leading to a ray-trace accuracy of $\sim 85\%$ based on the criterion of ~ 48 -h computational time on a 2.8-GHz PC. The results obtained for that system were consistent with the results obtained with 97% accuracy, confirming the feasibility of the system. This simple analysis, however, points to the reason we originally chose microlenslets of smaller diameter: We can run simulations at higher accuracy with the intrinsic understanding that diffraction is limiting and can be reduced with larger microlenslets. If the system is made of simple plano-convex lenses, as considered for the feasibility investigation, both monochromatic and chromatic aberrations will limit the image quality. However, because the sine condition is quasi-satisfied (i.e., $<0.02\%$ discrepancy), if the lenslets located in the subpupils are aspherized, coma will be negligible. Furthermore, per modulation transfer function analysis astigmatism limits the image quality and can be corrected by aspherization of the lenslets in the first array,

which is the entrance window. Distortion for any pair of lenslets is nonnegligible and requires further investigation in how it practically affects image quality. Finally, given that simple plano-convex lenslets were used, the system will suffer both axial and transverse chromatic aberrations. An analysis shows that axial chromatism is significant and will need to be corrected with a lenslet doublet in the pupil. Lateral color, however, is less than 5 μm at the edge of the field of view and will thus most likely not require any further minimization. However, if an application required no lateral color, another lenslet doublet located in the entrance window could be used.

In conclusion, we have studied the imaging properties of magnification systems based on a stack of two microlenslet arrays and have demonstrated that ultracompact imaging optical relay systems can be designed with an overall length of only a few millimeters. Any design of such a magnifier has to be application driven. However, in all cases of imaging gray-scale or color images, lensletization will likely need to be minimized below the level at which it is perceived. Beyond that point, applications may impose different compactness and resolution requirements, which will lead to more or less complexity in the design of each array. In HMPDs, for example, compactness and low weight are critical; however, some loss in resolution will likely be tolerable and even desired to remove the pixelization of the microdisplay being magnified through the main HMPD optics.

This work was supported in part by the U.S. Army Simulation, Training, and Instrumentation Command. We thank Breault Research Organization for the educational license of ASAP and Optical Research Associates for the educational license of CODE V, which were used for this research. V. Shaoulov's e-mail address is vesko@odalab.ucf.edu.

References

1. R. H. Anderson, *Appl. Opt.* **18**, 477 (1979).
2. V. Shaoulov and J. Rolland, *Appl. Opt.* **42**, 6838 (2003).
3. V. Shaoulov and J. Rolland, *Proc. SPIE* **4832**, 74 (2002).
4. L. Erdmann and K. J. Gabriel, *Appl. Opt.* **40**, 5592 (2001).
5. J.-S. Jang, F. Jin, and B. Javidi, *Opt. Lett.* **28**, 1421 (2003).
6. J.-S. Jang and B. Javidi, *Opt. Lett.* **27**, 1767 (2002).
7. R. Martins and J. Rolland, *Proc. SPIE* **5079**, 277 (2003).
8. V. Shaoulov, R. Martins, and J. Rolland, "Compact microlenslet array imager," U.S. patent pending, 2003.
9. W. Cassarly, *Proc. SPIE* **5186**, 1 (2003).

**APPENDIX: B MAGNIFYING MINIATURE DISPLAYS WITH
MICROLENSLET ARRAYS**

Vesselin Shaoulov*, Ricardo Martins and Jannick Rolland

CREOL / School of Optics

University of Central Florida

Orlando, Florida 32816

**[Email: vesko@odalab.ucf.edu](mailto:vesko@odalab.ucf.edu)*

ABSTRACT

Current technology trends are focused on miniaturizing displays, although for specific applications such as the use of head-mounted displays (HMD) this limits the advancements for a wider field-of-view (FOV) and a negligible overall weight of the optics. Due to the advancements of electronics that benefit from smaller miniature displays, universities and companies are focused on developing this technology to meet the growing demand of this global market. Higher resolution displays with added brightness are being developed, but these displays are decreasing in their viewable area. HMDs can benefit from these higher resolution and brighter displays but they will undergo an increased optical weight to compensate for the smaller display size. To overcome this hindrance in HMDs, we demonstrate in this chapter how to incorporate microlenslet arrays as an optical relay system to magnify miniature displays. Microlenslet arrays provide respectively shorter focal length which yields a smaller overall object to image distance and an incremental overall weight compared to an otherwise increased optical lens assembly. The contribution of this chapter is a patented concept of magnifying/demagnifying miniature displays with microlenslet arrays that can be integrated in a spaced limited area.

1. INTRODUCTION

Many applications require the integration of an ultra-compact optical system to magnify miniature displays. For example, a driving application for our research comprises of the magnification of miniature displays in head-mounted displays (HMDs).¹ A key component of any HMD is the microdisplay, specifically its size, resolution, and illumination scheme, which drive the design, and thus the final layout after packaging. Several technologies, such as liquid crystal displays (LCD), organic light emitting diodes (OLED) and liquid crystal on silicon displays (LCOS) currently compete for

the microdisplay market.^{2,3,4} They all have specific advantages and are best fit for different design requirements and applications.

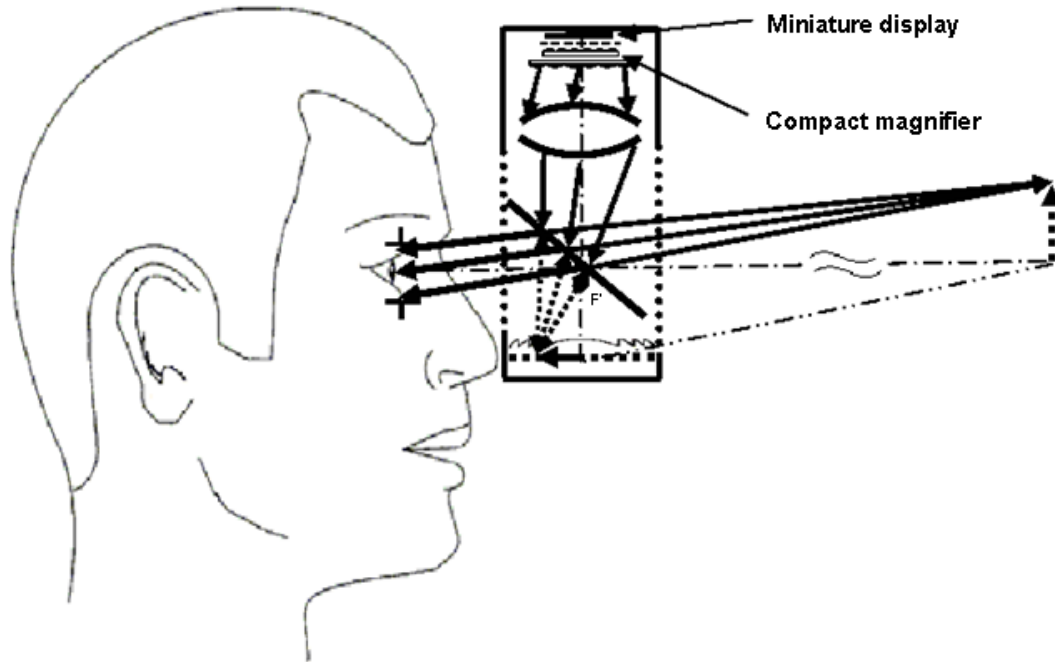


Fig. 1. Conceptual design of an HMD with integrated miniature display, magnified by a compact magnifier.

An example of an integrated system comprising of a miniature display magnified by a compact magnifier is presented in Fig. 1 for a recently conceived HMD.⁵ In such configuration, magnification of the miniature display is needed to minimize the overall length of the optical assembly to further increase the field of view (FOV) of the HMD. As part of our previous work, we designed a state-of-the-art 1:2 magnifying system utilizing bulk macro optics, however while compact, this system still had an overall object to image length (OAL) of 120mm and weighted over 700 grams.⁶ Therefore an alternative approach had to be investigated. Given the compactness requirements imposed on any HMD system, a magnifying system with size of a few millimeters and weight of a few grams is desired. Optical magnifying systems based on microlenslet arrays could provide a useful solution for such applications. The key contribution of our investigation is the replacement of bulk macro optics with multi-aperture micro-optics.

2. KEY CHALLENGES IN IMAGING WITH MICROLENSLET ARRAYS

The basic theory of imaging with microlenslet arrays, developed by R.H. Anderson, was driven by requirements of optical scanning devices.⁷ In his work, Anderson demonstrated that arrays of simple lenses combined with appropriate baffles could be used in close-up imaging systems for black and white document copiers, oscilloscope cameras, as well as binary code scanners. Microlenslet-array based imaging systems were consequently further investigated for optical scanners and copiers,^{8,9} and 3D integral photography.¹⁰ The imaging capabilities of microlenslet arrays for either grayscale or color images were previously investigated, and it was demonstrated that 1:1 compact relays for such images could be conceived with OAL of less than 7mm.¹¹

The two key challenges when imaging with multi-aperture stacks of microlenslet arrays are the formation of ghost images in the system and lensletization.¹¹ The formation of ghost images in a multi-aperture imaging system comprising of a stack of microlenslet arrays is caused by the light emitted from the object in all directions taking more than one optical path through the system. The formation of ghost images in such optical system is demonstrated in Fig. 2(a). To suppress the ghost image formation an appropriate baffle should be placed in the location of either the entrance or the exit pupil of the optical system as demonstrated in Fig. 2(b).

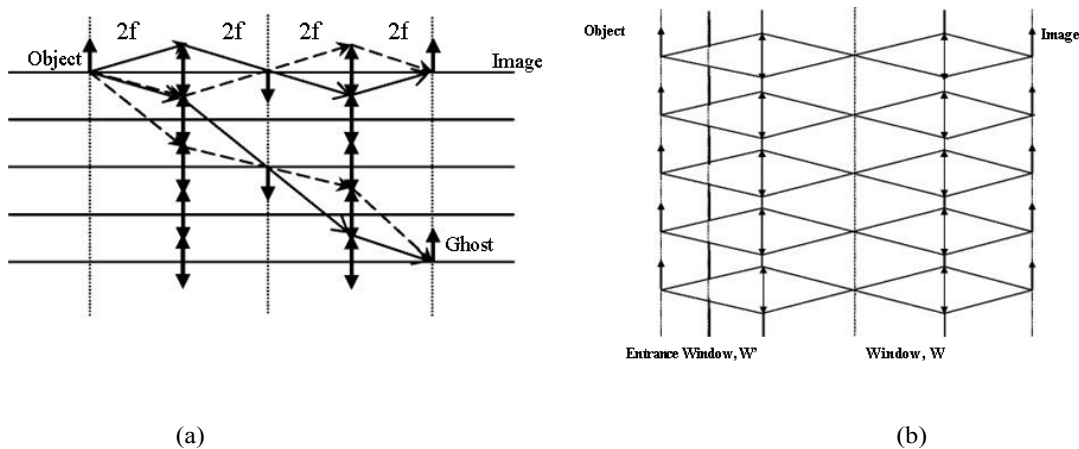


Fig. 2. First order optical layout of a compact imaging system, consisting of a multi-aperture stack of microlenslet arrays, demonstrating (a) the formation of ghost images in the system without an appropriate baffle, and (b) the suppression of ghost images formation with an appropriate baffle placed in the location of the entrance pupil.

The lensletization is another property of optical imaging with a multi-aperture stack of two microlenslet arrays that describes the sampling of the object by each pair of microlenslets in the stacks, where each pair operates over a limited field of view. Overcoming this effect is less straightforward than

suppressing ghost images and requires overlapping the individual sub-fields of view of each individual pair of lenses, as demonstrated in Fig. 3(a) and 3(b). The overlap of the individual sub-fields of view occurs at the expense of an increase in the OAL and a natural decrease in resolution.¹¹

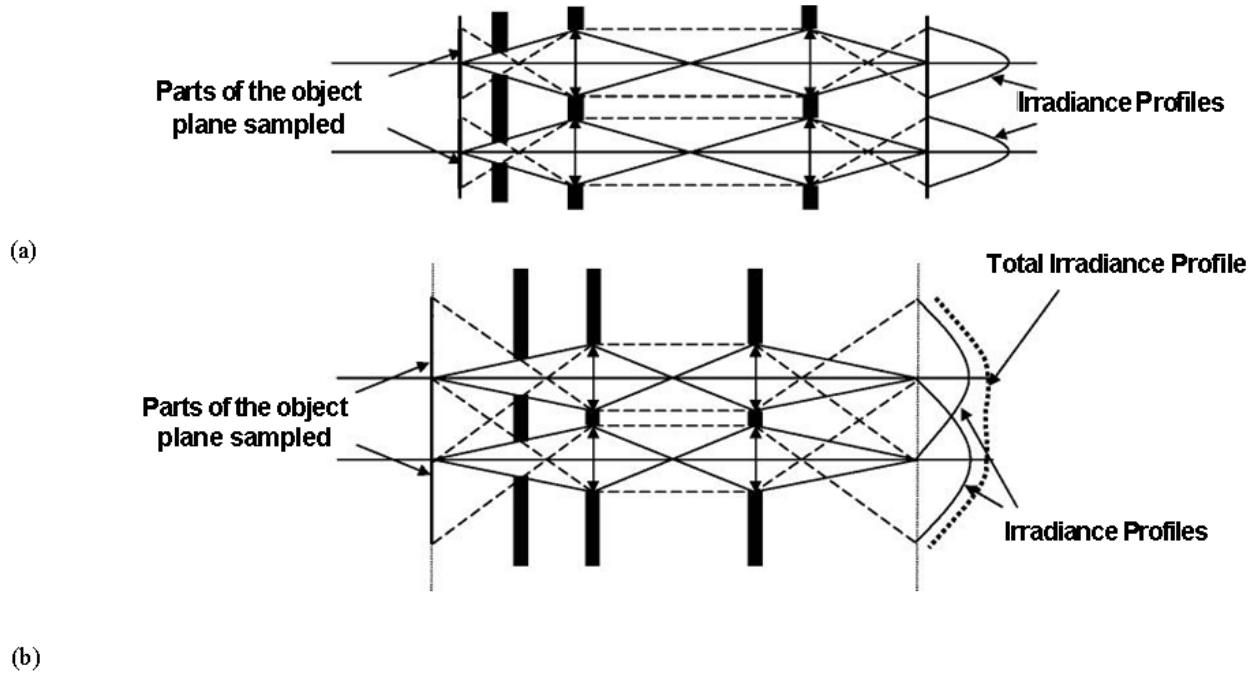


Fig. 3. First order optical layout of a compact imaging system, consisting of a multi-aperture stack of microlenslet arrays, demonstrating the lensletization effect (a) without overlapping the individual sub-FOVs leading to sampling of the object by each individual pair of lenses in the stack, and (b) with overlapping the individual sub-FOVs suppressing the lensletization effect and achieving an uniform image.

3. OPTICAL LAYOUT OF MAGNYFYING MINIATURE DISPLAYS WITH A STACK OF TWO MICROLENSLET ARRAYS

The concept of imaging with a multi-aperture stack of two microlenslet arrays was further extended to the most general case, where two dissimilar arrays were used to achieve a system with overall magnification or demagnification, as demonstrated in Fig 4.

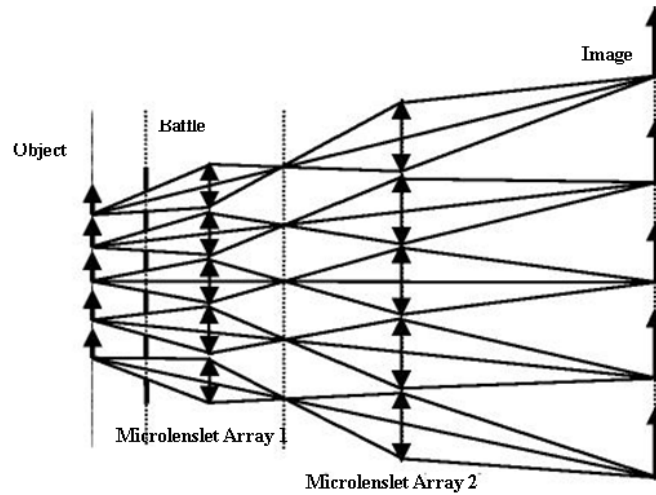


Fig. 4. First order optical layout of compact magnifying system consisting of a multi-aperture stack of microlenslet arrays.

In this configuration the first and the second microlenslet arrays are of focal lengths f_1 and f_2 , diameters D_1 and D_2 , and operate at magnifications m_1 and m_2 , respectively. The overall magnification of such system is $M=m_1m_2$. An appropriate baffle is placed in the location of the entrance pupil of the system to suppress the ghost image formation and the system is configured with enough overlap to minimize the lensletization. The optical and the geometrical relationships used to achieve such configuration were discussed previously.^{12,13}

4. THEORETICAL MODELING

In order to further analyze the imaging properties of microlenslet array based magnifiers, a computer model was developed using custom-designed software based on ASAPTM. The first aspect of modeling is

to define an appropriate light source or equivalently an object to be imaged. Since the driving application for our research was to magnify miniature displays, a complex grayscale light source, such as a bitmap portrait, was selected to assess the grayscale imaging capability of the proposed microlenslet array based magnifier. In the case of grayscale images, image quality may be assessed subjectively as well as with more sophisticated quantitative approaches.^{11,12}

The optical layout of a 1:2 system using two arrays of each 11 by 11 microlenses, combined with an associated baffle located at the entrance pupil of the system is shown in Fig 5.

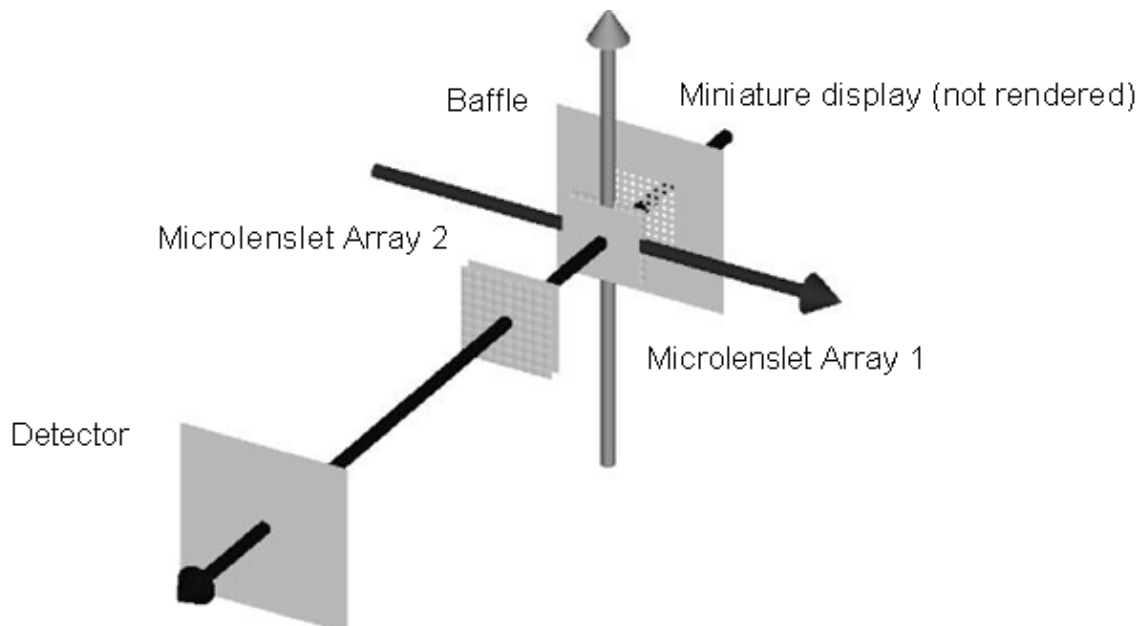


Fig. 5. ASAP™ model of a compact magnifying system consisting of a multi-aperture stack of microlenslet arrays.

Each lens in the first array was considered an F/5 square plano-convex, of $150\mu\text{m}$ thickness, and $500\mu\text{m}$ focal length. Each lens in the second array was an F/8.3 square plano-convex lens, of $150\mu\text{m}$ thickness, and $1000\mu\text{m}$ focal length. Because we use simple plano-convex singlets, which inherently have significant axial chromatic aberration, we only consider imaging single color grayscale image, which we selected without loss of generality to be λ equal 656nm . In our previous work we demonstrated that one level of optimization in optical raytracing is to direct the rays towards the entrance pupil of the optical system.¹¹ While in the case of microlenslet arrays no single pupil exists but instead multi-sub-pupils must be considered, a fictitious pupil is defined that encompasses all the sub-pupils.¹¹ Building on this scattering technique, which is standard in ASAP™ software, the raytrace was further optimized. The rays were first traced from the source to the diffuser, and then only the scattered rays were traced

from the diffuser towards the fictitious entrance pupil of the system. An analysis of the minimum number of rays to achieve 97% accuracy, which is enough for a first order feasibility assessment, demonstrated that a total of 150 million rays should be traced through the system.¹⁴

Results of feasibility simulations using a grayscale light source and 150 million rays are shown in Fig. 5 for the imaging configuration shown in Fig. 6.

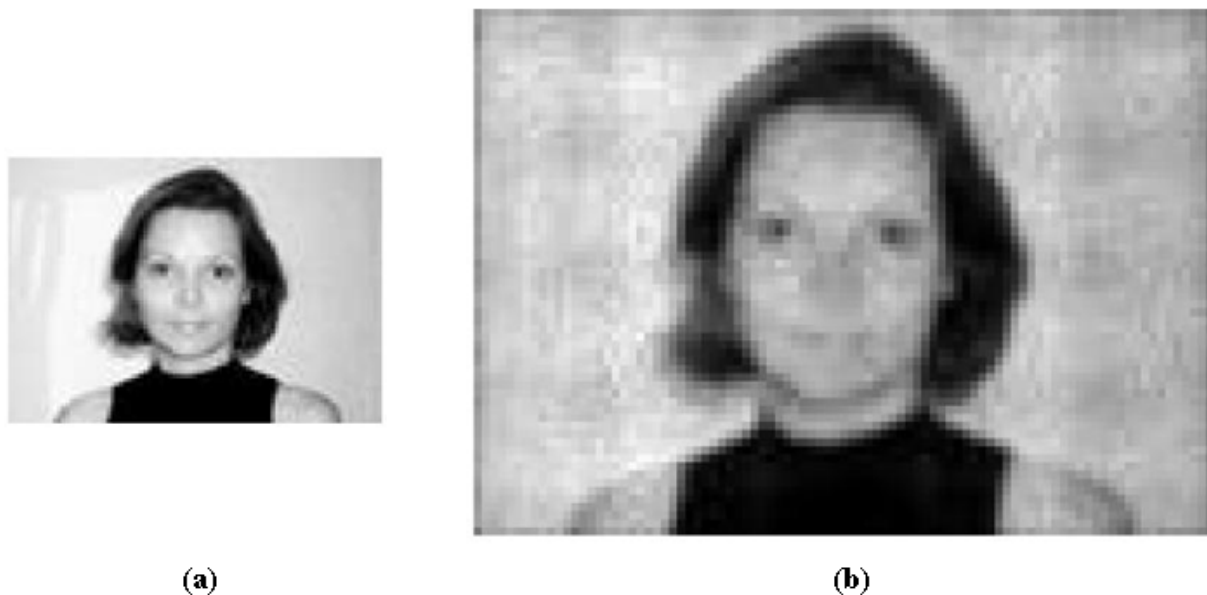


Fig. 6. Simulation of imaging of a grayscale object projected by a miniature display through a stack of two dissimilar microlenslet arrays: (a) a grayscale object and (b) magnified image through the system.

5. CONCLUSION AND FUTURE WORK

Results presented in this chapter demonstrate that ultra-compact multi-aperture magnification system based on a stack of two dissimilar microlenslet arrays is feasible since a final image with no apparent ghosting and a small residual lensletization can be formed. That will allow for efficient magnification of miniature displays in an HMD. As part of the future work, we will investigate the higher order image properties of such systems and will optimize for best performance to satisfy a spatial frequency of approximately 24cycles/mm to drive 0.6 inch 800x600 miniature displays.

ACKNOWLEDGMENTS

We thank BRO Corporation for the educational license of ASAP™ to the School of Optics/CREOL/FPCE. This research was supported in part by the US Army Simulation, Training, and Instrumentation Command (STRICOM) and funded in part by grant number N00014-03-10677 awarded by the Office of Naval Research.

REFERENCES

1. J. P. Rolland, H. Fuchs, "Optical versus Video See-Through Head-Mounted Displays", in "Fundamentals of wearable computers and augmented reality", W. Barfield, T. Caudell, Lawrence Erlbaum Associates, New Jersey 2001.
2. W.C. O'Mara, C. William, "Liquid Crystal Flat Panel Displays: Manufacturing Science & Technology" Van Nostrand Reinhold, New York, 1993.
3. M. E. Thompson, S. R. Forrest, P. Burrows, Z. Shen, G. Gu and V. Bulovic, "The stacked OLED (SOLED), a new type of organic device for achieving high-resolution full-color displays", Synthetic Metals Vol. 91(1-3), p. 9-13, December 1997.
4. Intel(R) LCOS Technology Brief, <ftp://download.intel.com/design/celect/technology/lcos/30042801.pdf>, 2004.
5. R. Martins and J. Rolland, "Diffraction of Phase Conjugate Material in a New HMD Architecture", SPIE Proceedings Vol. 5186, p. 277-283, SPIE AeroSense: Helmet and Head-Mounted Displays VIII: Technologies and Applications, Editors: C. E. Rash and C. E. Reese, September 2003. J.P. Rolland, H. Hua, and V. Shaoulov, "Design of a compact relay lens", Technical Report TR02- 05, University of Central Florida 2002.
6. R.H. Anderson, "Close-up imaging of documents and displays with lens arrays", Applied Optics Vol. 18(4), p. 477-484, February 1979.
7. J. Mir, "High resolution optical-addressing device and electronic scanner and/or printer apparatus employing such device", US Patent 4,377,753, 22 March 1983.
8. M. Kawazi and Y. Ogura, "Application of gradient index fiber arrays to copying machines", Applied

Optics 19(7), p. 1105-1112, April 1980

9. L. Erdmann, K. J. Gabriel, "High-Resolution Digital Integral Photography by use of a Scanning Microlens Array", Applied Optics 40(31), p. 5592-5599, November 2001.
10. V. Shaoulov, J. Rolland, "Design and Assessment of Microlenslet-Array Relay Optics", Applied Optics 42(34), p. 6838-6845, December 2003.
11. V. Shaoulov, R. Martins, J. Rolland, "Compact microlenslet array-based magnifier", Optics Letters 29(7), p. 709-711, April 2004.
12. V. Shaoulov, R. Martins and J. Rolland, "Imaging with microlenslet arrays", Annual Meeting of SPIE 2003, SPIE Proceedings Vol. 5174, p. 11-18, Novel Optical Systems Design and Optimization VI; Eds. Jose M. Sasian, R. John Koshel, Paul K. Manhart, November 2003.
13. W. Cassarly, "Art of making efficient illuminator design fun", Annual Meeting of SPIE 2003, SPIE Proceedings Vol. 5186, p. 1-4, Design of Efficient Illumination Systems, Editor: R. John Koshel, November 2003.

**APPENDIX: C HEAD-MOUNTED DISPLAY BY INTEGRATION OF
PHASE-CONJUGATE MATERIAL**

(12) **United States Patent**
Martins et al.

(54) **HEAD-MOUNTED DISPLAY BY INTEGRATION OF PHASE-CONJUGATE MATERIAL**

(75) Inventors: **Ricardo F. Martins**, Orlando, FL (US); **Jannick Rolland**, Chuluota, FL (US); **Yonggang Ha**, Orlando, FL (US)

(73) Assignee: **Research Foundation of the University of Central Florida, Inc**, Orlando, FL (US)

(*) Notice: Subject to any disclaimer, the term of this patent is extended or adjusted under 35 U.S.C. 154(b) by 0 days.

(21) Appl. No.: **11/128,514**

(22) Filed: **May 13, 2005**

Related U.S. Application Data

(60) Division of application No. 10/418,623, filed on Apr. 19, 2003, which is a continuation-in-part of application No. 10/090,070, filed on Mar. 1, 2002, now Pat. No. 6,731,434.

(60) Provisional application No. 60/292,942, filed on May 23, 2001.

(51) **Int. Cl. GO2B 27/14**(2006.01)

(52) **U. S. C1. 359/630; 345/7**

(58) **Field of Classification Search** 359/639-631, 359/636-640, 649; 345/7-9

See application file for complete search history.

(56) **References Cited**

U.S. PATENT DOCUMENTS

3,200,702 A 8/1965 Giordano 353/7

(10) **Patent No.:** **US 6,999,239 B1**

(45) **Date of Patent:** **Feb. 14, 2006**

4,348,185 9/1982	Breglia et al.434/43
A	
4,669,810 6/1987	Wood350/3.7
4,753,522 6/1988	Nishina et al.350/470
5,013,135 5/1991	Yamamura359/630
5,172,272 12/1992	Aoki359/654
5,189,452 2/1993	Hodson et al.353/94
5,526,183 6/1996	Chen359/629
5,572,229 11/1996	Fisher
5,621,572 4/1997	Ferguson 359/630
5,808,801 9/1998	Nakayama et al. ... 359/630
6,100,862 8/2000	Sullivan 345/88
6,147,805 11/2000	Ferguson 359/630
6,160,666 12/2000	Rallison et al. 359/630
6,236,511 5/2001	Brown359/634

* cited by examiner

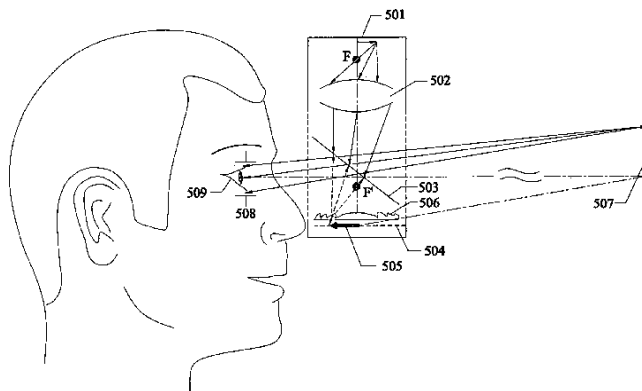
Primary Examiner—Huy Mai

(74) *Attorney, Agent, or Firm—Brian S. Steinberger; Law Offices of Brian S. Steinberger, P.A.*

(57) **ABSTRACT**

This invention has incorporated projective optics and phase conjugate material thus eliminating the requisite use of an external phase conjugate material to provide a see-through head mounted projective display. A key component of the invention is the use of optical imaging technology in combination with projective optics to make this revolutionary technology work. In previous head mounted projective displays the phase conjugate material had to be placed in the environment to display images, but in this invention one is not limited to the use of an external phase conjugate material but further extends its use to outdoor see-through augmented reality to produce images using the see-through head mounted projective display system. Furthermore, this invention extends the use of projective head mounted displays to clinical guided surgery, surgery medical, an outdoor augmented see-through virtual environment for military training and wearable computers.

9 Claims, 14 Drawing Sheets



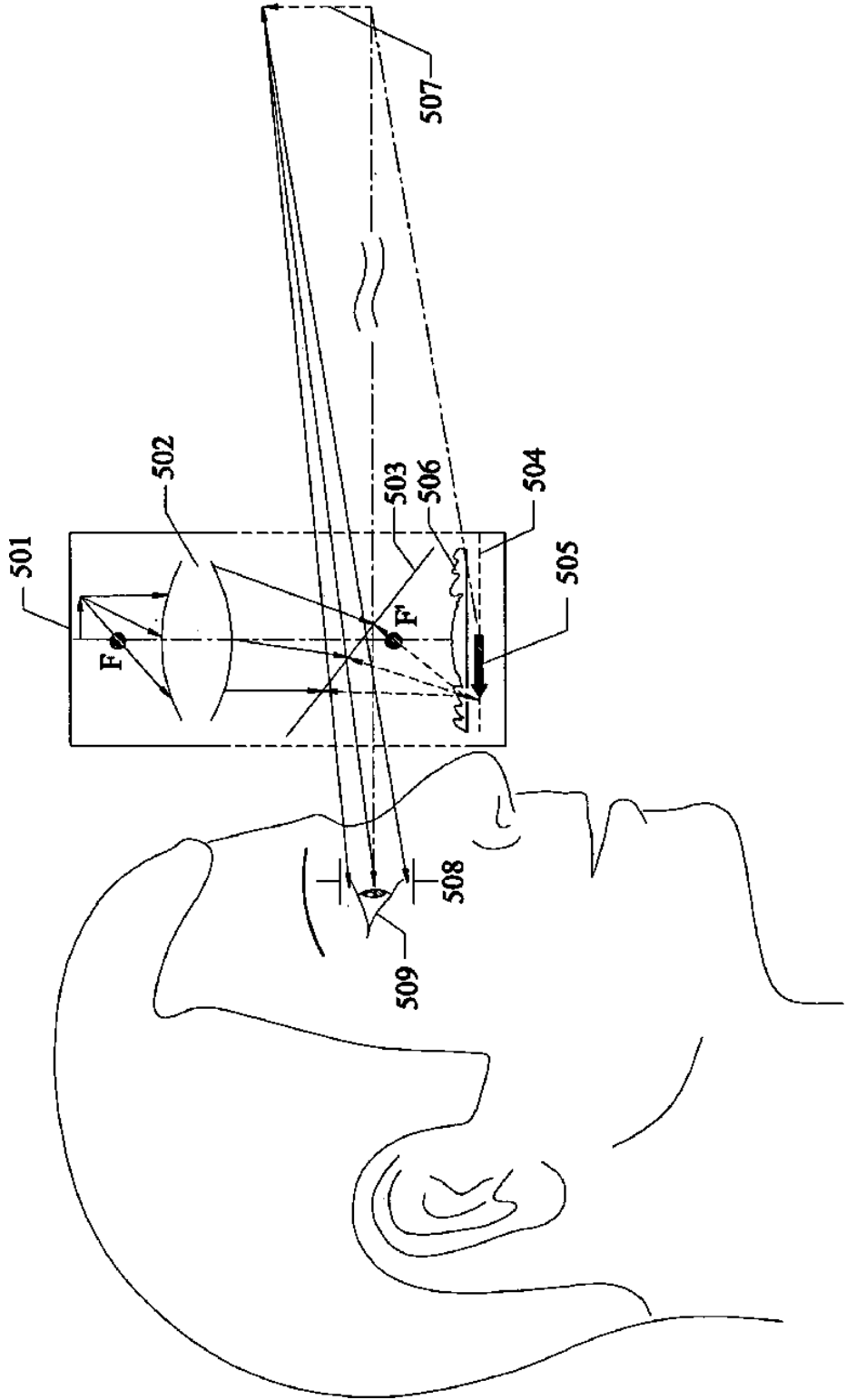


Fig. 1

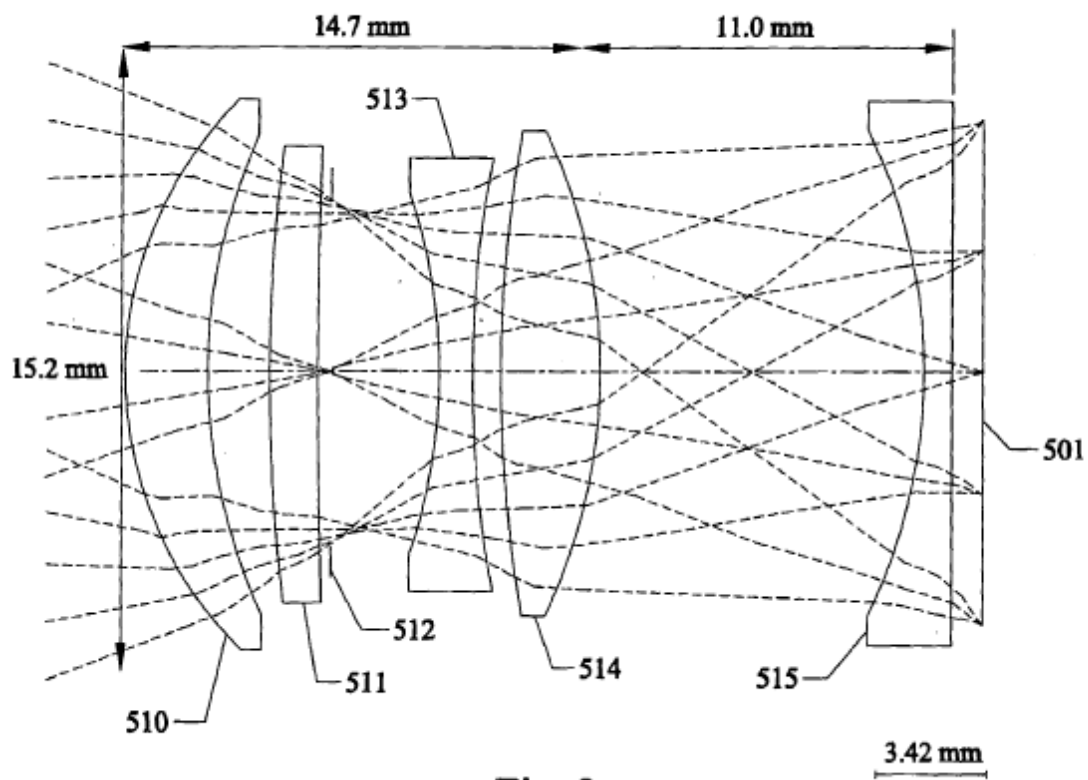


Fig. 2

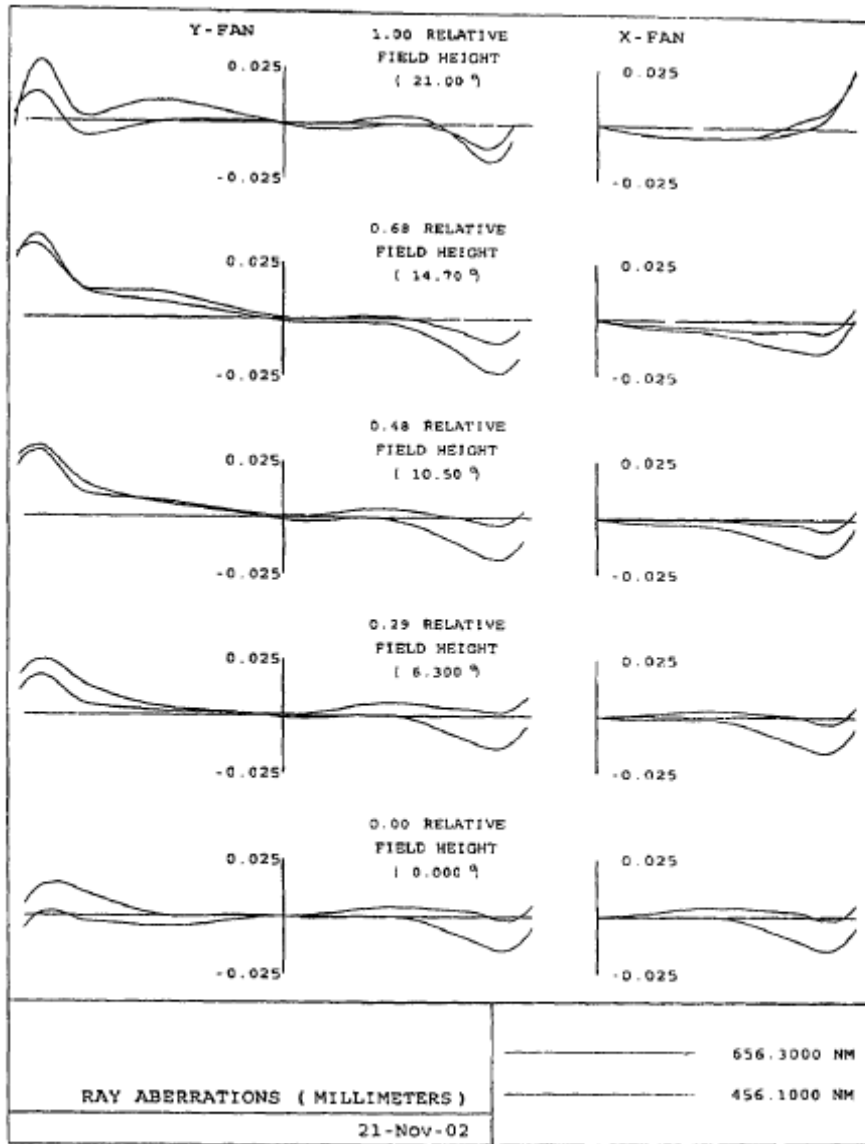


FIG. 3

**LOGITUDINAL
SPHERICAL ABER.**

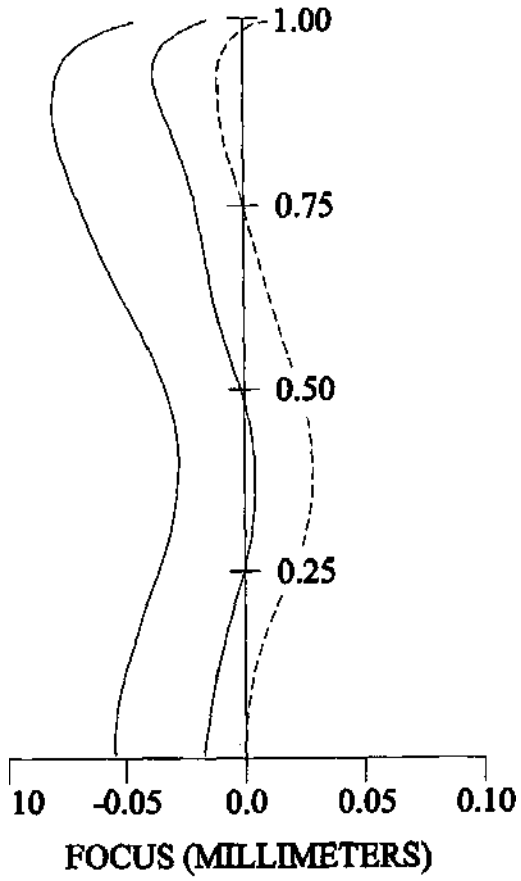


Fig. 4

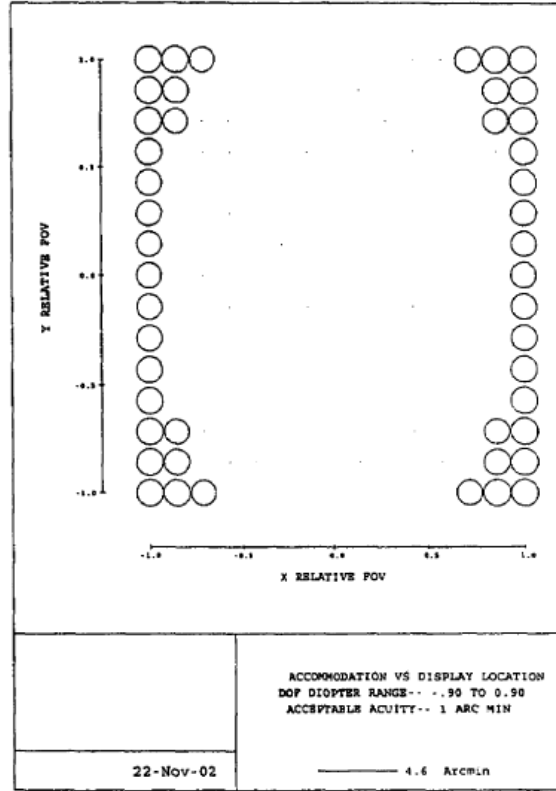


FIG. 5

ASTIGMATIC
FIELD CURVES

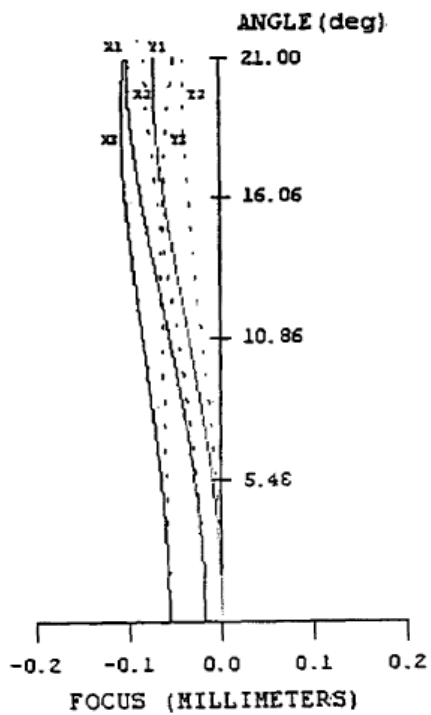


Fig. 6

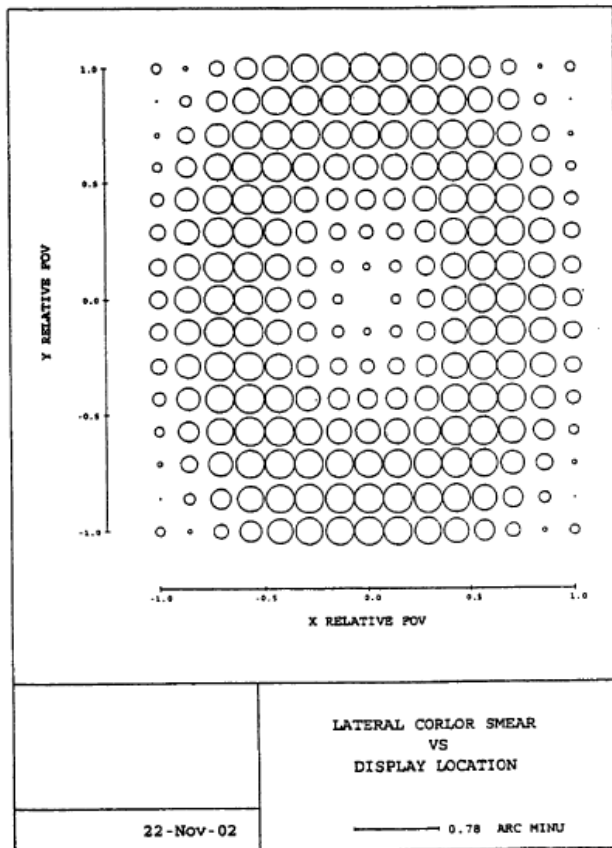


FIG. 7

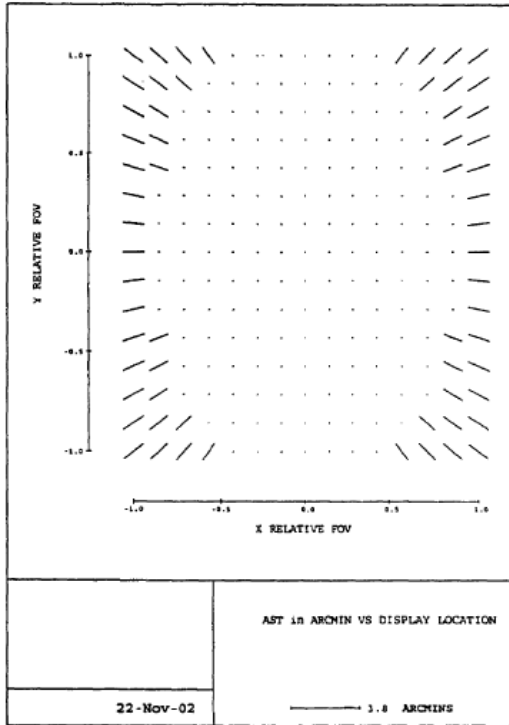


FIG. 8

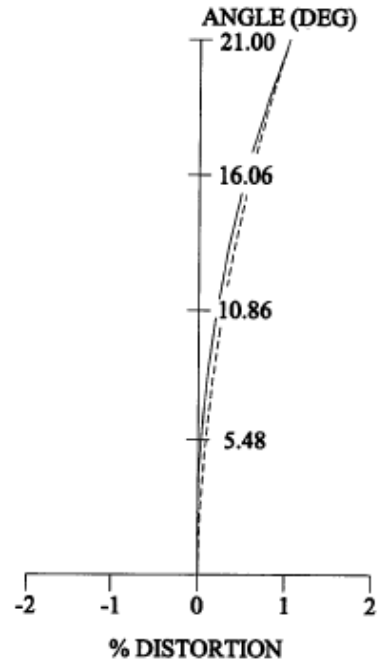


Fig. 9

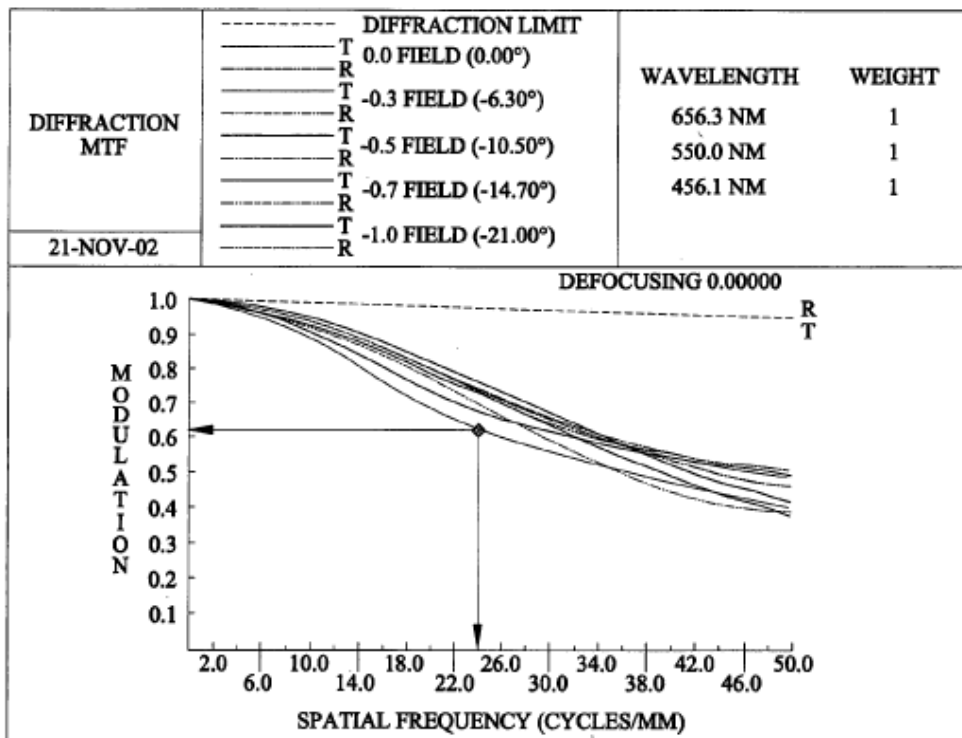


Fig. 10

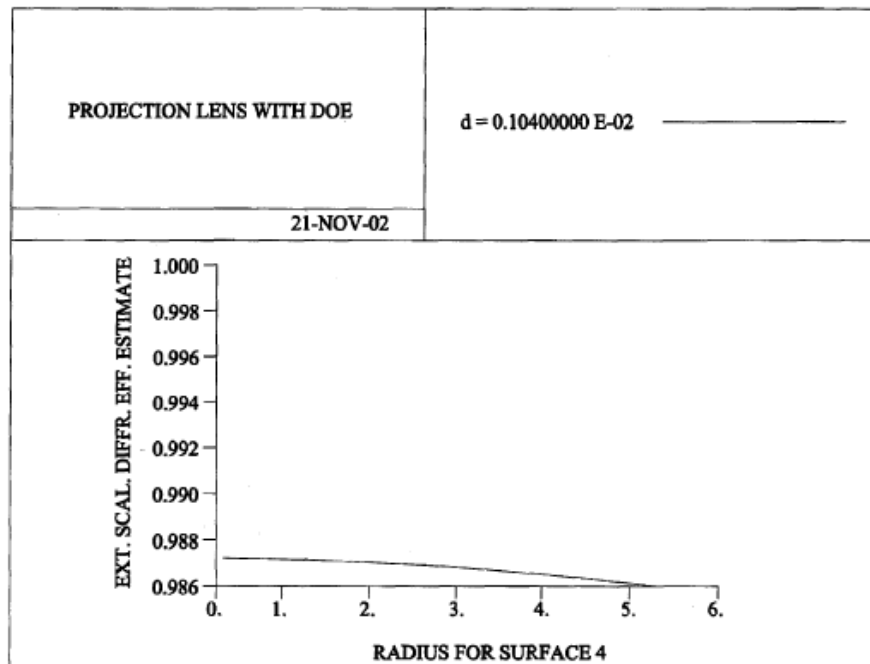


Fig. 11

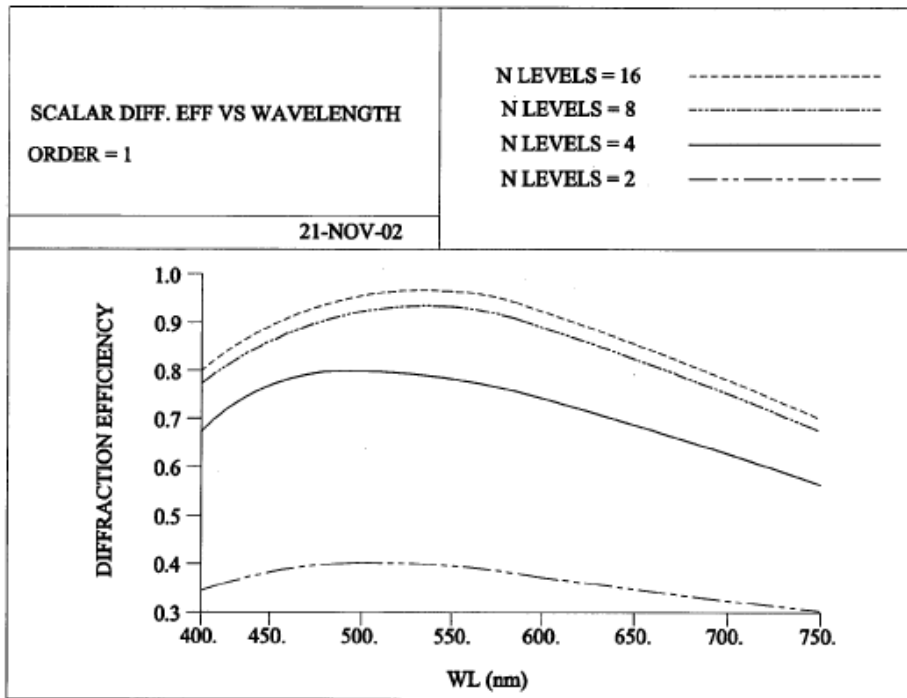


Fig. 12

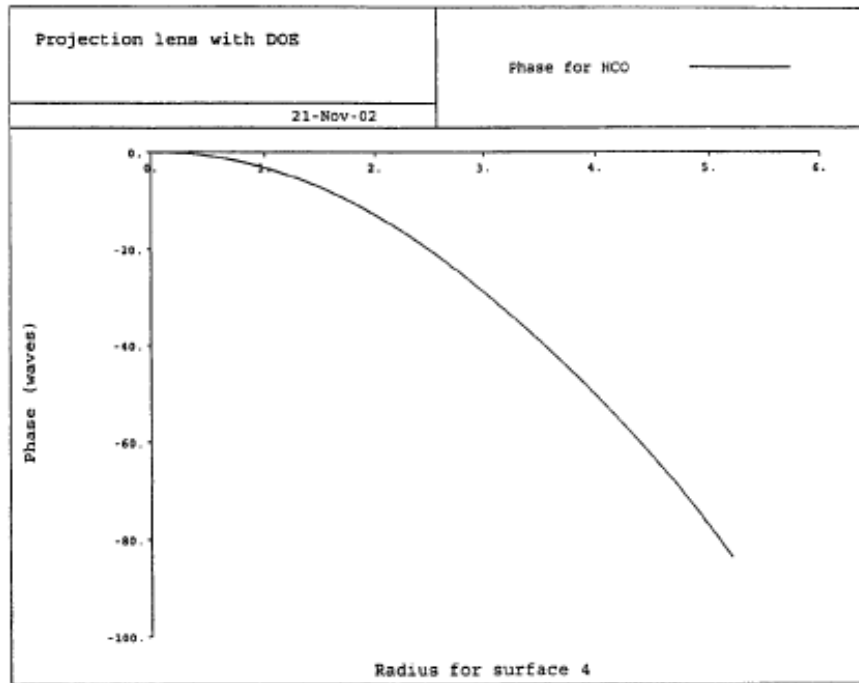


FIG. 13

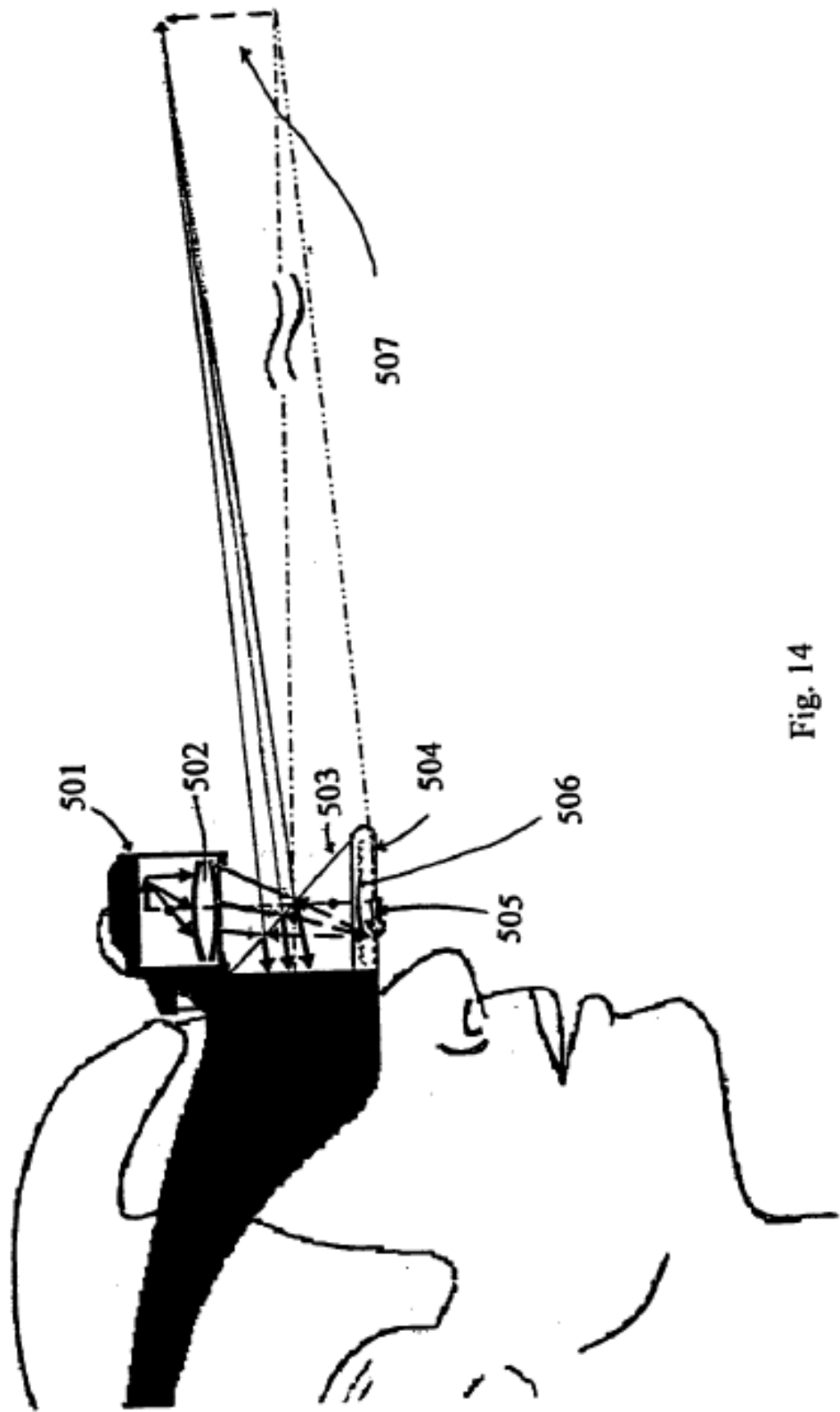


Fig. 14

1

HEAD-MOUNTED DISPLAY BY INTEGRATION OF PHASE-CONJUGATE MATERIAL

This invention is a Divisional Application of U.S. application Ser. No. 10/418,623 filed Apr. 19, 2003, now allowed, which is a Continuation-In-Part (CIP) of U.S. application Ser. No. 10/090,070 filed Mar. 1, 2002, now U.S. Pat. No. 6,731,434 which claims the benefit of priority of U.S. Provisional Application 60/292,942 filed May 23, 2001, and 10 was funded in part by grant number 6502562 awarded by the Army STRICOM SNE.

FIELD OF INVENTION

This invention relates to a head mounted projection display (HMPD), and in particular to a compact lens assembly having a projection display interior of the HMPD for a teleportal augmented reality system.

BACKGROUND AND PRIOR ART

Networked virtual environments allow users at remote locations to use a telecommunication link to coordinate work and social interaction. Teleconferencing systems and 25 virtual environments that use 3D computer graphic displays and digital video recording systems allow remote users to interact with each other, to view virtual work objects such as text, engineering models, medical models, play environments and other forms of digital data, and to view each 30 other's physical environment.

A number of teleconferencing technologies support collaborative virtual environments which allow interaction between individuals in local and remote sites. For example, video-teleconferencing systems use simple video screens 35 and wide screen displays to allow interaction between individuals in local and remote sites. However, wide screen displays are disadvantageous because virtual 3D objects presented on the screen are not blended into the environment of the room of the users. In such an environment, local users 40 cannot have a virtual object between them. This problem applies to representation of remote users as well. The location of the remote participants cannot be anywhere in the room or the space around the user, but is restricted to the screen.

Head-mounted displays (HMDs) have been widely used for 3D visualization tasks such as surgical planning, medical training, or engineering design. The main issues of the conventional eyepiece-based HMD technology include tradeoffs between resolution and field-of-view (FOV), and 50 between compactness and eye clearance, the presence of large distortion for wide FOV designs, the conflict of accommodation and convergence, the occlusion contradiction between virtual and real objects, the challenge of highly precise registration, and often the brightness conflict with 55 bright background illumination. The concept of head-mounted projective displays (HMPDs) is an emerging tech-

2

IEEE 1997 Virtual Reality Annual International Symposium, IEEE Computer Soc. Press. 1997, pp. 130-7. Los Alamitos, Calif., USA.].

Also on Apr. 15, 1997, a U.S. Pat. No. 5,621,572 was also issued to Ferguson on the conceptual idea of a display, i.e. optical, system for head mounted display using phase conjugate material and method of displaying an image. Independently, the technology of HPMD was developed by Parsons and Rolland as a tool for medical visualization [See Parsons and Rolland, "A non-intrusive display technique for providing real-time data within a surgeon's critical area of interest. "Proceedings of Medicine Meets Virtual Reality 98, 1998, pp. 246-251"]. After the initial proof of concept using off-the-shelf components, a first-generation custom-designed HMPD prototype was built to investigate perception issues and quantify some of the properties and behaviors of phase conjugate materials in an imaging system. Since, the projection system of the first-generation prototype was custom designed using a double-Gauss lens structure and built from commercially available components. The total weight of each lens assembly was about 50 grams (already a significant reduction compared to using off-the-shelf optics) with mechanical dimensions of 35 mm in length by 43 mm in diameter.

Common to all these teleconferencing systems is the use of lenses of various configurations and weights with distortions, lack of clarity and smearing of the televised images. Representative of lenses that might at first glance appear to be useful in the teleconferencing systems are also shown in: U.S. Pat. No. 5,526,183 by Chen who teaches the use of a lens combining diffractive elements of both glass and plastic to reduce the weight and size of the lens within a conventional helmet mounted display rather than the necessary projective helmet mounted display;

U.S. Pat. No. 5,173,272 by Aoki which discloses a four element high aperture lens with glass elements making it too heavy for helmet mounting;

U.S. Pat. No. 4,753,522 by Nishina et al which lens features all 4 plastic elements and is fully symmetrical which latter property is imposed by its restricted application—a copy machine lens; and,

U.S. Pat. No. 4,669,810 by Wood which shows a head-mounted display with many (more than 4) optical elements in the relay optics.

Consequently, there is a need for a HMPD augmented reality display that mitigates the above mentioned disadvantages and has the capability to display virtual objects and environments, superimposes virtual objects on the "real world" scenes, provides "face-to-face" recording and display, be used in various ambient lighting environments, and corrects for optical distortion, while minimizing weight, computational power and time. Lightweight, compactness, enhanced mobility and improved fidelity of the field of view are always of basic importance and/or highly desirable, particularly, for head-mounted devices.

nology that can be thought to lie on the boundary of conventional HMDs, and projective displays such as the CAVE Technology.

The basic HMPD concept of projection head-mounted display was early disclosed by Fisher Nov. 5, 1996, in U.S. Pat. No. 5,572,229.

Also a first international presentation was done by Kijima and Ojika in 1997 [See Kijima and Ojika, "Transition 65 between virtual environment and workstation environment with projective head-mounted display." Proceedings of

SUMMARY OF THE INVENTION

The first object of the present invention is to provide a HMPD with phase conjugate material integrated for use of see-through augmented reality within the HMPD.

The second object of this invention is to allow extension of the HMPD to mobile outdoors environment, as well as those environments in which the phase conjugate material can not be used in the environment, such as surgical procedures.

US 6,999,239 B1

3

The third object of this invention is to provide a user of the HMPD the means of a mobile teleportal augmented reality system with or without the use of phase conjugate material located in the environment.

A preferred embodiment of the invention encompasses a head mounted projection display (HMPD) comprising in combination: a component assembly for displaying computer generated image from a micro display; an optical assembly for projecting virtual images and said computer generated images to a user's eye or eyes for monocular or 10 binocular viewing; phase conjugate material for receiving and projecting said virtual images; an imaging lens for magnification of said phase conjugate material; and, all of which are located internally of the housing of said HMPD assembly. The lens can be other optical elements that may be 15 used for imaging, including Fresnel lens, microlenslet arrays, prisms, folding flat or curved mirrors, adaptive optics components, micro-optics components, phase plates and any combinations of the optical lenses. An additional preferred embodiment relates to a method of forming a HMPD 20 assembly comprising the steps of: positioning the HMPD helmet on the user's head; displaying virtual images to said user's eye or eyes by a micro display disposed within said helmet; providing a phase conjugate material for also displaying said virtual images from a display source integrated 25 with the interior surface of said helmet to said user's eye; and, providing an imaging lens, such as a Fresnel lens and others noted above for magnification of said phase conjugate material whereby said magnified screen is projected to the user's eye or eyes.

Further objects and advantages of this invention will be apparent from the following detailed description of presently preferred embodiments which are illustrated schematically in the accompanying drawings.

35

BRIEF DESCRIPTION OF THE FIGURES

FIG. 1 is a concept illustrative cross-sectional view of the projection head mounted display (HMPD) assembly placed on the user's head, where the novel aspects of the invention are shown.

FIG. 2 shows the cross-sectional layout of the novel projection lens layout of the invention.

FIG. 3 shows the residual ray aberrations in the image

4

FIG. 12 shows the Scalar Diffraction Efficiency versus Wavelength of the Diffractive Optical Element (DOE) optical element.

FIG. 13 shows the surface profile of the DOE.

FIG. 14 shows how the HMPD can be attached to the user's head.

DESCRIPTION OF THE PREFERRED EMBODIMENTS

Before explaining the disclosed embodiments of the present invention in detail, it is to be understood that the invention is not limited in its application to the details of the particular arrangements shown since the invention is capable of other embodiments. Also, the terminology used herein is for the purpose of description and not of limitation.

It would be useful to discuss the meanings of some words used herein and their applications before discussing the compact lens assembly of the invention including: HMPD—helmet mounted projection display; Singlet—single lens element;

EFL—effective focal length;

F"—f-number;

OAL—overall length;

FOV—field of view (given in degrees for the diagonal of the display);

EPD—entrance pupil diameter;

AMLCD—active matrix display;

Conjugate—image of each other;

Fresnel lens—a lens in which one collapses a surface into annular zones to a thin plate;

Microlenslet array—an array of miniature lenses comprised to replace a conventional lens;

Phase conjugate material—retro-reflective screen;

Distortion—warping of the image;

Arcminutes—an arcminute is the limit of visual acuity of the visual human system with one degree visual angle corresponds to 60 arcminutes;

Color Smear—a small spreading of the color spectrum in a point image;

Modulation—contrast;

DOE—diffractive optical element; and,

MTF—modulation transfer function.

plane over points in the field of view.

FIG. 4 shows the longitudinal spherical aberration curves shifted on the longitudinal axis denoting some residual lateral color occurring in visual space across the spectral wavelengths.

FIG. 5 illustrates the residual blur of the perceived image 50 which shows to be about 1.3 arcmin at all points in the image vs. display location.

FIG. 6 shows the astigmatic field curves over the entire field of view with the residual lateral color.

FIG. 7 shows the residual lateral color smear vs. display location to be less than about 1 arcmin over the entire field of view.

FIG. 8 shows the astigmatism in arcminutes versus display location of the final image being projected from the 60 miniature display inside the HMPD on the image plane.

FIG. 9 shows the amount of residual distortion to be about 1% over the entire field of view.

FIG. 10 shows the Diffraction MTF curves which illustrate how different spatial frequency of a scene is perceived.

FIG. 11 shows the Scalar Diffraction Efficiency Estimate versus apparent height of the diffraction optical element.

Referring now to FIG. 1 of the instant Application, a miniature display 501 is located beyond the focal point of a projection lens 502 which is used to display computer-generated images into a virtual environment. Rays traveling from the computer generated miniature active matrix display 501 (exemplified by a 0.6 inch OLED microdisplay purchased from eMagin Corporation) through the novel projection lens 502 (exemplified by an about 42 degree lens produced according to the disclosure of U.S. patent application Ser. No. 10/090,070 filed Mar. 1, 2002) provide an intermediary image 507 which is conjugate to the projected image 505.

When the phase conjugate material screen 504 (purchased from 3M Corporation) is at either the focal plane or within the focal plane of the lens 506 (commercially available from Edmund Scientific), it reflects rays at the same incoming angle in the reverse and opposite direction traveling toward the beamsplitter 503 (commercially available from Edmund Scientific) into the eye 509 of the user of the novel HMPD of the invention. When the lens 506 is placed at its focal plane and combined phase conjugate material at optical infinity For the case of placing the lens 506 within the focal plane, the phase conjugate material 504 is optically placed at a finite distance from the user's eye 509. The user's eye

US 6,999,239 B1

5

509 will perceive the projected image 505 from the exit pupil 508 of the optical system. The unique novelty of the head mounted display of the invention is that all components, i.e., 501-506 and 508-509, is within the helmet of the HMPD as indicated by the dotted lines of FIG. 1.

Refer now to FIG. 2 which shows in cross-section the projection lens 502 referenced in FIG. 1. The lens 502 is composed of a two glass singlet lenses, 510 and 514 respectively, two plastic singlet lenses, 511 and 513 respectively, and the stop surface 512 which is in the middle of glass-plastic and plastic-glass composition. In particular, the second surface of plastic singlet lens 511 is designed with a diffractive optical element (DOE), and the first surface of plastic singlet 513 is an aspherical surface. A single field flattener 515 is placed relatively close to the miniature display 501 to compensate field aberrations. Such a novel optical design makes it possible to achieve compactness, light-weight (<10 g per eye), as well as good performance over the visual spectrum.

As noted above with reference to lens 502, projective lens systems of this type are taught in co-pending U.S. patent application Ser. No. 10/090,070 filed Mar. 1, 2002 of common assignee with the instant Application and fully incorporated herein by reference thereto; and, in co-pending United States Patent Application designated UCF-380C1P-002 filed Nov. 1, 2002 of common assignee also with the instant Application and fully incorporated herein by reference thereto.

The specification of the highly useful novel 42 degree lens 502 as disclosed in the design system shown in FIG. 2 is:

6

axis called barrel distortion or pincushion causing the sides of the virtual image to move inward.

FIG. 10 shows the MTF plot which has a design criterion of 20% modulation at 24 cycles/mm. In the design of the invention, it is shown that at 24 cycles/mm, the modulation is above 60%. A minimum of 20% is typically required. Thus, this lens performance supersedes the requirements.

FIG. 11 shows the scalar diffraction efficiency which is estimated for a lens radius of 5.517 mm at 98.7%.

FIG. 12 shows the scalar diffraction efficiency vs. wavelength for the number of zones "N" levels of the diffractive optical element (DOE), with a vertical axis as percentage and the horizontal axis representing the visible spectrum.

FIG. 13 shows the continuous phase profile across the DOE radius in lens unit.

FIG. 14 shows a HMPD attached to a user's head and containing fully the integration of the phase conjugate material 504, material and the lens, 506 and as earlier emphasized in the discussion of FIG. 1 with respect to the 06 invention detailed herein, all the components, i.e., 501-506, and 508-509, which provides the virtual environment seen by the user's eye, 509 are located within the helmet (dotted lines) although one or more of the components 501, 502, 503, 504, 506, 507, 508 and projected image, 505, can when appropriate be located outside of the helmet.

Refer again to FIG. 2 for showing of the final layout of the projection lens. As shown therein,

501---Miniature display

502---Projection lens

510---Glass singlet 1

Effective focal length (EFL)=19.5382 mm; F#=1.62; Overall-length (OAL)=25.6459 mm; Field of view (FOV)=42°; EPD=12 mm

The evaluation of the projective lens, shown in FIG. 2, has been analyzed and the resulting plots have been provided in FIGS. 3-4, 6, 9-13 along with the visual performance graphs shown in FIGS. 5, 7 and 8. The overall assessment of the projective lens design is shown to have negligible aberration in visual space.

FIG. 3 shows various points in the field 0, 0.3, 0.7 and 1 in order to determine what residual aberrations are present in the referenced optical lens system. The X-Y ray fan plot has a maximum vertical range of ± 0.025 mm having residual aberrations which are further evaluated.

FIG. 4 quantifies spherical aberration across wavelengths. The shapes of the curves are the same for all three wavelengths meaning no spherochromatism. The curves are shifted on the longitudinal axis denoting some residual lateral color will occur in visual space. Lateral color in visual space is further quantified in FIG. 9.

FIG. 5 shows the accommodation vs. display location the largest circle measures approximately 0.8 mm on the Figure, corresponding to about 1.3 arcmin which is about human visual acuity.

FIG. 6 shows the astigmatic field curves of the projection lens which are further evaluated in FIG. 8.

FIG. 7 shows lateral color smear vs. display location. The variation is about 0.25 arcmin, which can not be resolved by the human eye; therefore one can neglect lateral color.

FIG. 8 shows astigmatism curves expressed in arcminutes. The amount of astigmatism results in about 1.2 arcminutes which is about human visual acuity.

FIG. 9 shows an amount of distortion of 1% at the edge of the field of view. Distortion warps the virtual image displayed by either an elongation in the longitudinal image

- 511----Plastic singlet 1
- 512----Stop
- 513----Plastic singlet 2
- 514----Glass singlet 2
- 515----Single field flattener

TABLE 1

<u>Optical lens specification</u>	
Parameter	Specification
<u>Object: Color OLED</u>	
a. Size	Approximately 0.6" inch in diagonal
b. Active display area	approximately 9 mm x approximately 12 mm
c. Resolution	800 x 600 pixels
<u>Lens:</u>	
a. Type	Projection lens
b. Effective focal length	Approximately 19.5 mm
c. Exit pupil diameter	Approximately 12 mm
d. Eye relief	Approximately 25 mm
e. No. of diffractive surface	Approximately 1
<u>Other Parameters:</u>	
Wavelength range	Approximately 656 to approximately 486 nm
FOV	Approximately 42.0° in diagonal
Distortion	Approximately <2.0% over entire FOV

OVERALL DESCRIPTION AND USES

The nature of this invention is to incorporate projective optics and phase conjugate material without the inhibiting, hindering and limiting requisite use of an external phase conjugate material to provide a see-through head mounted projection display. A key component of the invention is not only the integration of the phase conjugate material and projection optics within the HMPD but surprisingly also the

7

use of a lens in combination with this novel projection enclosed system markedly facilitates the operability of this revolutionary technology. In previous head mounted projection displays phase conjugate material had to be placed in the environment to display images, but in this invention the user is not limited by the requisite use of an exterior phase conjugate material.

Refer again to FIG. 1 for showing of the final layout of the components within the HMPD which are identified with reference numbers 501 through 507. As shown therein,

501---Miniature display
 502---Projection lens
 503---Beam splitter
 504---Phase conjugate material
 505---Projected image
 506---Lens
 507---Intermediary image
 508---Entrance pupil
 509---Eye

As shown in FIG. 1, the light from the miniature display 501 strikes the beam splitter 503 after passing through the projection lens 502. The miniature display 501 may display a virtual image as well as a computer generated image. A portion of the light striking the beam splitter 503 is reflected to produce the intermediary image 507. The remainder of the light passes through the beam splitter 503 and lens 506 and produces the projected image 505 (hollow arrow) on the phase conjugate material 504. The light from the projected image 505 is reflected back to the beam splitter as shown by the upwardly directed arrows. The reflected light strikes the beam splitter 503 and is reflected toward the eye 509 within the area shown as the pupil entrance 508. The lens 506 can be an optical element such as a Fresnel lens, microlenslet array, prism, flat mirror, curved mirror, folding mirror, phase plate, adaptive optic component, micro-optics component and micro-phase plate component or any combination of the optical lenses. Placement of the lens 504 and phase conjugate material 504 at a location outside of the user's line of sight extends usage to see-through augmented reality to produce images using the see-through head mounted projective display system.

The invention improves upon not being limited to use of the phase conjugate material in the environment but dramatically extends the use of outdoor see-through augmented reality. Furthermore, this invention extends the use of projection head mounted displays to clinical guided surgery, medical surgery, outdoor augmented see-through virtual environment for military training and wearable computers, and for use with binoculars. In these latter applications, a head mounted projection display (HMPD) optical lens assembly comprising in combination a projection lens having a field of view (FOV) of up to approximately ninety degrees and of an overall weight of less than approximately 10 grams; and a micro display ranging from approximately

8

0.2 inches up to approximately 2 inch diagonal size whereby an intermediate image will be viewed by the user's eye is surprisingly and particularly useful.

While the invention has been described, disclosed, illustrated and shown in various terms of certain embodiments or modifications which it has presumed in practice, the scope of the invention is not intended to be, nor should it be deemed to be, limited thereby and such other modifications or embodiments as may be suggested by the teachings herein are particularly reserved especially as they fall within the breadth and scope of the claims here appended.

We claim:

1. Ahead mounted projection display(HMPD) optical lens assembly comprising in combination:

(a) a projection lens having a field of view (FOV) of up to approximately ninety-degrees and of an overall weight of less than approximately 10 grams; and
 (b) a micro display ranging from approximately 0.2 inches up to approximately 2 inch diagonal size

whereby an intermediate image will be viewed by a user's eye.

2. The assembly of claim 1 also including in combination a lens for imaging of said micro display whereby said imaged displays is further projected to the user's eyes.

3. The assembly of claim 1 also including in combination a lens means for magnification of said micro display whereby said magnified display is further projected to the user's eyes.

4. The assembly of claim 1, further comprising: a single phase conjugate component for receiving and projecting virtual images to the user's eyes.

5. Ahead mounted projection display(HMPD) optical lens assembly, the assembly comprising in combination:

a projection lens with a field of view (FOV) of up to approximately ninety-degrees; and
 a display having a diagonal size of up to approximately 2 inches, wherein an intermediate image is viewable by a user's eye.

6. The assembly of claim 5, wherein the assembly includes an overall weight of less than approximately 10 grams.

7. The assembly of claim 5, further comprising: an imaging lens for imaging of said display wherein said imaged display is further projected to the user's eyes.

8. The assembly of claim 5, further comprising: a magnification lens for magnifying said display wherein said magnified display is further projected to the user's eyes.

9. The assembly of claim 5, further comprising:
 a single phase conjugate component for receiving and

projecting virtual images to the user's eyes

APPENDIX: D COMPACT MICROLENSLET ARRAYS IMAGER

(12) **United States Patent**
Chaoulov et al

(54) **COMPACT MICROLENSLET ARRAYS
IMAGER**

(75) Inventors: **Vesselin I. Chaoulov**, Orlando, FL (US);
Ricardo F. Martins, Orlando, FL (US);
Jannick P. Rolland, Chuluota, FL (US)

(73) Assignee: **Research Foundation of the University
of Central Florida, Inc.**, Orlando, FL
(US)

(*) Notice: Subject to any disclaimer, the term of this
patent is extended or adjusted under 35
U.S.C. 154(b) by 0 days.

(21) Appl. No.: **10/910,148**

(22) Filed: **Aug. 3, 2004**

(65) **Prior Publication Data**

US 2005/0007673 A1 Jan. 13, 2005

Related U.S. Application Data

(63) Continuation-in-part of application No. 10/418,623, filed
on Apr. 19, 2003, now Pat. No. 6,963,454, and a
continuation-in-part of application No. 10/285,855, filed
on Nov. 1, 2002, now Pat. No. 6,804,066, which is a
continuation-in-part of application No. 10/090, 070,
filed on Mar. 1, 2002, now Pat. No. 6,731,434.

(60) Provisional application No. 60/492,453, filed on Aug. 4,
2003, provisional application No. 60/292,942, filed on
May 23, 2001.

(51) **Int. Cl.**

G02B 27/10 (2006.01)

(52) U. S. C1. 359/622; 359/630; 345/8 (58) **Field of
Classification Search** 359/619,

(10) **Patent No.: US 7,009,773 B2**

(45) **Date of Patent: Mar. 7, 2006**

359/621, 622, 626, 630; 349/11; 345/7-9 See
application file for complete search history.

(56) **References Cited U.S.**

PATENT DOCUMENTS

5,561,538 A *	10/1996 Kato et al.	349/5
5,621,572 A *	4/1997 Ferguson	359/630
5,796,522 A *	8/1998 Meyers	359/626
5,822,125 A *	10/1998 Meyers	359/621
6,310,713 B1 *	10/2001 Doany et al.	359/247
6,731,434 B1 *	5/2004 Hua et al.	359/619
6,804,066 B1 *	10/2004 Ha et al.	359/771

* cited by examiner

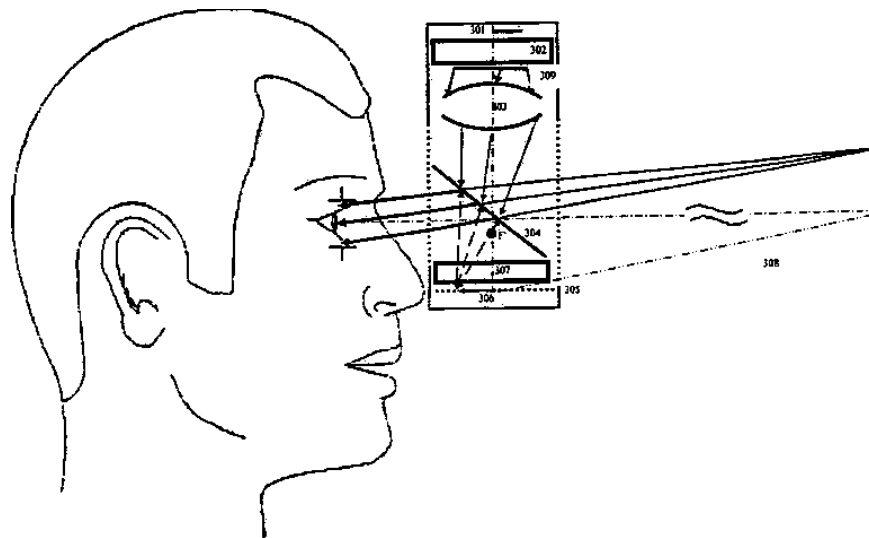
Primary Examiner—Huy Mai

(74) *Attorney, Agent, or Firm—Brian S. Steinberger; Law
Offices of Brian S. Steinberger, P.A.*

(57) **ABSTRACT**

Extremely compact and light-weight optical systems, apparatus,
devices and methods to image miniature displays. Such
systems include, for example, head-mounted projection
displays (HMPD), head-mounted displays (HMDs), and cameras
for special effects, compact microscopes and telescopes as well
as applications in which magnification and compactness are
design criteria. The invention includes an ultra-compact
imaging system based on microlenslet arrays and demonstrates
that such a system can achieve an object-to-image distance as
low as approximately 1.7 mm. with the usage of commercially
available microlenslet arrays. The replacement of bulk macro-
optical system by multi-aperture micro-optics is achieved.

10 Claims, 3 Drawing Sheets



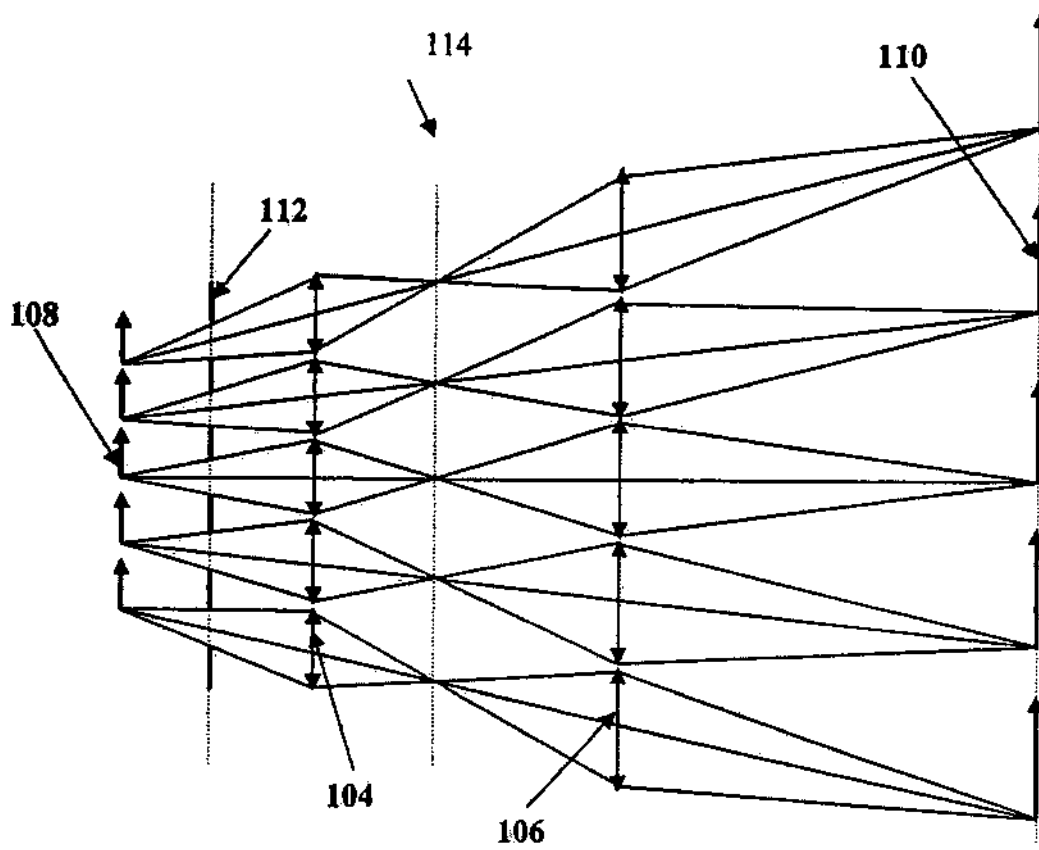


Figure 1

Object

Magnified Image



201

202

Figure 2

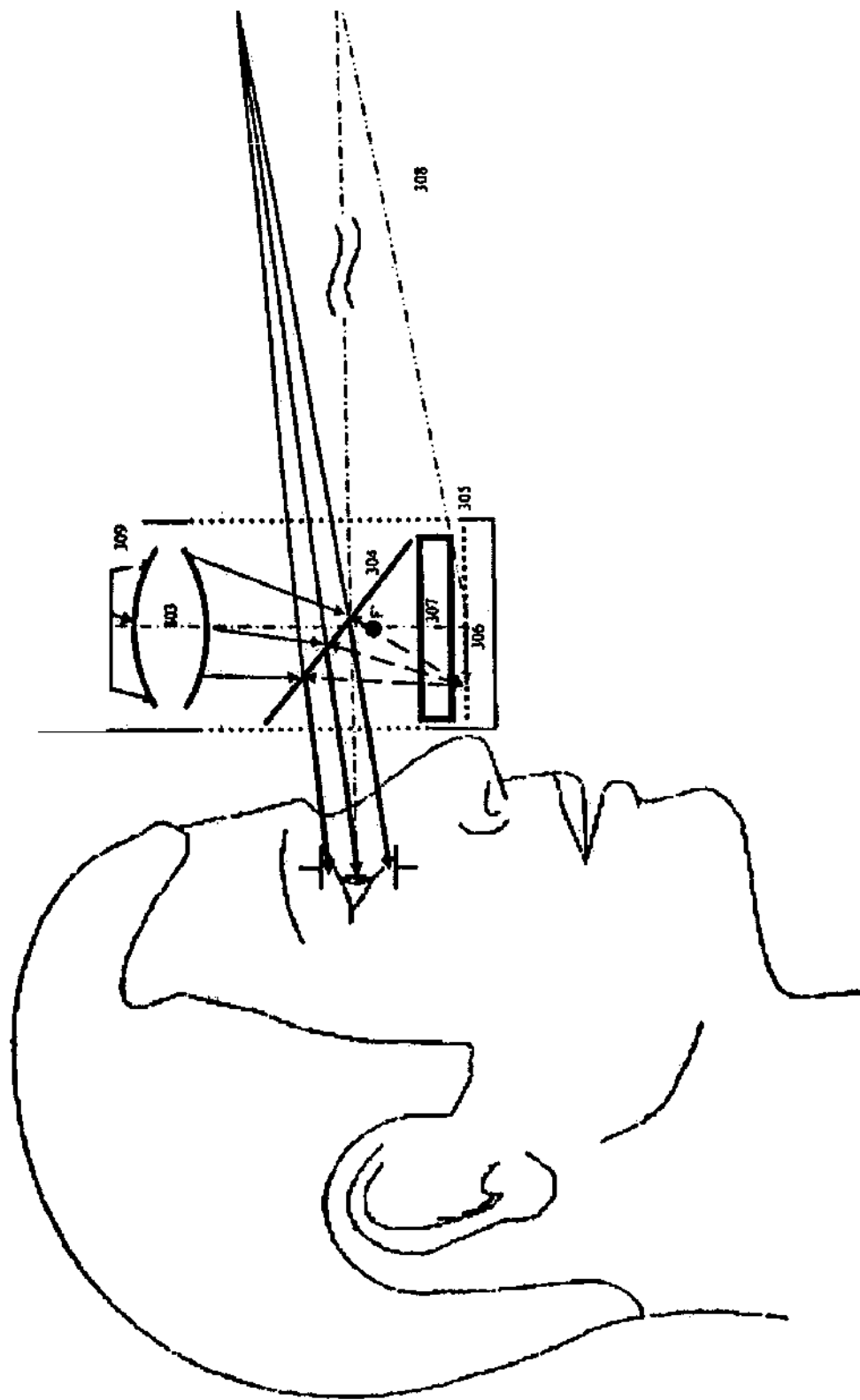


Figure 3

COMPACT MICROLENSLET ARRAYS IMAGER

This invention claims the benefit of priority to U.S. Provisional Patent Application No. 60/492,453 filed Aug. 4, 2003, and this application is a Continuation-In-Part of both U.S. patent application Ser. No. 10/285,855 filed Nov. 1, 2002, now U.S. Pat. No. 6,804,066 and U.S. patent application Ser. No. 10/418,623 filed Apr. 19, 2003, now U.S. Pat. No. 6,963,454 which are both a Continuation-In-Part of U.S. 10 patent application Ser. No. 10/090,070 filed Mar. 1, 2002, now U.S. Pat. No. 6,731,434, which claimed the benefit of priority to U.S. provisional application 60/292,942 filed May 23, 2001.

FIELD OF INVENTION

This invention relates to the replacement of a bulk single-aperture macro-optical systems by multi-aperture micro-optical systems, and more particularly to assemblies, systems, apparatus, devices and methods of utilizing arrays of lenses combined with appropriate baffles, so that an ultra-compact imaging system with chosen magnification or demagnification can be achieved.

BACKGROUND AND PRIOR ART

Networked virtual environments allow users at remote locations to use a telecommunication link to coordinate work and social interaction. Teleconferencing systems and virtual environments that use 3D computer graphic displays and digital video recording systems allow remote users to interact with each other, to view virtual work objects such as text, engineering models, medical models, play environments and other forms of digital data, and to view each other's physical environment.

A number of teleconferencing technologies support collaborative virtual environments which allow interaction between individuals in local and remote sites. For example, video-teleconferencing systems use simple video screens and wide screen displays to allow interaction between individuals in local and remote sites. However, wide screen displays are disadvantageous because virtual 3D objects presented on the screen are not blended into the environment of the room of the users. In such an environment, local users cannot have a virtual object between them. This problem applies to representation of remote users as well. The location of the remote participants cannot be anywhere in the room or the space around the user, but is restricted to the screen.

Head-mounted displays (HMDs) have been widely used for 3D visualization tasks such as surgical planning, medical training, or engineering design. The main issues of the conventional eyepiece-based HMD technology include tradeoffs between resolution and field-of-view (FOV), and between compactness and eye clearance, the presence of large distortion for wide FOV designs, the conflict of accom-

was built to investigate perception issues and quantify some of the properties and behaviors of the retro-reflective materials in imaging systems. The projection system of the first-generation prototype was custom designed using a double-Gauss lens structure and built from commercially available components. The total weight of each lens assembly was approximately 50 grams (already a significant reduction compared to using off-the-shelf optics) with mechanical dimensions of 35 mm in length by 43 mm in diameter.

Consequently, there is a need for a HMPD augmented reality display that mitigates the above mentioned disadvantages (in part by an internally mounted projected display that provides visible spectrum images without smears and of reduced weight) and has the capability to display virtual objects and environments, superimposes virtual objects on the "real world" scenes, provides "face-to-face" recording and display, be used in various ambient lighting environments, and corrects for optical distortion, while minimizing weight, computational power and time.

Useful lens assemblies of reduced weight and/or increased field of view (FOV) are taught in co-pending U.S. patent application Ser. No. 10/090,070, filed Mar. 1, 2002, now U.S. Pat. No. 6,731,434, which is incorporated by reference, of common assignee with the instant application. The double-Gauss lens disclosed therein has a FOV of approximately 52 degrees with an effective focal length of approximately 35 mm. Co-pending U.S. patent application Ser. No. 10/418,623, filed Apr. 18, 2003, which is incorporated by reference, of common assignee also with the instant application, discloses a compact lens assembly useful for HMPD systems of miniature display of 0.6" diagonal with a FOV of approximately 42 degrees and an effective focal length of approximately 17 mm.

Lightweight, compactness, enhanced mobility and improved fidelity of the field of view are always of basic importance and/or highly desirable, particularly, for head-mounted devices and for these reasons the quest for useful compact and lightweight continues. A key to novel solutions in compact light weight HMDs is to pre-magnify, within a very compact space, the microdisplay in the HMD before it is further imaged toward the eyes. Such an approach is the subject of the current invention. However, the ultra-compact magnifier is broadly applicable to all imaging applications where such magnification is required. Such applications include, but are not limited to, imaging systems that perform magnified-relaying (i.e. magnification greater than 1), demagnified-relaying (i.e. magnification is less than one), or relaying (i.e. magnification equal to one). Examples of such imaging systems include, but are not limited to, images in scanners, copiers, cameras, microscopes, projection systems, eyepieces, and telescopes,

SUMMARY OF THE INVENTION

The first object of the present invention is to provide an imaging assembly, system, apparatus, device and method of

modation and convergence, the occlusion contradiction between virtual and real objects, the challenge of highly precise registration, and often the brightness conflict with too bright background illumination. The concept of head-mounted projection displays (HMPDs) is an emerging technology that can be thought to lie on the boundary of conventional HMDs, and projection displays such as the CAVE technology.

After the initial proof of concept using off-the-shelf components, a first-generation custom-designed HMPD prototype

using an imaging system of reduced size utilizing arrays of lenses, for example microlenslet arrays.

The second object of this invention is to allow an increase of the apparent size of the miniature display in the HMD or HMPD, thereby making the system more compact.

The third object of the present invention is to allow for an object to be magnified (i.e. magnification greater than one), demagnified (i.e. magnification less than one) or relayed (i.e.

US 7,009,773 B2

3

. magnification equal to one) by using a compact magnifying or demagnifying optical system based on baffled arrays of microlenses.

The fourth object of the present invention is to replace single aperture bulk macro-optical system with compact multi-aperture micro-optical system.

The fifth object of the present invention is the use of microlenslet arrays in combination with the appropriate baffles to magnify the miniature display integrated in the HMPD or HMD.

Preferred embodiments of the invention encompasses assemblies, apparatus, systems, devices and methods of a lens useful in a head mounted projection display (HMPD) or equivalently a head-mounted display (HMD) having at least two microlenslet arrays in combination with appropriate baffles to magnify the miniature display.

Further objects and advantages of this invention will be apparent from the following detailed description of the presently preferred embodiments that are illustrated schematically in the accompanying drawings.

BRIEF DESCRIPTION OF THE FIGURES

FIG. 1 shows the cross-sectional layout of the novel optical imaging system, subject of this invention.

FIG. 2 shows the object and the magnified image, produced by the novel optical system presented in FIG. 1.

FIG. 3 shows the novel magnifying lens layout used in within an HMPD or HMD to magnify the miniature display integrated in an HMPD or HMD.

DESCRIPTION OF THE PREFERRED EMBODIMENTS

Before explaining the disclosed embodiments of the present invention in detail, it is to be understood that the invention is not limited in its application to the details of the particular arrangements shown since the invention is capable of other embodiments. Also, the terminology used herein is for the purpose of description and not of limitation.

As previously noted, this invention claims the benefit of priority to U.S. Provisional Patent Application No. 60/492, 453 filed Aug. 4, 2004, and this application is a Continuation-In-Part of both U.S. patent application Ser. No. 10/285, 855 filed Nov. 1, 2002, now allowed, and U.S. patent application Ser.

4

However, utilizing arrays of microlenses is part of the preferred embodiment since it leads to more compact HMPD and HMD systems.

EFL—effective focal length;

F"—f-number;

OAL—overall length;

FOV—field of view (given in degrees for the diagonal of the display).

Microlens(or microlenslet) arrays, as defined above, can be arrays of refractive microlenses, fabricated by various commercially available technologies, such as the gray-scale technology used by MEMS Optical Inc. or those developed by Adaptive Optics Inc. for example. Usually many microlenslet arrays can be replicated from a single master. Some companies such as MEMS Optical can design and fabricate refractive, diffractive, anamorphic, spherical, and aspherical positive and negative microlenses.

A typical microlens array has nearly diffraction limited performance, high internal transmittance, various lenslet and array geometry, high fill factor and low manufacturing cost, once the master is fabricated. Commonly, microlens arrays can be made of compression molded plastic or epoxy replicated on standard glass window of various thickness. If glass substrate is used, broadband anti-reflection coating is provided on the glass side of the window. Often the customer supplies their own glass substrate as well. The most common geometries of the lenslets are circular, square, and hexagonal and the most common geometry of the array itself is square. The aperture of each lenslet can be as small as approximately 15 microns or less, and the focal length can be as short as approximately 30 microns or less. Microlens arrays containing lenslets of various apertures and focal lengths are commercially designed and fabricated.

Micro-baffles can be sets of transparent holes designed and fabricated on opaque screen. Such micro-baffles can be commercially fabricated by various technologies, such as etching holes on a silicon substrate or masking out holes in glass slide with a chromed surface, for example.

The alignment and packaging of systems containing microlenslet arrays and micro-baffles is usually completed by the company that designs and fabricates the individual components. Various approaches including laser alignment are

No. 10/418,623 filed Apr. 19, 2003 which are both a Continuation-In-Part of U.S. patent application Ser. No. 10/090,070 filed Mar. 1, 2002, now U.S. Pat. No. 6,731,434, which claimed the benefit of priority to U.S. provisional application 60/292,942 filed May 23, 2001, all of which are incorporated by reference in the subject invention.

It would be useful to discuss the meanings of some words used herein and their applications before discussing the compact lens assembly of the invention including:

HMPD—head-mounted projection display. HMD—head-mounted display
Microlens (also called microlenslet)—miniature lenses of 60 diameter from a few microns (e.g. approximately 15 microns) to hundreds of microns (e.g. approximately 500 microns), and of focal length fractions of millimeters (e.g. approximately 0.016 mm) to a few millimeters (e.g. approximately 5 mm). It is to be understood that utilizing arrays of 65 microlenses is not a limitation of the current invention, since the invention can utilize arrays of lenses of any sizes.

US 7,009,773 B2

5

1000 microns and the diameter of each lenslet is approximately 120 microns. The compact imaging system 102 is capable of providing a magnification factor of approximately 2 in the image 110 with an overall object to image length of approximately 9 mm for a weight of approximately 5 1 gram.

In the compact microlenslet array imager, the first microlenslet array assembly 104, can be located in front of the object 108, and can be used to form an intermediary image in an intermediary image plane 114. The final image 110 can 10 be formed by the second microlenslet array assembly 106. The baffle 112, can be placed between the object 108 and the first microlenslet array assembly 104, and can consist of a set of micro-baffles with computed diameter of, for example, approximately 40 microns, and is used to limit the optical 15 paths through the system and thus suppresses the formation of undesired secondary images (also referred to in the optics literature as ghost images). Each microlenslet array assembly 104, 106 can be made of multiple arrays. Each array within an assembly can be made of optical materials such as, 20 but not restricted to, spherical lenses, aspherical lenses, lenses of multiple glasses, plastic lenses of various plastic materials, gradient index lenses, and liquid crystal lenses.

Referring now to FIG. 2, the first picture 201 shows the object to be imaged and the second picture 202 shows the 25 magnified image after the compact imaging system 102.

FIG. 3 shows the microlenslet array based imager 302, integrated within the concept of HMPD or equivalently HMD, used to magnify the miniature display 301. A min

used.

Further discussion of microlenslet arrays can be found in V. Shaoulov and J. Rolland, "Compact Relay Lenses Using Microlenslet Arrays", Proceedings of the SPIE: International Optical Design Conference 2002, Editors P. K. Manhart and J. M. Sasian, pp 74-79; V. Shaoulov and J. Rolland, "Design and assessment of Microlenslet array relay Optics", Applied Optics 42(34), 6838-6845, (December 2003); and V. Shaoulov, R. Martins, and J. P. Rolland, "Compact microlenslet array-based magnifier", Optics Letters 29(7), 1-3 (April 2004), for example.

Referring to FIG. 1, which shows, in cross-section, the compact imaging system 102 according to the instant invention, which as seen can consist of two dissimilar microlenslet arrays, a first microlenslet array 104 and a second microlenslet array 106, which in combination are used to magnify the object 108 into the image 110. The compact imaging system 102 has an opaque glass baffle 112 of circular shape, with dimension of approximately 45 microns diameter, interposed at the appropriate location between the object 108 and the first microlenslet array 104 [Shaoulov, Martins, Rolland, 2004]. The first microlenslet array 104 has a focal length of approximately 500 microns and the diameter of each lenslet is approximately 100 microns. The second microlenslet array 106 has a focal length of approximately

6

to a miniature display of approximately 0.5" with a FOV of approximately 42 degrees. The compact imaging system of the current invention markedly reduces the size and the weight of the optics used in HMPD and HMD systems and provides an increase in the FOV of the latter application Ser. No. 10/418,623 by increasing the miniature display size via the microlenslet array based imager before it is projected with the projection optics.

The evaluation of the microlenslet array-based projective 10 lens shown in FIG. 1, indicates a magnification of the miniature display by a factor of approximately 2 and indicates overall object to image length of approximately 9 mm (one eleventh the length of a conventional magnifying lens) and a weight of less than approximately 1 gram (one 15 seven-hundredth the weight of a conventional lens).

The HMPD can be based on novel innovative technology when one uses the compact lens of the earlier described inventions and now the remarkable novel microlenslets array of this invention for 3D visualization.

The foregoing discussion of the HMPD of the invention has increased FOV, reduced weight, remarkable mobility, and as a major component of a teleportal augmented reality system by using the combination of a plurality of baffled microlenslet arrays for generating a new generation of HMPDs into which has been placed the teleportal system. U.S. patent application Ser. No. 2002/0080094, filed Dec. 22, 2000 of common co-assignee with the instant application, discloses a teleportal augmented reality system that allows 3D visualization with a HMPD and real-time stereo-

miniature display 301 is used to display computer-generated 30 scopific face capture that can be teleported via the network to image. The magnified image 309 is then projected by the projection lens 303 toward the beam splitter 304. The image 306 is formed on the retro-reflective screen 305 and further magnified by a second compact lens, such as a single microlenslet array or a Fresnel lens based imager 307. A 35 final virtual image 308 can be formed in front of the viewer's eye.

When the retro-reflective screen 305 is at either the focal plane or within the focal plane of the second microlenslet array based imager 307, or other imager 307 such as Fresnel 40 of the invention are as a component of wearable computers, lenses, the retro-reflective screen 305 reflects rays at the same angle and in the reverse direction traveling towards the beam splitter 304 forming the final image 308 viewed by the user's eye.

As noted above, other useful lens assemblies are taught in 45 of the invention is not intended to be, nor should it be deemed to be, limited thereby and such other modifications or embodiments as may be suggested by the teachings herein are particularly reserved especially as they fall within the breadth and scope of the claims here appended.

co-pending U.S. patent application Ser. No. 10/090,070, filed Mar. 1, 2002, now U.S. Pat. No. 6,731,434, of common assignee with the instant application and fully incorporated herein by reference thereto. The double-Gauss lens disclosed therein has a FOV of approximately 52 degrees with 55 an effective focal length of 35 mm. Co-pending U.S. patent application Ser. No. 10/285,855, filed Nov. 1, 2002 of common assignee also with the instant application and fully incorporated herein by reference thereto, discloses a double-Gauss lens that has a FOV of approximately 70 degrees with 55 an effective focal length of approximately 25.8 mm. Co-pending U.S. patent application Ser. No. 10/418,623, filed Apr. 18, 2003, of common assignee also with the instant application and fully incorporated herein by reference 60 thereto, discloses a compact lens assembly useful for HMPD systems of miniature display of 0.6" diagonal with a FOV of approximately 42 degrees and an effective focal length of approximately 17 mm.

While the original U.S. Pat. No. 6,731,434 implemented an approximately 52 degree FOV with an approximately 65 1.3" miniature display for use inside the HMPD, the latter application Ser. No. 10/418,623 expanded the optical design

a remote location for face-to-face collaboration.

A purpose of this invention is to replace single aperture bulk macro-optical system with compact multi-aperture micro-optical system. A key component of the invention is the use of microlenslet arrays in combination with the appropriate baffles to magnify the miniature display integrated in the HMPD or HMD to make this revolutionary technology work.

Other applications of the compact imaging system subject of the invention are as a component of wearable computers, lenses, within telescopes and microscopes, and many others.

While the invention has been described, disclosed, illustrated and shown in various terms of certain embodiments or modifications which it has presumed in practice, the scope of the invention is not intended to be, nor should it be deemed to be, limited thereby and such other modifications or embodiments as may be suggested by the teachings herein are particularly reserved especially as they fall within the breadth and scope of the claims here appended.

We claim:

1. A compact optical assembly useful for head mounted projection display (HMPD) or head-mounted displays (HMDs) comprising:

- (a) a first baffled microlenslet array and a second cooperating microlenslet array which provide an optical means for magnifying images written on a microdisplay within the HMPD or the HMD before imaging to the users' eye
- (b) miniature projection optics for further magnifying the images in HMPD or an eyepiece optics for further magnifying the images in HMD; and
- (c) retro-reflective means for receiving said magnified images by disposing them on a micro-structures retro-reflective screen integrated on the interior surface of said HMPD or said HMD and within the field of view of said miniature projection optics or said eyepiece optics; and wherein both of said miniature projection

US 7,009,773 B2

7

optics or said eyepiece optics and said retro-reflective means are located internally of the external housing of said HMPD or HMD assembly, respectively.

- 2. The assembly of claim 1, wherein a baffle is located between the second array and the image plane.
- 3. The assembly of claim 1, wherein a baffle is located between an object and the first microlens array and wherein another baffle is located between the second microlens array and the image plane.
- 4. The assembly of claim 1, where the microlenslet arrays are aspherical shaped.
- 5. The assembly of claim 1 wherein the first baffled microlenslet arrays comprises: multiple arrays.
- 6. The assembly of claim 1 wherein the second microlenslet array comprises: multiple arrays.
- 7. A method of forming a head mounted display (HMD) or head mounted projection display (HMPD) having a compact lens display assembly comprising the steps of:
 - (a) combining a baffle with a first microlenslet array; and
 - (b) combining said combined baffle and first microlenslet array with a second microlenslet array;
 - (c) providing images of an object to be viewed by a user wearing the HMD or (HMPD) incorporating the com-

8

compact lens display assembly with said combined baffle and said first microlenslet array and said second microlenslet array.

- (d) further magnifying the images with a miniature projection optics in the HMPD or an eyepiece optics in the HMD; and
- (e) disposing the magnified images on a retro-reflective screen, wherein said miniature projection optics or eyepiece optics are integrated on an interior of said HMPD or HMD.
- 8. The method described in claim 7, further comprising the step of: combining said the baffle with the second microlenslet array.
- 9. The method described in claim 7, further comprising the step of: combining said baffles with the first and the second microlenslet array.
- 10. The method of claim 7, further comprising the step of: providing a distance between the object and the image as low as approximately 1.7 mm.

LIST OF REFERENCES

- [Arrington, K.F., and Geri, G.A., 2000] Arrington, K.F., and Geri, G.A., “Conjugate-Optical Retroreflector Display System: Optical Principles and Perceptual Issues,” *Journal of the SID*, August 2000.
- [Azuma, R., 1993] Azuma, R., “Tracking Requirements for Augmented Reality”, *Communications of the ACM*, **36**, 7, 50-51, July 1993.
- [Azuma, R., 1995] Azuma, R., “A Survey of Augmented Reality”, *Presence: Teleoperators and Virtual Environments*, **6**, 4, 355 – 385, 1995.
- [Azuma, R., and Gary B., 1994] Azuma, R. and Gary B., “Improving Static and Dynamic Registration in an Optical See-Through HMD”, *Proceedings of SIGGRAPH '94*, Orlando, FL, 24-29, *Computer Graphics*, Annual Conference Series, 197-204, 1994.
- [Azuma, R., and Gary B., 1995] Azuma, R., and Gary B., “A Frequency-Domain Analysis of Head-Motion Prediction”, *Proceedings of SIGGRAPH '95*, Los Angeles, CA, 6-11, *Computer Graphics*, Annual Conference Series, 401-408, 1995.
- [Barfield, W., et. al., 1995] Barfield, W., Rosenberg, C., & Lotens, W. A., Augmented-reality displays, in *Virtual environments and advanced interface design*, Oxford University Press, 1995.
- [Biocca, F., and Rolland, J., 1998] F. Biocca and J. Rolland, “Virtual eyes can rearrange your body: Adaptation to visual displacement in see-through head-mounted displays,” *Presence*, vol. **7** no. 3, 262–278, 1998.
- [Biocca, F., 1992] Biocca, F., “Will simulation sickness slow down the diffusion of virtual environment technology,” *Presence*, vol. **1**, 334-343, 1992.

- [Biocca, F., and Rolland, J., 2000] F. Biocca and J.P. Rolland, "Teleportal face-to-face system," *Patent Application Filed* (2000).
- [Bogaert, L. et. al., 2007] Bogaert, L., Meuret, Y., Giel, B.V., & Thienpont, H., "LED based full color stereoscopic projection system," *Proc. SPIE*, **6489**, 2007.
- [Buckert-Donelson, 1995] Buckert-Donelson, A., Linden Rhoads, Virtual I/O, *Virtual Reality World*, 35-36, 1995.
- [Buxton, D., and Fitzmaurice, G. W., 1998] Buxton, D., and Fitzmaurice, G. W., "HMDs, caves and chameleon: a human-centric analysis of interaction in virtual space," *Computer Graphics*, vol. **32**, no. 4, 69-74 (AMC, 1998).
- [Cakmakci, O., and Rolland, J., 2006] Cakmakci, O., Rolland, J., "Head-worn Displays: A Review," *Journal of Display Technology*, vol. **2** no. 3, 2006.
- [Caldwell, J. B., 1999] Caldwell, J. B., "Diffractive apochromatic double-Gauss lens," *Optics and Photonics News*, 43-45 (Oct. 1999).
- [Cruz-Neira, C., et. al., 1993] Cruz-Neira, C., Sandin, D. J., and DeFanti, T. A., "Surround-screen projection-based virtual reality: the design and implementation of the CAVE," *Conference of Computer Graphics 1993*, Proc. Of ACM SIGGRAPH 93, p. 135-142, ACM, New York, NY, USA, Anaheim, CA, USA, 1st-6th August 1993.
- [Curatu, C., et. al., 2005] Curatu, C., Hua, H., and Rolland, J. P., "Projection-based head-mounted display with eye-tracking capabilities," *Proc. SPIE* , **5875**, 2005.
- [Curatu, C., et. al., 2006] Curatu, C., Rolland, J. P., and Hua, H., "Dual Purpose Lens for an Eye-Trackted Projection Head-Mounted Display," in *International Optical Design*, Technical Digest (CD), 2006.

- [Davis, L., et. al., 2002] Davis, L., et. al., “Application of Augmented Reality to Visualizing Anatomical Airways,” Proceedings of SPIE Proceedings, *SPIE AeroSense: Helmet- and Head-Mounted Displays VII: Technologies and Applications*, Editors: Clarence E. Rash, Colin E. Reese, Editors, Vol. **4711**, p.400-405, August 2002.
- [Davis, L., et. al., 2003] Davis, L., Rolland, J. P., Hamza-Lup, F., Ha, Y., Norfleet, J., and Imielinska, C., “Alice in the ARC: seamless transition between levels of immersion in virtual environments,” *IEEE Computer Graphics and Applications*, 23(2), 10-12, 2003.
- [Dereniak, E. L., and Boreman, G. D., 1996] Dereniak, E. L., and Boreman, G. D., “Radiometry,” in *Infrared Detectors and Systems*, (John Wiley & Sons, Inc., 1996), pp. 38-55.
- [DiZio, P., and Lackner, J. R., 1992] DiZio, P., & Lackner, J. R., “Spatial orientation, adaptation, and motion sickness in real and virtual environments,” *Presence*, vol. **1**, 319-328, 1992.
- [Fidopiastis, C., 2006] Fidopiastis, C., User-centered virtual environment assessment and design for cognitive rehabilitation applications. Ph.D. Dissertation, University of Central Florida 2006.
- [Fischer, R. E., 1994] Fischer, R. E., “Optics for head-mounted displays,” *Information Disp.*, **10**, 1994.
- [Fischer, R. E., 1996] Fischer, R. E., “Head-mounted projection display system featuring beam splitter and method of making same.” US Patent: 5,572,229, November 5, 1996.
- [Genc, Y., et. al., 2000] Genc, Y., Sauer, F., Wenzel, F., Tuceryan, M., Navab, N., “Optical see-through HMD calibration: a stereo method validated with a video see-through system”,

Augmented Reality Proceedings, IEEE and ACM International Symposium on 5-6 Oct. 2000, 165 – 174, 2000.

[Goodman, J.W., 1968] Goodman, J.W., “*Introduction to Fourier optics*,” McGraw-Hill physical and quantum electronics series, New York, 1968.

[Ha, Y., and Rolland, J. P., 2002] Ha, Y., and Rolland, J. P., “Optical assessment of head-mounted displays in Visual Space,” *Applied Optics* 42(25), 5282-5289 (2002).

[Ha, Y., and Rolland, J. P., 2004] Ha, Y., and Rolland, J. P., “Compact lens assembly for the teleportal augmented reality system,” US Proc. of SPIE Vol. 5442 109 Patent: US Patent: University of Central Florida, Issued August 2004.

[Hockel, H., et. al., 2005] Hockel, H., Martins, R. F., Sung, J., & Johnson, E. G., “Design and fabrication of trihedral corner-cube arrays using analog exposure based on phase masks,” *Proc. SPIE Int. Soc. Opt. Eng.*, **5720**, 2005.

[Holloway, R., 1994] Holloway, R., “An Analysis of Registration Errors in a See-Through Head-Mounted Display System for Craniofacial Surgery Planning”, Ph.D. dissertation, University of North Carolina at Chapel Hill, 1994.

[Hua, H. and Gao, C., 2007] Hua, H. and Gao, C., "Design of a bright polarized head-mounted projection display," *Appl. Opt.*, **46**, 2600-2610, 2007.

[Hua, H., et. al., 2001] Hua, H., Rolland, J.P., and Biocca, F., “Compact Lens-Assembly for Wearable Displays, Projection Systems, and Cameras,” US Patent: University of Central Florida, Filed 2001.

[Hua, H., et. al., 2000] Hua, H., Girardot A., C. Gao, and Rolland, J. P., “Engineering of head-mounted projective displays,” *Applied Opt.*, **39** (22), 3814-3824, 2000.

- [Hua, H., et. al., 2002] Hua, H., C. Gao, and Rolland, J. P., “Imaging properties of retro-reflective materials used in head-mounted projective displays (HMPDs),” *Helmet- and Head-Mounted Displays VII*, C. E. Rash, and C. E. Reese, eds., Proc. SPIE 4711, pp. 194-201 (August 2002).
- [Hua, H., et. al., 2002] Hua, H., Ha., Y., Rolland, J. P., “Design of an ultra-light and compact projection lens,” *Applied Opt.*, **42**(1), 97-107, 2002.
- [Inami, M., et. al., 2000] Inami, M., Kawakami, N., Sekiguchi, D., Yanagida, Y., Maeda, T., and Tachi, S., “Visuo-haptic display using head-mounted projector,” in *Proceedings of IEEE Virtual Reality 2000*, pp. 233–240, 2000.
- [Inami, M., et. al., 2003] Inami, M., Kawakami, N., and Tachi, S., “Optical camouflage using retro-reflective projection technology,” in *Proceedings of ISMAR 2003*, 348–349, 2003.
- [Julier, S., et. al., 2000] Julier, S., Baillot, Y., Lanzagorta, M., Brown, D., and Rosenblum, L., “BARS: Battlefield Augmented Reality Systems”, *NATO Symposium on Information Processing Techniques for Military Systems*, Istanbul, Turkey, 2000.
- [Kalawsky, R. S., 1993] Kalawsky, R. S., *The Science of Virtual Reality and Virtual Environment*, Wokingham, England, Addison-Wesley, 1993.
- [Kawakami, N., et. al., 1999] Kawakami, N., Inami, M., Sekiguchi, D., Yangagida, Y., Maeda, T., and Tachi, S., “Object-oriented displays: a new type of display systems—from immersive display to object-oriented displays,” in *Proceedings of IEEE SMC 1999, IEEE International Conference on Systems, Man, and Cybernetics*, vol. **5**, pp. 1066–1069, 1999.

- [Kijima, R., and Ojika, T., 1997] Kijima, R., and Ojika, T., “Transition between virtual environment and workstation environment with projective head-mounted display,” in *Proceedings of IEEE VR 1997*, 130–137, 1997.
- [Liepmann, T. W., 2004] Liepmann, T. W., “How retroreflectors bring the light back,” *Laser Focus World* **30**, pp. 129-132, 1994.
- [Martins, R., and Rolland, J.P., 2003] Martins, R.F. and Rolland, J.P. “Head-mounted display by integration of phase-conjugate material,” *US Patent 6999239*, (Feb. 2006)
- [Martins, R., and Rolland, J.P., 2003] Martins, R.F. and Rolland, J.P. "Diffraction of Phase Conjugate Material in a New HMD Architecture," *SPIE AeroSense: Helmet and Head-Mounted Displays VIII: Technologies and Applications*, SPIE Proceedings Vol. **5186**, p. 277-283, , Editors: C. E. Rash and C. E. Reese, September 2003.
- [Martins, R., et. al., 2004] Martins, R., Shaoulov, V., Ha, Y., and Rolland, J. P., “Projection based head-mounted displays for wearable computers,” *Proc. SPIE* **5442**, 104–110, 2004.
- [Martins, R., et. al., 2007] Martins, R., Shaoulov, V., Ha, Y., and Rolland, J. P, "A mobile head-worn projection display," *Opt. Express* **15**, 14530-14538, 2007.
- [Metzger, P. J., 1993] Metzger, P. J., “Adding reality to the virtual,” *Virtual Reality Annual International Symposium '93*, Los Alamitos, CA: IEEE Computer Society Press, 1993.
- [Milgram, P. and Kishino, F., 1994] P.Milgram and F. Kishino, “A taxonomy of mixed reality visual displays,” *IECE Trans. Information and Systems (Special Issue on Networked Reality)*, vol. E77-D, no. 12, 1321-1329 (1994).
- [O’Brien, D. C., et. al., 1999] O’Brien, D. C., Faulkner, G. E., and Edwards, D. J., “Optical properties of a retroreflecting sheet”, *Appl. Opt.* **38**, pp. 4137-4144, 1999.

- [Ogawa, H., 1999] Ogawa, H., “Optical system with refracting and diffracting optical units, and optical instrument including the optical system,” US patent 5,930,043 (1999).
- [Oranchak, A., and Rolland, J., 2006] Oranchak, A., and Rolland, J., “Elastic head mounting platform cap”, US Patent Filed July 2006.
- [Parsons, J., and Rolland, J. P., 1998] Parsons, J., and Rolland, J. P., “A non-intrusive display technique for providing real-time data within a surgeons critical area of interest,” in *Proceedings of Medicine Meets Virtual Reality 1998*, 246–251, 1998.
- [Pausch, R., and Conway, M., 1992] Pausch, R., Crea, T., and Conway, M., “A literature survey for virtual environments: Military flight simulator visual systems and simulator sickness,” *Presence*, vol. **1**, 344-363, 1992.
- [Rapaport, A., et al., 2006] Rapaport, A., Milliez, J., Cassanho, A., Jenssen, H., & Bass, M., "Review of the properties of Up-Conversion Phosphors for new Emissive Displays," *IEEE/OSA J. Display Technol.*, **2**, 2006.
- [Rolland, J., et al., 1995] J. P. Rolland, R. L. Holloway, and H. Fuchs (1995), “Comparison of optical and video see-through, head-mounted displays,” *Proceeding SPIE*, **2351**, 293, 1995.
- [Rolland, J., et al., 2001] Rolland, J. P., Shaoulov, V., and Gonzalez, F. J., "The art of back-of-the-envelope paraxial raytracing", *IEEE Transactions in Education* (2001).
- [Rolland, J., et al., 2004] Rolland, J. P., Biocca, F., Hua, H., Ha, Y., Gao, C., and Harrison, O., *Teleportal Augmented Reality System: Integrating virtual objects, remote collaborators, and physical reality for distributed networked manufacturing*, Chapter 11, Springer-Verlag, June 2004.

- [Rolland, J. P. et. al., 2005] Rolland, J. P., Biocca, F., Hamza-Lup, F., Ha, Y. and Martins, R., “Development of head-mounted projection displays for distributed, collaborative, augmented reality applications,” *Presence: Teleoperators and Virtual Environments* **14**, 528–549, 2005.
- [Seward, G. H., and Cort, P. S., 1999] Seward, G. H., and Cort, P. S., “Measurement and characterization of angular reflectance for cube-corners and microspheres”, *Opt. Eng.* **38**, pp. 164-169, 1999.
- [State, A., et. al., 2005] State, A., Keller, K. P., and Fuchs, H., 2005, “Simulation-Based Design and Rapid Prototyping of a Parallax-Free, Orthoscopic Video See-Through Head-Mounted Display,” In *Proceedings of the Fourth IEEE and ACM international Symposium on Mixed and Augmented Reality*, ISMAR. IEEE Computer Society, Washington, DC, 28-31, 2005.
- [Sutherland, I., 1965] Sutherland, I., "The ultimate display," *Information Processing 1965: Proc. of IFIP Congress*, **65**, 506-508, 1965.
- [Yamazaki, T., et. al., 1990] Yamazaki, T., Kamijo, K., and Fukuzumi, S., “Quantitative evaluation of visual fatigue encountered in viewing stereoscopic 3D displays: near-oint distance and visual evoked potential study”, *Proceedings of the Society for Information Dispalys*, **31**, 245-247, 1990.
- [Yuan, J., et. al., 2002] Yuan, J., Chang, S., Li, S., and Zhang, Y., “Design and fabrication of micro-cube-corner array retro-reflectors”, *Optics Communications*, **209** (1-3), 75-83 (2002).
- [Zurasky, J. L., 1976] Zurasky, J. L., “Cube corner retroreflector test and analysis,” *Appl. Opt.* **15**, pp. 445-452, 1976.

[Zhang, R. and Hua, H., 2008] Zhang, R. and Hua, H., "Design of a polarized head-mounted projection display using ferroelectric liquid-crystal-on-silicon microdisplays," *Appl. Opt.* **47**, 2888-2896, 2008.

[Zhu, X., et. al., 2000] Zhu, X., Hsu, V. S., and Kahn, J. M., "Optical Modeling of MEMS Corner Cube Retroreflectors with Misalignment and Non-flatness", *IEEE Journal on Selected Topics in Quantum Electronics*, (July 2000).